

## Neogene integrative stratigraphy, biotas, and paleogeographical evolution of the Qinghai-Tibetan Plateau and its surrounding areas

Tao DENG<sup>1,2,3\*</sup>, Xiaomin FANG<sup>3,4</sup>, Qiang LI<sup>1,2,3</sup>, Shiqi WANG<sup>1,2</sup>, Feixiang WU<sup>1,2</sup>,  
Sukuan HOU<sup>1,2,3</sup>, Jiao MA<sup>1,2</sup>, Qigao JIANGZUO<sup>1,2,5</sup>, Danhui SUN<sup>3</sup>, Yan ZHENG<sup>1,2</sup>,  
Qinqin SHI<sup>1,2</sup>, Boyang SUN<sup>1,2</sup> & Lu LI<sup>1,2</sup>

<sup>1</sup> Key Laboratory of Vertebrate Evolution and Human Origins, Institute of Vertebrate Paleontology and Paleoanthropology, Chinese Academy of Sciences, Beijing 100044, China;

<sup>2</sup> CAS Center for Excellence in Life and Palaeoenvironment, Beijing 100044, China;

<sup>3</sup> University of Chinese Academy of Sciences, Beijing 100049, China;

<sup>4</sup> CAS Center for Excellence in Tibetan Plateau Earth Sciences and Key Laboratory of Continental Collision and Plateau Uplift, Institute of Tibetan Plateau Research, Chinese Academy of Sciences, Beijing 100101, China;

<sup>5</sup> Key Laboratory of Orogenic Belts and Crustal Evolution, School of Earth and Space Sciences, Peking University, Beijing 100871, China

Received December 23, 2022; revised April 28, 2023; accepted May 8, 2023; published online December 6, 2023

**Abstract** The remarkable uplift of the Tibetan Plateau in the Neogene had great impacts on the climate and environment of East Asia and even the world. Therefore, establishment of the Neogene stratigraphic framework of the Tibetan Plateau is of great significance to research in various fields of geosciences. Based on marine sediments, the international chronostratigraphic system of the Neogene is divided into six stages in the Miocene and two stages in the Pliocene. Since the beginning of the Cenozoic, the share of terrestrial strata on continents has increased rapidly. By the Neogene, it had far exceeded that of marine strata, and almost all deposits on the Tibetan Plateau and its surrounding areas were terrestrial strata. In China, the Miocene includes five stages and the Pliocene includes two stages. Except for the Tunggurian of the Miocene, which has a lower boundary at 15 Ma, the other stages have the same paleomagnetic definitions and time intervals as the corresponding international marine stages. Mammalian fossils play a very important role in the division and correlation of Cenozoic terrestrial strata, and rodent, carnivore, proboscidean, perissodactyl and artiodactyl fossils are especially important in Neogene terrestrial biostratigraphy. There are many basins with well-exposed strata and abundant mammalian fossils in the Tibetan Plateau. The lower boundary stratotype sections of the Neogene Xiejian and Bahean stages are located respectively in the Xining and Linxia basins, and there are precise paleomagnetic dates in coordination with mammalian fossils. The lower boundary stratotypes of other stages can also be effectively determined in the Tibetan Plateau. Many first appearing mammalian genera in East Asia also appeared in the Tibetan Plateau and its surrounding areas, especially in the Linxia Basin on the northeast margin and in the Siwaliks on the southwest margin. Among them, *Prodeinotherium* first appeared at the bottom of the Miocene in the Siwaliks, and the earliest *Hipparion* of the Old World first appeared at the bottom of the Bahean Stage in the Linxia Basin. Carbon and oxygen isotope analysis of enamel and paleosols of Cenozoic sediments and mammal fossils in the Tibetan Plateau and its surrounding areas have been used to reconstruct the climate, environment and vegetation development characteristics, and revealed that these changes were not only related to global change, but also had regional features. Evidence of the Late Miocene C<sub>4</sub> plant expansion event based on carbon isotope changes comes from the southern margin of the Tibetan Plateau, but in sharp contrast,  $\delta^{13}\text{C}$  indicates that there was still no clear or significant C<sub>4</sub> plant signal on the northern margin of the Tibetan Plateau until the end of the Neogene. The  $\delta^{18}\text{O}$  analysis shows that there were several major climate change events in the Cenozoic, especially in the Late Miocene at about 7 Ma, when positive drift of  $\delta^{18}\text{O}$  indicates that the northern and southern sides of the Tibetan Plateau were changing to drier environments. The strong uplift of the Tibetan Plateau in the Late Miocene strengthened the thermal contrast

\* Corresponding author (email: [dengtao@ivpp.ac.cn](mailto:dengtao@ivpp.ac.cn))

between sea and land, which strengthened monsoon circulation and led to the expansion of C<sub>4</sub> vegetation in South Asia. However, the East Asian summer monsoon, which can bring atmospheric precipitation and a climate suitable for C<sub>4</sub> plants to northern China, was not enough to affect the northern Tibetan Plateau. The Tibetan Plateau on the whole rose to an altitude of about 3000 m in the Miocene, becoming a barrier to mammalian migration; it reached its modern altitude of more than 4000 m in the Pliocene, thus forming a cryosphere environment, which led to the emergence of ancestral types of the Ice Age fauna.

**Keywords** Tibetan Plateau, Neogene, Terrestrial stratum, Mammalian fossil, Paleomagnetism

---

**Citation:** Deng T, Fang X, Li Q, Wang S, Wu F, Hou S, Ma J, Jiangzuo Q, Sun D, Zheng Y, Shi Q, Sun B, Li L. 2024. Neogene integrative stratigraphy, biotas, and paleogeographical evolution of the Qinghai-Tibetan Plateau and its surrounding areas. *Science China Earth Sciences*, 67(4): 1326–1359, <https://doi.org/10.1007/s11430-022-1115-5>

---

## 1. Introduction

Following the break-up of Gondwana in the Mesozoic, a series of collisions between drifting continental blocks occurred in the Cenozoic, and this process continued to evolve in the Neogene. Among them, the collision between the Indian and Eurasian plates in the early Paleogene completely closed the Neo-Tethys Ocean, the Himalayas were taking shape, and the Tibetan Plateau gradually transformed into its present state (Ding et al., 2017). This collision is the most important orogenic event in the past 500 million years on Earth (Yin and Harrison, 2000). In the Neogene, the global climate began to gradually cool, accompanied by fluctuations of different scales (Zachos et al., 2001). The uplift of the Tibetan Plateau had a considerable impact on the climate and environment in East Asia and even globally. Its scope of influence has extended far beyond the Tibetan Plateau (Wang, 2021), affecting the hinterland of Central Asia, Southeast Asia and eastern China (Tapponnier et al., 1982, Ruddiman and Kutzbach, 1989), and these effects have become a focus of global geoscience (Molnar, 2005). Since the late Neogene, the large-scale mountain uplift of the Tibetan Plateau has pushed parts of the Paleogene-Neogene sedimentary basins to the tops of mountains. Most of these sediments have been denuded, leaving incomplete sedimentary records of the pre-existing basins; thus, they are called remnant basins (Zhang et al., 2010). Fossils are an important basis for stratigraphic division and correlation, and the uplift of the Tibetan Plateau has also had a significant impact on the biota. During the Paleogene, the uplift of the Tibetan Plateau was not strong. The elevation of basins such as the Nima and Lunpola basins in northern Xizang Autonomous Region was about 2000 m in the Oligocene, and the terrain of the entire Tibetan Plateau was not high enough to hinder the exchange of large animals. Mammals such as the giant rhino could still travel between the north and south of the plateau in the Oligocene (Deng et al., 2021a). During the Late Eocene, seawater completely withdrew from the Tibetan Plateau; thus, the Neogene was characterized by continental sedimentation. The Gyirong, Lunpola and Hoh Xil basins had risen to altitudes of about 3000 m in the Miocene, becoming barriers to the exchange of mammals such as *Platybelodon*

(Deng et al., 2019b). By the Pliocene, basins such as the Zanda and Kunlun Pass basins reached modern altitudes of more than 4000 m, thus forming a cryosphere environment, leading to the emergence of ancestral forms of the Ice Age fauna (Deng et al., 2011b).

## 2. Review of Neogene studies on the Tibetan Plateau

The Neogene System includes the Miocene Series in the lower part and the Pliocene Series in the upper part. The Miocene started at 23.03 Ma and ended at 5.333 Ma; it is divided into the Aquitanian, Burdigalian, Langhian, Serravallian, Tortonian and Messinian stages from bottom to top. The Pliocene began at 5.333 Ma and ended at 2.58 Ma; the lower part of the Pliocene is the Zanclean Stage and the upper part is the Piacenzian Stage. Because of the detailed study of marine microfossils in Mediterranean coastal areas, Neogene chronostratigraphy has been particularly well established worldwide. In the International Chronostratigraphic Chart, lower boundary stratotypes have been established for six of the eight stages of the Neogene, and the remaining Burdigalian and Langhian stages also have accurate lower boundary ages. Based on marine strata as the standard, Neogene terrestrial strata, which are widely distributed across different continents, can be well correlated between sea and land (Ogg et al., 2016; Raffi et al., 2020).

Since the beginning of the Cenozoic, the proportion of terrestrial strata on land has increased rapidly, and by the Neogene, this proportion far exceeded that of marine strata, especially in Asia and North America. The global chronostratigraphic standard and geochronological system established based on marine deposits have been greatly restricted at the stage/age level in the Cenozoic, especially in the Neogene. Neogene strata in China are mainly terrestrial deposits, but before 1978, biostratigraphic studies focused more on the description of mammalian fossils. Fossils of other biological groups were limited to local reports, and chronostratigraphy had not received due attention. Chiu et al. (1979) reviewed and summarized the research on Neogene mammalian faunas in China, and put forward a chronological

framework of these faunas for the first time. Li et al. (1984), Qiu (1990), Qiu and Qiu (1990, 1995), Tedford (1995), Tong et al. (1995), Qiu et al. (1999, 2013), Deng (2006a), Woodburne et al. (2013), Deng and Hou (2014), and Deng et al. (2019a) have successively established and improved the division scheme of Neogene mammalian ages and chronostratigraphic stages in China (Figure 1).

In early works, the strata containing the three-toed horse *Hipparion* in China, such as the Baode Formation (Fm.) in Shanxi, Bahe Fm. in Shaanxi, and Woma Fm. in Xizang Autonomous Region, were referred to the Pliocene (Chiu et al., 1979; Huang W B et al., 1980). This was because of a historical error, which may have been influenced by the views of American paleontologists: They believed that in the evolutionary history of horses, *Anchitherium* lived in the Miocene, *Hipparion* in the Pliocene, and *Equus* in the Quaternary. The effect of this mistaken view has persisted for a long time (Qiu et al., 1987). Since the Third National Stratigraphy Conference of China in 2000, the stage establishment of the Neogene in China has been greatly promoted. Based on mammalian ages and in accordance with the principles of the *International Stratigraphic Guide* (Salvador, 1994), the Neogene in China is divided into the Miocene Xiejian, Shanwangian, Tunggurian, Bahean, and Baodean stages, and the Pliocene into the Gaozhuangian and Maze-gouan stages. This scheme has been applied to the *Stratigraphic Chart of China* (Wang Z J et al., 2014), and the correlation with international marine stages is consistent or close for most lower boundaries. Only the division of the Tunggurian has its own characteristics (Qiu et al., 2013; Deng et al., 2019a).

The remarkable uplift of the Tibetan Plateau in the Neogene caused large-scale geomorphic inversion in East Asia, and the current macro-geomorphologic pattern of China, high in the west and low in the east, was ultimately established in the Neogene (Wang, 2005). Therefore, the establishment of the Neogene stratigraphic framework of the Tibetan Plateau is of great significance to the study of various fields of geoscience.

The Neogene strata of the Tibetan Plateau have long been discussed. The British botanist John Forbes Royle (1839) first illustrated vertebrate fossils from China, which were found in the Neogene strata of the Zanda Basin in the Ngari region, Xizang Autonomous Region, China, north of the Niti Pass in the Himalayas. These fossils included a caprine skull and upper cheek teeth, which were named “*Pantholops*” *hundsensis* (Lydekker, 1881) but were recently referred to the genus *Qurlignoria* (Wang et al., 2023), as well as an incomplete upper cheek tooth of a rhinoceros, which may have belonged to the Tibetan woolly rhino *Coelodonta tibetana* created by Deng et al. (2011b). Also in 1839, the British naturalist Hugh Falconer formally described for the first time in a report some Neogene mammalian fossils from

the Zanda Basin, including materials from Royle (1839), as well as additional rhinocerotid teeth and limb bones (Falconer, 1868).

By the first half of the 20th century, Birger Bohlin had made outstanding achievements in the investigation of the Cenozoic, especially Neogene stratigraphy and paleontology in the northern part of the Tibetan Plateau (Bohlin, 1937, 1942, 1946). What laid a systematic foundation for the Neogene stratigraphic work in the hinterland of the Tibetan Plateau was the preliminary division and comparison of a series of Cenozoic basins by Li (1955), including the northern bank of the Nujiang River, the basins in the northern Tibetan lake area, and the upper reaches of the Yarlung Zangbo river valley. However, because there was a lack of mammalian fossils, which were very important for the Neogene division at that time, it was summarized as Tertiary.

With the development of geological mapping and comprehensive scientific expeditions on the Tibetan Plateau, a series of achievements involving Neogene stratigraphic division and fossil discoveries have been made. Hsu et al. (1973) reported *Quercus* fossils found in the Mount Xixabangma area, and inferred that the relevant strata would not be older than the middle and late Pliocene according to the sporopollen fossils. Wang et al. (1975) studied the sporopollen of the Lunpola Basin in northern Xizang Autonomous Region, and Wu and Chen (1980) reported fish fossils in the basin. They proposed that the Dingqing Formation belongs to the Miocene to Pliocene. The discovery of Neogene mammalian fossils provided an important basis for the division and correlation of Neogene strata in the Tibetan Plateau. The most important localities of the *Hipparion* fossils are the Bulong Basin in Biru County, northern Xizang Autonomous Region, and the Woma Basin in Gyirong County, Himalayan Mountains (Huang W B et al., 1980; Ji et al., 1980; Zheng, 1980). Later, fossils of the *Hipparion* fauna were also found in the Zanda Basin in the Ngari region (Zhang et al., 1981; Li and Li, 1990). In the Hengduanshan area on the eastern margin of the Tibetan Plateau, Neogene strata are still preserved in some fault basins, especially in Lufeng, Yuanmou, Baoshan, Yanyuan, and other basins in the southern part, where coal-bearing strata are well developed and mammalian fossils are abundant (Zong et al., 1996). Research carried out in a series of Cenozoic basins on the northern margin of the Tibetan Plateau, such as the Xining Basin in Qinghai Province and the Danghe and Linxia basins in Gansu Province, has led to many achievements in the understanding of Neogene strata. In recent years, Neogene stratigraphic investigation and research in the Lunpola, Nima, and Hoh Xil basins, as well as other basins in northern Xizang Autonomous Region, have also yielded rich evidence.

On the southern margin of the Tibetan Plateau, the Siwalik area is a typical site for recording Cenozoic sediments. Research began as early as the 1930s, mainly on the Potwar

Neogene System		Europe		Chiu	Li	Qiu	Tong	Deng	Hilgen	Qiu	Deng	Deng	This	
Series	Stage	Steininger, 1999		et al.	et al.	and Qiu	et al.		et al.	et al.	and Hou	et al.	Paper	
Epoch	Age	ELMA	MN	1979	1984	1990	1995	2006a	2012	2013	2014	2019a		
Pleistocene			17	SM Fm.	Nihewanian					Nihewanian				
Pliocene	Late	Vilanyian	16	Jingle Fm.	Youshan				Yushean	Maze-gouan	Maze-gouan	Maze-gouan	Maze-gouan	
	Early		Ruscianian	15 14 13	BD Fm. Jinglean Bahe Fm.	Jinglean Yushean	Yushean	Yushean		Gaozhuangian Yushean	Maze-gouan Yushean	Maze-gouan Yushean	Maze-gouan Yushean	Maze-gouan Yushean
Miocene	Late Miocene	Tortonian	12	Tunggur Fm.	Baodean	Baodean	Baodean	Baodean	Baodean	Baodean	Baodean	Baodean	Baodean	
			11		Baodean	Baodean	Baodean	Baodean		Baodean	Baodean	Baodean	Baodean	
			10		Baodean	Baodean	Baodean	Baodean		Baodean	Baodean	Baodean	Baodean	
			9		Baodean	Baodean	Baodean	Baodean		Baodean	Baodean	Baodean	Baodean	
			8		Baodean	Baodean	Baodean	Baodean		Baodean	Baodean	Baodean	Baodean	
	Middle Miocene	Langhian	Vallesian	7	Tunggur Fm.	Bahean	Bahean	Bahean	Bahean	Baodean	Bahean	Bahean	Bahean	Bahean
				6		Bahean	Bahean	Bahean	Bahean		Bahean	Bahean	Bahean	Bahean
				5		Bahean	Bahean	Bahean	Bahean		Bahean	Bahean	Bahean	Bahean
				4		Bahean	Bahean	Bahean	Bahean		Bahean	Bahean	Bahean	Bahean
				3		Bahean	Bahean	Bahean	Bahean		Bahean	Bahean	Bahean	Bahean
Early Miocene	Burdigalian	Astaracian	2	Shanwang Fm.	Tunggurian	Tunggurian	Tunggurian	Tunggurian	Tunggurian	Tunggurian	Tunggurian	Tunggurian	Tunggurian	
			1		Tunggurian	Tunggurian	Tunggurian	Tunggurian		Tunggurian	Tunggurian	Tunggurian	Tunggurian	
			0		Tunggurian	Tunggurian	Tunggurian	Tunggurian		Tunggurian	Tunggurian	Tunggurian	Tunggurian	
			0		Tunggurian	Tunggurian	Tunggurian	Tunggurian		Tunggurian	Tunggurian	Tunggurian	Tunggurian	
			0		Tunggurian	Tunggurian	Tunggurian	Tunggurian		Tunggurian	Tunggurian	Tunggurian	Tunggurian	
Oligocene	Chattian	MP 30	1	Xiejia Fm.	Shanwangian	Shanwangian	Shanwangian	Shanwangian	Shanwangian	Shanwangian	Shanwangian	Shanwangian	Shanwangian	
			0		Shanwangian	Shanwangian	Shanwangian	Shanwangian		Shanwangian	Shanwangian	Shanwangian	Shanwangian	

**Figure 1** History of the division of the Neogene in China and its correlation to the international Neogene scheme. Abbreviations: BD, Baode; Fm., Formation; SM, Sanmen.

Plateau of Pakistan and the Siwalik Hills in northern India. Stratigraphically, the Siwalik Group represents molasse deposits weathered from the Himalayas and Karakoram and accumulated on the southern edge of the Tibetan Plateau. This group is several kilometers thick and extends more than 2000 km from east to west. In this area, the Neogene strata are completely developed fluvial sediments and rich in mammalian fossils (Barry et al., 2013; Flynn et al., 2013).

### 3. Neogene biostratigraphy of the Tibetan Plateau

Neogene marine fossils with important biostratigraphic significance are represented by planktonic organisms, and include planktonic foraminifera, calcareous nannofossils, diatoms, radiolarians, silicoflagellates and dinoflagellates. Among these, planktonic foraminifera and calcareous nannofossils are the dominant groups and the basis for zonation. For the terrestrial Neogene, ostracods and sporopollens play a biostratigraphic role similar to that of foraminifera and calcareous nannofossils. Mammals originated in the Mesozoic. In the Cenozoic, mammalian fossils play a very important role in the division and correlation of terrestrial strata. For the Neogene, biostratigraphy is particularly dependent on fossils of Rodentia, Carnivora, Proboscidea, Perissodactyla, and Artiodactyla. Since 1978, great progress has been made in Chinese Neogene terrestrial stratigraphy. Many localities with well-exposed strata and rich mammalian fossils have also been found on the Tibetan Plateau, such as the Bulong, Gyirong, and Zanda basins in Xizang Autonomous Region (Huang W B et al., 1980; Wang X M et al., 2013a, 2013b), the Qaidam Basin in Qinghai (Wang et al., 2007), and the Linxia Basin in Gansu (Deng et al., 2013b). In addition, a large number of paleomagnetic dates based on mammalian fossils have been determined. The biggest difference between mammal fossils and other fossils is that mammal fossils are characterized by a fast evolutionary speed and distinctive morphological features that are easy to distinguish (Figure 2). Even with few or even incomplete fossils, it is relatively easy for paleomammalogists to arrange a sequence of fossils at the initial time of discovery based on their evolutionary levels without a detailed study of the fossil-bearing strata.

#### 3.1 Rodentia

Rodents breed fast, have large populations, and evolve rapidly. In addition, their teeth are easily preserved, comparable to marine microfossils. With the application and development of screening wash technology, the collection of small mammal fossils has been greatly enriched, and such fossils have become important standard fossils in Cenozoic

strata. In the Neogene of the Tibetan Plateau, rodent fossils are also key evidence for age constraint.

The first stage of the Miocene, the Xiejian Stage, was named at Xiejia in Tianjiazhai Township, Huangzhong County, Qinghai Province. The Xiejia fauna was found in the Xiejia Formation at this locality (Li and Qiu, 1980). Among the Rodentia, the marker fossils of the Xiejian include *Yindirtemys suni*, *Parasminthus xinningensis*, *P. huangshuiensis*, *Litodomys lajeensis*, and *Cricetodon youngi*. These fossils all appear in the Xiejia fauna (Qiu et al., 2013), and the characteristic genus of the Xiejian, *Tachyoryctoides* is represented by *T. kokonorensis* in this fauna. The characteristic genus *Prodistylomys*, the first appearing genera *Sayimys*, *Sinotamias*, *Democricetodon*, *Sicista*, and *Cricetodon*, and the last appearing genera *Tataromys*, *Yindirtemys*, and *Parasminthus* of the Xiejian are found in the Zhangjiaping fauna of the Huangyangtuo Fm. in the Lanzhou Basin. In the Siwaliks, *Prosayimys* and *Primus* first appeared at the lower boundary of the Miocene, and *Prokanisamys* and *Democricetodon* first appeared at approximately 22 Ma (Flynn et al., 2013).

The Shanwangian Stage is named in the Shanwang Basin, Linqu County, Shandong Province. Recently, Shanwangian rodent fossils were found in the Linxia Basin, Gansu Province on the Tibetan Plateau. They were produced from the Shangzhuang Formation, and included 6 families, 10 genera, and 12 species of rodents (Qiu et al., 2023). Among these, *Sayimys* and *Atlantoxerus* are characteristic genera, *Protolactaga* and *Megacricetodon* are first appearing genera, and *Litodomys* is a last appearing genus of the Shanwangian (Qiu et al., 2013). *Sayimys* is also found in the Dingqing Fm. of the Lunpola Basin. In the Danghe area in the west of Gansu Province, the Tiejianggou Fm. of the Xishui section produces *Heterosminthus intermedius* and *Litodomys xishuiensis*. *H. intermedius* from Danghe is primitive compared with the Middle Miocene *H. orientalis*, and more derived than the Late Oligocene *H. lanzhouensis*; *L. xishuiensis* appears at a higher horizon (Wang, 2003) than *L. huangheensis* (Wang and Qiu, 2000). The Duitinggou fauna of the Shimagou Fm. in the Lanzhou Basin contains the rodents *Atlantoxerus*, *Heterosminthus*, *Litodomys*, *Protolactaga*, *Democricetodon* and *Megacricetodon* (Flynn et al., 1999; Qiu et al., 2013). *Heterosminthus* and *Megacricetodon* also occur in the Chetougou Fm. of the Xining Basin (Qiu et al., 1981). On the southern edge of the Tibetan Plateau, *Prokanisamys arifi* first appeared at 20.1 Ma, *Sayimys intermedius* at 19 Ma, and *Kochalia gespei* at 16.1 Ma (Flynn et al., 2013), which are equivalent to the Shanwangian.

The Tunggurian Stage is named at the Tunggur tableland in Sunid Left Banner, central Inner Mongolia. Most members of the Quantougou micromammalian fauna of the Xiajie Formation in the Lanzhou Basin are the same as those of the Tunggur fauna, and contain the characteristic and last ap-

ATNTS 2012		Neogene System		China	Rodentia	Carnivora	Proboscidea	Perissodactyla	Artiodactyla
Date (Ma)	Chron	Series Epoch	Stage Age	Stage Age					
	C2	Pleistocene	Nihewanian		<i>Marmota</i>	<i>Canis</i>		<i>Equus</i>	<i>Leptobos</i>
3	C2A	Pliocene Late	Piacenzian 2.59	Mazegouan		<i>Sivapathera</i> <i>Lynx</i> <i>Homotherium</i>	<i>Elephas</i>		<i>Ovis</i>
4		Pliocene Early	Zanclean 3.60	Gaozhuangian	<i>Apyocricetus</i> <i>Mimomys</i>	<i>Pliocrocuta</i> <i>Chasmaporthetes</i> <i>Nyctereutes</i>		<i>Coelodonta</i> <i>Proboscideipparion</i>	<i>Antilospira</i>
5	C3		5.33	5.3					
6	C3A		Messinian	Baodean			<i>Sinomastodon</i> <i>Mammut</i>	<i>Dihoplus</i> <i>Shansirhinus</i>	<i>Hexaprotodon</i>
7	C3B		7.25	7.25					
8	C4					<i>Eomellivora</i> <i>Plesiogulo</i> <i>Simocyon</i>			<i>Gazella</i>
9	C4A		Tortonian	Bahean	<i>Huerzelerimys</i> <i>Abudhabia</i> <i>Nannocricetus</i> <i>Sinocricetus</i> <i>Prosiphneus</i> <i>Pseudorhizomys</i> <i>Pararhizomys</i>	<i>Indarctos</i> <i>Aderocuta</i> <i>Hyaenictitherium</i> <i>Ictitherium</i> <i>Promephitis</i> <i>Machairodus</i> <i>Agriotherium</i> <i>Parataxidea</i>		<i>Sinotherium</i> <i>Tapirus</i>	<i>Urmitherium</i> <i>Cervavitus</i> <i>Honanotherium</i> <i>Schansitherium</i> <i>Selenoportax</i> <i>Chleuastochoerus</i>
10	C5						<i>Tetralophodon</i>	<i>Hipparion</i>	
11			11.63	11.6					
12	C5A		Serravalian	Tunggurian	<i>Spermophilinus</i>				<i>Palaeotragus</i>
13	C5AA								
14	C5AB		13.82		<i>Myomimus</i>				
15	C5AC		Langhian		<i>Gobicricetodon</i>				
16	C5AD								
17	C5B		15.97		<i>Kochalia</i>	<i>Pseudaelurus</i>			
18	C5C								
19	C5D		Burdigalian	Shanwangian	<i>Protalactaga</i>	<i>Kinometaxia</i>		<i>Plesiaceratherium</i>	<i>Turcocerus</i>
20	C5E				<i>Megacricetodon</i>		<i>Platybelodon</i>		<i>Listriodon</i>
21	C6								
22	C6A		20.44	20.4	<i>Sicista</i> <i>Sayimys</i> <i>Sinotamias</i> <i>Democricetodon</i> <i>Cricetodon</i> <i>Primus</i> <i>Prosayimys</i>			<i>Phyllotillon</i>	
23	C6AA								
	C6B		Aquitanian	Xiejian					
	C6C		23.03	Tabenbulukian			<i>Prodeinotherium</i>		
		Oligocene							

Figure 2 Asian first appearances of mammalian genera in the Tibetan Plateau and surrounding areas.

pearing genera *Heterosminthus* and *Megacricetodon*, as well as the index fossil *Plesiodipus* of the Tunggurian (Qiu, 2000, 2001a, 2001b). *Plesiodipus* has also been recorded in the

Guanjiashan Fm. of the Xining Basin. Two localities of the Dongxiang Fm. in the Linxia Basin, Galijia and Shinanu, are rich in micromammalian fossils, including 10 families, 19

genera, and 25 species of rodents (Qiu et al., 2023). *Gobicricetodon* is a first appearing genus, *G. flynni* is an index fossil, *Sayimys* is a last appearing genus, *Heterosminthus* and *Megacricetodon* are last appearing and characteristic genera, and *Democricetodon* is the characteristic genus of the Tunggurian. In the upper Tunggurian Hujialiang Fm. at Lanjiashan in the Linxia Basin, 6 species of rodent fossils belonging to 6 genera and 3 families have been found, all of which were also found at Galijia except for *Plesiodipus*. *Spermophilinus kumkolensis*, *Myomimus maritsensis*, *Dipus nanus*, and *Democricetodon lindsayi* occur at the top of the Shimagou Fm. in the Kumkol Basin, Ruoqiang County, Xinjiang Autonomous Region, where *Democricetodon* is a characteristic genus of the Tunggurian (Li et al., 2020). *Monosaulax tungurensis* and *Plesiodipus* sp. are found in the stratum of about 13.1 Ma in the Dahonggou section of the Qaidam Basin; both of these taxa are characteristic genera of the Tunggurian (Li and Wang, 2015; Wang W T et al., 2017). The Orbotu fauna is found in the Hongyazi Basin at the southern foot of the South Dange Mountains. Among them, the rodents *Democricetodon lindsayi*, *Megacricetodon sinensis*, and *Heterosminthus orientalis* are characteristic genera and species, and *Sayimys* is a last appearing genus of the Tunggurian (Li et al., 2013). On the southern edge of the Tibetan Plateau, *Myomimus* first appeared at 13.8 Ma, *Sayimys chinjiensis* at 12.3 Ma, and *Progonomys hussaini* at 11.7 Ma (Flynn et al., 2013).

The Bahean Stage is named after the Bahe River in Lantian County, Shaanxi Province, and its lower boundary stratotype is selected near the bottom of the Liushu Formation in the Guonigou section of the Linxia Basin. The Yihachi fauna found in the lower part of the Liushu Fm. is very rich in small mammals, including 23 species of rodents belonging to 21 genera and 10 families (Qiu et al., 2023): *Nannocricetus primitivus* and *Huerzelerimys* are the index fossils; *Paralactaga*, *Dipus*, *Sinocricetus*, *Pararhizomys*, *Pseudorhizomys*, *Abudhabia*, and *Prosiphneus* are first appearing genera; and *Protolactaga*, *Mycricetodon*, and *Heterosminthus* are last appearing genera; *Prosiphneus* and *Protalactaga* are characteristic genera of the Bahean. There are many small mammalian fossils in the Upper Youshashan Fm. at Shengou in the Qaidam Basin, Qinghai; this small mammalian assemblage is most similar to that found in the lower layer of the Bahe Fm. in Lantian (Qiu and Li, 2008). *Nannocricetus primitivus*, *Myocricetodon lantianensis* and *Huerzelerimys* of the Shengou fauna are index fossils; *Nannocricetus*, *Lophocricetus*, *Sinocricetus* and *Pararhizomys* are first appearing genera; *Protolactaga* is a characteristic and last appearing genus; and *Myocricetodon* is a last appearing genus of the Bahean. In the Late Miocene, *N. primitivus* was quickly replaced by *N. mongolicus*, which successfully migrated to most areas of northwestern China (Li, 2010). By the Early Pliocene, they had spread to the northern edge of the

high-altitude platform of the Tibetan Plateau (Kunlun Pass) (Li Q et al., 2014), and *N. qiui* of the Zanda Basin is another plateau representative of this genus in the Early Pliocene. *Qaidamomys fortelii* is found near the core of the Oboliang III anticline in the Qaidam Basin, representing the first occurrence of the genus in the Bahean (Li and Wang, 2014). At the southern edge of the Tibetan Plateau, *Hystrix sivalensis* first appeared at 8.1 Ma (Flynn et al., 2013).

The Baodean Stage is the earliest stage name used in the Chinese Neogene. The name originated from the “*Hipparion* red clay” containing the *Hipparion* fauna described by Zdansky (1923) in Baode County, Shanxi Province. *Prosiphneus* is a characteristic genus of the Baodean. *P. licenti* is found in the *Hipparion* red clay in the Tianshui Basin on the eastern margin of the Tibetan Plateau, and *P. tianzuensis* is found in the Tianzhu area on the northern margin; both of these species are Late Miocene (roughly equivalent to MN12 in the European MN zones) (Zheng and Li, 1982; Guo et al., 2002).

The Gaozhuangian Stage is named in the Yushe Basin, Shanxi Province. The Gaozhuang Formation contains abundant small mammalian fossils. *Mimomys bilikeensis* discovered in the Gaozhuangian Tuolin Fm. of the Pliocene in the Zanda Basin, southwestern Xizang Autonomous Region, with an age of about 4.4 Ma, represents a first appearing and characteristic genus of the Gaozhuangian, and is also found in the Qiangtang Fm. of the Kunlun Pass Basin and the Shizigou Fm. of the Qaidam Basin in Qinghai. *Nannocricetus qiui* in the Zanda Basin is a last appearing genus of the Gaozhuangian, and shows that *Nannocricetus* migrated from its origin center, the Mongolian Plateau or northern China, to the hinterland of the high-altitude Tibetan Plateau in the Early Pliocene. *N. mongolicus* is also found in the Kunlun Pass Basin (Li Q et al., 2014). *N. qiui* of the Zanda Basin is slightly larger than *N. mongolicus* of the Kunlun Pass Basin (Li, 2010) and obviously larger than *N. primitivus* from Shengou in the Qaidam Basin (Qiu and Li, 2008). Another hamster in the Zanda Basin, *Aepyocricetus liuae*, represents the first appearance of this genus in the Gaozhuangian (Li Q et al., 2017).

The Mazegouan Stage is also named in the Yushe Basin, which is also rich in small mammal fossils. Rodent fossils of 3 families and 5 genera were found in the Hewangjia Formation of the Linxia Basin, including *Kowalskia*, *Mimomys*, *Mesosiphneus*, *Eospalax*, and *Allosiphneus*. Among them, *Kowalskia* and *Mesosiphneus* are last appearing genera, and *Mimomys* and *Mesosiphneus* are characteristic genera of the Mazegouan (Qiu et al., 2023). *Mimomys* cf. *hengduan-shanensis* was found in the Wangbuding Fm. in Dege County, eastern Tibetan Plateau (Zong et al., 1996).

### 3.2 Carnivora

In the early Neogene, carnivores were not yet prosperous,

and remnants of the primitive creodonts still occupied the position of predators in the fauna. For example, *Hyaenodon* in the Zhangjiaping fauna of the Lanzhou Basin is a last appearing genus of the Xiejian.

The primitive *Kinometaxia guangpui* occurs in the Tiejiaogou Formation in the Danghe area, Gansu Province. This genus is the earliest member of the subfamily Lepartarctinae, family Mustelidae, in the world (Wang X M et al., 2004), and is also an index fossil of the Shanwangian (Qiu et al., 2013). The Shinanu fauna of the Dongxiang Fm. in the Linxia Basin contains *Pseudoelurus guangheensis*, which is similar to *P. turnauensis* (MN3-9) and *P. lorteti* (MN4b-9); *Pseudoelurus* is a first appearing genus of the Shanwangian (Qiu et al., 2013). However, a recent study on small mammalian fossils of the same fauna suggests that *P. guangheensis* belongs to the Tunggurian (Qiu et al., 2023).

There are abundant carnivoran fossils in the Hujialiang Formation of the Linxia Basin. The index genera of the Tunggurian are *Percrocuta* and *Gobicyon*, which exist as *P. tungurensis* and as *G. macrognathus* and *G. acutus*, respectively (Jiangzuo et al., 2019). *Amphicyon zhanxiangi* and *Hemicyon* sp. represent the last occurrences of their respective genera (Sun et al., 2022).

*Ictitherium*, *Adcrocuta eximia*, *Plesiogulo*, *Eomellivora*, and *Promephitis parvus* occur in the Bahean layers of the Upper Youshashan Formation in the Qaidam Basin, and are the first appearing genera of the Bahean. *Promephitis* is also a characteristic genus of the Bahean. *Dinocrocuta xizangensis* (Zheng, 1980), a giant hyena, occurs in the Bulong Basin, Biru County, northern Xizang Autonomous Region. *Dinocrocuta* is an index genus of the Bahean, and *D. gigantea* is also a typical fossil in the Bahean strata of the Linxia Basin (Qiu et al., 1988). *Machairodus aphanistus*, *Adcrocuta eximia*, *Hyaenictitherium hyaenoides*, *H. wongii*, *Ictitherium viverrinum*, *Yoshi* sp., *Agriotherium inexpectans*, *Indarctos* sp., *Plesiogulo* cf. *crass*, *Pekania* sp., *Martes* sp., *Parataxidea sinensis*, and *Simocyon* aff. *batalleri* represent the first appearances of their respective genera (Qiu et al., 1991; Deng et al., 2013b; Li C X et al., 2021; Jiangzuo et al., 2023). *Indarctos* is also a characteristic genus of the Late Miocene. *Promephitis*, a first appearing and characteristic genus of the Bahean, is represented by two species in the Linxia Basin, *P. parvus*, and *P. hootoni* (Wang and Qiu, 2004).

A hyena fossil found in the Woma Formation of the Gyirong Basin (Ji et al., 1980) may be ascribed to *Adcrocuta*, which is a last appearing and characteristic genus of the Baodean (Qiu et al., 2013). *Indarctos zdanskyi*, *Eomellivora wimani*, and *Adcrocuta eximia* at the top of the Liushu Fm. in the Linxia Basin record the last occurrences of their respective genera. *Ursavus sylvestris* of the Shihuiba Fm. in the Lufeng Basin also represents the last occurrence of its genus (Qiu et al., 2014).

*Nyctereutes* is a first appearing and characteristic genus,

and *Chasmaporthetes* and *Pliocrocuta* are first appearing genera of the Gaozhuangian. They exist in the Tuolin Formation of the Zanda Basin as *Nyctereutes* cf. *tingi*, *Chasmaporthetes gangsriensis* and *Pliocrocuta perrieri*. *Chasmaporthetes* also first appeared in the Kunlun Pass Basin in Qinghai Province and the Linxia Basin in Gansu Province. *Hyaenictitherium wongii* of the Hewangjia Fm. in the Linxia Basin recorded the last occurrence of its genus in the Gaozhuangian (Deng et al., 2011a).

The first appearing *Pliocrocuta perrieri* and *Lynx* of the Mazegouan were found in a mudstone lens of the Late Pliocene Jishi Formation in the Linxia Basin (Jiangzuo et al., 2023), and the evolutionary level of the Linxia *Pliocrocuta* is similar to that of the Mazegouan in the Yushe Basin. *Meles chiai*, *Homotherium hengduanshanensis*, *Lynx shansius* and *Sivapanthera* sp. are found in the Wangbuding Fm. in Dege County, western Sichuan, and *Meles*, *Homotherium*, *Lynx* and *Sivapanthera* are the first appearing genera of the Mazegouan.

### 3.3 Proboscidea

The appearance of the Proboscidea in Eurasia is a sign of the beginning of the Neogene. Proboscidean incisor fragments were found in the Xiejian Huangyangtou Fm. in the Lanzhou Basin (Qiu, 1990; Qiu and Qiu, 1995). At the southern margin of the Tibetan Plateau, *Prodeinotherium* first appeared at the lower boundary of the Miocene in the Siwaliks.

*Platybelodon dangheensis* is found in the lower part of the Tiejiaogou Formation in the Danghe area, Gansu Province (Wang and Qiu, 2002). It is the earliest known shovel-tusked elephant in China and an index fossil of the Shanwangian (Qiu et al., 2013).

The Tunggurian strata have the most abundant proboscidean fossils. A large number of *Platybelodon* fossils, a characteristic genus of the Tunggurian, have been found in the Hujialiang Fm. in the Linxia Basin, Gansu Province (Qiu et al., 2013). *Gomphotherium* is a last appearing genus of the Tunggurian, which occurs in the Hujialiang Fm. as *Gomphotherium tassyi* (Wang S Q et al., 2017b). The Guanjiashan Fm. in the Xining Basin contains *Gnathabelodon connectus* and *Protanancus? wimani*. *Stegolophodon latidens* is found in the Xiaolongtan Fm. in Yunnan Province.

*Prodeinotherium sinensis* is found in the lower part of the Liushu Formation in the Linxia Basin; that is, in the Bahean strata (Qiu et al., 2007). Although *Prodeinotherium* appeared earlier in the Siwaliks, it is a first appearing genus of the Bahean in East Asia. The Bahean index fossil *Tetralophodon* is found in the lower part of the Liushu Fm., as well as in the Upper Youshashan Fm. of the Qaidam Basin.

*Mammut* cf. *obliquelophus* found in the upper part of the Liushu Formation in the Linxia Basin represents a first appearing genus of the Baodean (Wang S Q et al., 2017a), and *Mammut* also exists in the Baodean Shihuiba and Zhaotong



formations in Yunnan Province (Wang et al., 2016). In the Zhaotong Fm., the Baodean first appearing genus *Sinomas-todon* is represented by *Si. praeintermedius*, and *Stegodon* by *St. zhaotongensis* (Wang et al., 2016, 2019).

Following its appearance in the Baodean, *Stegodon* greatly developed in the Pliocene, becoming a characteristic genus of the Gaozhuangian. *Stegodon yuanmouensis*, *St. elephantoides* and *St. zhaotongensis* are present in the Shagou Formation in Yuanmou County, Yunnan Province (Qian et al., 1991).

At the southern margin of the Tibetan Plateau, *Elephas planifrons* first appeared at 3.5 Ma, which is equivalent to the Mazagouan (Flynn et al., 2013).

### 3.4 Perissodactyla

The Xiejia fauna in the Xining Basin and the Zhangjiaping fauna in the Lanzhou Basin contain *Turpanotherium elegans*, the last giant rhino to survive after the Oligocene prosperity of this group. *Turpanotherium* is also a last appearing genus of the Xiejian. *Aprotodon lanzhouensis* and *Phyllotillon huangheensis* in the Zhangjiaping fauna are index fossils, and *Aprotodon* is a characteristic genus of the Xiejian.

*Plesiaceratherium* sp. was found in the upper part of the Dingqing Fm. of the Lunpola Basin in the central Tibetan Plateau (Deng et al., 2012), and represents the first appearing fossil and characteristic genus of the Shanwangian. *Aprotodon lanzhouensis* occurs in the Sigou fauna of the Shangzhuang Fm. in the Linxia Basin. Deng et al. (2013b) suggested that this species belongs to the Shanwangian, and the accompanying small mammal fossils further confirm this attribution (Qiu et al., 2023), representing the last appearance of *Aprotodon*.

The Shinanu fauna of the Dongxiang Fm. in the Linxia Basin contains *Anchitherium* sp. and *Hispanotherium matritense* (Deng et al., 2004), and the overlying Hujialiang Fm. contains *Anchitherium gobiense* and *H. matritense* (Deng, 2003; Sun and Deng, 2021). *Hispanotherium* is an index fossil, and *Anchitherium* is a characteristic genus of the Tunggurian (Qiu et al., 2013). *H. matritense* is also found in the Lower Youshashan Fm. in the Qaidam Basin (Deng and Wang, 2004a).

*Hipparion*, *Sinotherium*, and *Tapirus* are first appearing genera, *Diceros*, *Parelasmotherium*, and *Iranotherium* are index fossils, *Chalicotherium* is a last appearing genus, and *Chilotherium* and *Acerorhinus* are characteristic genera of the Bahean (Qiu et al., 2013). On the Tibetan Plateau, the Late Miocene Liushu Fm. in the Linxia Basin is rich in perissodactyl fossils, including the important Bahean genera *Hipparion dongxiangense*, *H. weihoense*, *H. dermatorhinum*, *Sinotherium lagrelli*, *Tapirus hezhengensis*, *Diceros gansuensis*, *Parelasmotherium simplum*, *P. linxiaense*, *Iranotherium morgani*, *Chilotherium primigenius*, *C. wimani*,

and *Acerorhinus hezhengensis*. The lower part of the Upper Youshashan Fm. in the Qaidam Basin contains *Hipparion weihoense*, *H. teilhardi*, *Chalicotherium brevirostris*, and *Acerorhinus tsaidamensis* (Deng and Wang, 2004b). *H. chiai* (= *H. weihoense*) was collected from the Jidike Fm. in the Kuqa area of the northern Tarim Basin (Sun et al., 2009). *Hipparion xizangense* occurs in the Bulong Basin. At the southern margin of the Tibetan Plateau, *Hipparion (Hippotherium)* first appeared at 10.8 Ma (Flynn et al., 2013).

*Shansirhinus* and *Dihoplus* are first appearing genera, *Sinohippus* is a last appearing genus, *Ancylotherium* is an index fossil, and *Chilotherium* and the medium-sized *Hipparion* are characteristic genera of the Baodean. Common occurrence of the first and last appearing genera is a reliable method to determine the age of a deposit. At the top of the Liushu Fm. in the Linxia Basin, *Shansirhinus ringstroemi*, *Dihoplus ringstroemi* and *Sinohippus robustus* occur together, along with the medium-sized *Hipparion forstenae* and *H. hippidiodus*, as well as *Ancylotherium* and *Chilotherium anderssoni*. *Hipparion forstenae* and *Chilotherium xizangense* occur in the Woma Fm. of the Gyirong Basin. *Dihoplus ringstroemi* is present in the upper part of the Upper Youshashan Fm. in the Qaidam Basin.

The Tuolin Formation in the Zanda Basin bears *Coelodonta thibetana* and *Hipparion (Plesiohipparion) zandaensis*, whereas *Coelodonta* and *Hipparion (Plesiohipparion)* are a first appearing genus and subgenus of the Gaozhuangian. The Hewangjia Fm. in the Linxia Basin contains *Shansirhinus ringstroemi*, *Hipparion (Hipparion) hippidiodus*, *H. (H.) platyodus*, *Hipparion (Cremohipparion) licenti*, and *Proboscidipparion pater*, whereas *Proboscidipparion* is a first appearing genus, *Hipparion (Hipparion)* is a last appearing subgenus, and *Shansirhinus*, *Hipparion (Cremohipparion)* and *Proboscidipparion pater* are characteristic genera and species of the Gaozhuangian. *P. pater* also occurs in the Qiangtang Fm. of the Kunlun Pass Basin (Li Q et al., 2014).

### 3.5 Artiodactyla

In the Xiejia Fm. of the Xining Basin, *Sinopalaeceros xiejiaensis*, a representative bovid of the Early Miocene, is found (Li and Qiu, 1980). *Turcocerus* sp. occurs in the Shangzhuang Fm. of the Linxia Basin (Deng et al., 2013b), and *Turcocerus halamagaiensis* and *Amphimoschus xishuiensis* occurs in the lower part of the Tiejianggou Fm. in the Danghe area (Li Y et al., 2022), representing the first appearing and characteristic genera of the Shanwangian respectively. On the southern edge of the Tibetan Plateau, *Listriodon guptai* first appeared at 19.1 Ma (Flynn et al., 2013).

*Kubanochoerus minheensis* and *Stephanocemas chinghaiensis* are distributed in the Guanjiashan Formation of the

Xining Basin. *Listriodon mongoliensis*, *Kubanochoerus gigas*, *Stephanocemas guangheensis*, *Palaeotragus tungurensis* and *Turcocerus* sp. occur in the Dongxiang and Hujialiang formations of the Linxia Basin. *Kubanochoerus* and *Listriodon* are index fossils, *Palaeotragus* is a first appearing genus, and *Stephanocemas* and *Turcocerus* are characteristic genera of the Tunggurian. In the Siwaliks on the southern edge of the Tibetan Plateau, *Listriodon pentapotamiae* first appeared at 14.1 Ma (Flynn et al., 2013).

The Upper Youshashan Formation is rich in artiodactyls, including *Euprox*, a last appearing genus of the Bahean. Artiodactyls are more abundant in the Liushu Fm., including many fossils with important biostratigraphic significance, such as *Chleuastochoerus linxiaensis*, *C. stehlini*, *Euprox grandis*, *Cervavitus novorossiae*, *Schansitherium tafeli*, *Honanotherium schlosseri*, *Hezhengia bohlini*, *Shaanxipira linxiaensis*, *Miotragocerus* sp., *Sinotragus* sp. and *Gazella paotehensis* in the middle and lower parts of this formation (Deng et al., 2013b; Shi et al., 2014; Hou and Deng, 2014; Li, 2015; Hou et al., 2019). *Shaanxipira*, *Hezhengia* and *Miotragocerus* are index fossils; *Chleuastochoerus*, *Schansitherium*, *Honanotherium*, *Cervavitus*, *Sinotragus* and *Gazella* are first appearing genera of the Bahean. At the southern edge of the Tibetan Plateau, *Selenoportax* first appeared at 10.5 Ma, and *Giraffa punjabiensis* first appeared at 9.1 Ma (Flynn et al., 2013).

The top of the Liushu Fm. contains *Eostyloceros hezhengensis*, *Eucladoceros* cf. *proboulei*, and *Palaeotragus* cf. *coelophrys* (Li Y et al., 2017). The Woma Fm. contains *Palaeotragus microdon* (Ji et al., 1980), which is a typical representative of the Baode fauna (Qiu and Qiu, 1995). At the southern edge of the Tibetan Plateau, the hippopotamus *Hexaprotodon sivalensis* first appeared at 6.2 Ma (Flynn et al., 2013).

*Antilospira* of the Tuolin Formation in the Zanda Basin is a first appearing genus of the Gaozhuangian (Wang X M et al., 2013b). *Cervavitus novorossiae* and *Gazella blacki* of the Hewangjia Fm. in the Linxia Basin are also found in the Gaozhuang Fm. of the Yushe Basin. *Ovis* cf. *shantongensis*? was found in the Wangbuding Fm. in Dege County, western Sichuan (Zong et al., 1996), whereas *Ovis* is the first appearing genus of the Mazegouan (Qiu et al., 2013).

#### 4. Magnetostratigraphy

In the International Chronostratigraphic Chart, the Neogene is divided into eight stages. Aside from the Burdigalian and Langhian stages, the Global Boundary Stratotype Sections and Points (GSSPs, 'golden spikes') of the remaining six stages have been ratified, and their lower boundary ages are all calibrated according to the results of paleomagnetic dating. Because of the scarcity of material for isotopic dating,

paleomagnetism is the most widely used time scale in the study of the Neogene in China. Detailed magnetostratigraphic work has been carried out on many representative sections of the terrestrial Neogene, including many Cenozoic basins of the Tibetan Plateau. In particular, the stratotype sections of the Xiejian and Bahean stages were selected in the Xining and Linxia basins of the Tibetan Plateau, respectively. Both stages have accurate lower boundary positions determined by their magnetostratigraphic ages and can be compared with international stratotypes and other sections (Fang et al., 2016; Deng et al., 2019a).

The golden spike of the Aquitanian Stage is located at Lemme-Carrosio in Alexandria Province, Italy. It is located in a set of bathyal-facies sediments. The GSSP is 35 m from the top of the section. It is marked by the bottom of C6Cn.2n and the Mi-1 oxygen isotope event associated with this geomagnetic polarity age, with an age of 23.03 Ma (Steininger et al., 1997). The Xiejian Stage of terrestrial deposits in China completely corresponds to the Aquitanian, with a consistent definition of the lower boundary. At Xiejia in Huangzhong County in the Xining Basin, for which the Xiejian Stage is named, C6Cn.2n is not clearly identifiable. This boundary may be located within the continuous deposits of massive brownish-red mudstone in the lower part of the Xiejia Fm., 14 m from the bottom of this formation (Deng et al., 2019a). In the Linxia Basin, Gansu Province, the paleomagnetic marker of C6Cn.2n at the lower boundary of the Xiejian is located at the bottom of the Shangzhuang Fm. in the Maogou and Yagou sections of Dongxiang County (Sun L et al., 2023; Zheng et al., 2023).

The GSSP of the Burdigalian Stage has not yet been determined. In the currently recommended definition of its lower boundary, the lowest distribution layer close to the planktonic foraminifer *Globalerinaoides altiperturus* has been widely recognized. The boundary is close to the top of paleomagnetic zone C6An.2n, with an age of 20.44 Ma (Hilgen et al., 2012). The Shanwangian Stage in China roughly corresponds to the Burdigalian. Its lower boundary is defined by the first appearance of *Anchitherium* as a biostratigraphic marker, and the paleomagnetic age is also C6An.2n. In the Yagou section of the Linxia Basin, Gansu Province, C6An.2n is located in the upper part of the Shangzhuang Formation (Sun L et al., 2023).

The lower boundary of the Tunggurian Stage in China is not the same as that of the international marine stage, but is correlated to that of the terrestrial Astaracian Stage in Europe (Steininger, 1999). This lower boundary is marked by the first appearance of the lagomorph *Alloptox gobiensis* and the shovel-tusked elephant *Platybelodon grangeri*. Paleomagnetically, it is located at the bottom of C5Bn.1r, with an age of 15 Ma. In the Linxia Basin, this boundary is precisely presented at Mansancun, Niujiacun and Maogou, and is located in the middle of the Dongxiang Fm. (Sun L et al., 2023;

Zheng et al., 2023). In the Huaitoutala section of the Qaidam Basin, this boundary is at the bottom of the Upper Youshashan Fm. (Fang et al., 2007). In the Kumkol Basin, C5Bn.1r is located in the middle of the Shimagou Fm. (Lu et al., 2016).

The GSSP of the Tortonian Stage is located in the Monte dei Corvi beach section near Ancona, Italy, and the boundary is located at the midpoint of the 76th sapropel layer of this section. It is marked by the last common occurrence of the calcareous nannofossil *Discoaster kugleri* and the planktonic foraminifer *Globigerinoides subwadratus*, which corresponds to the bottom of paleomagnetic chron C5r.2n, with an age of 11.63 Ma (Hilgen et al., 2005, 2012). The Bahean Stage corresponds to the Tortonian, and their common lower boundary is defined as the bottom of paleomagnetic chron C5r.2n. The Guonigou section in the Linxia Basin is the most favorable candidate section for the lower boundary stratotype of the Bahean, which is marked by the first appearance of the three-toed horse *Hipparion* (Deng et al., 2015a). C5r.2n is located at the bottom of the Liushu Fm. (Fang et al., 2016), which is consistent with the location of the earliest three-toed horse *Hipparion dongxiangense* in Eurasia. This paleomagnetic boundary is located in the lower part of the Shibiliang Fm. in the Kumkol Basin (Lu et al., 2016), and in the middle of the Upper Youshashan Fm. in the Huaitoutala section of the Qaidam Basin (Fang et al., 2007).

The GSSP of the Messinian Stage is located in the Oued Akrech section in Morocco; the boundary is located at the bottom of the red layer of the 15th carbonate cycle. The biostratigraphic indicators are the first normal occurrence surface of the planktonic foraminifer *Globotalia miotumida* and the first occurrence datum of the calcareous nannofossil *Amaurolithus delicatus*, which correspond to paleomagnetic chron C3Br.1r at 7.246 Ma (Hilgen et al., 2000). The Baodean Stage corresponds to the Messinian, with C3Br.1r as its lower boundary. The first appearance of *Hipparion forstenae* can be used as the biostratigraphic marker of this boundary (Deng et al., 2019a). The boundary is located at the bottom of the Woma Formation in the Gyirong Basin (Yue et al., 2004a) and in the upper part of the Liushu Fm. in the Heilinding section of the Linxia Basin (Fang et al., 2016).

The GSSP of the Zanclean Stage is located in the Eraclea Minoa section on the southern coast of Sicily, Italy. The lower boundary is at the bottom of the Trubi Formation, close to the extinction surface of the calcareous nannofossil *Triquetrorhabdulus rugosus* (bottom of CN10b), and the lowest distribution layer of *Ceratolithus acutus*, located at the top of chron C3r, about 96 ka before the Thvera normal subchron (C3n.4n), with an age of 5.333 Ma (van Couvering et al., 2000). The Gaozhuangian Stage corresponds to the Zanclean, with the top of C3r as its lower boundary. The first appearance of the three-toed horse *Proboscoidipparion pater* is its biostratigraphic marker (Deng et al., 2019a). This pa-

leomagnetic boundary is clearly shown in the Duikang section of the Linxia Basin, accompanied by the first appearance of *P. pater* at the bottom of the Hewangjia Fm. (Zhang et al., 2019), at the lower part of the Shizigou Fm. (Fang et al., 2007) in the Huaitoutala section of the Qaidam Basin, in the middle part of the Woma Fm. in the Gyirong Basin (Yue et al., 2004a), and in the lower part of the Tuolin Fm. in the Zanda Basin (Wang et al., 2013b).

The GSSP of the Piacenzian is located in the Punta Piccola section of Sicily, Italy. The boundary is at the bottom of the beige marl of the 77th small-scale carbonate cycle (precession MPRS 347), which is equivalent to the extinction surface of the planktonic foraminifer *Globorotalia margaritae* (bottom of the PL3 zone) and *Pulleninatina primalis*, as well as the bottom of the C2An (Gauss) paleomagnetic polarity zone at 3.6 Ma (Castradori et al., 1998). The Mazegouan Stage corresponds to the Piacenzian, and also takes the bottom of C2An as the boundary. C2An is located at the top of the Woma Fm. in the Gyirong Basin (Yue et al., 2004a), at the bottom of the Guge Fm. in the Zanda Basin (Wang et al., 2013b), and in the upper part of the lower Qiangtang Fm. in the Kunlun Pass Basin (Li Q et al., 2014).

## 5. Geochronology

As mentioned above, the lower boundary stratotypes of various stages of the Neogene around the world are demarcated by paleomagnetism, and there are no direct isotopic age data. There is little material for isotopic dating of the terrestrial Neogene in China, and only the Shanwang section in Linqu, Shandong can be used for high-precision dating at the stratotype section (He et al., 2011). However, with the improvement and application of technology, the Cenozoic strata dating of the Tibetan Plateau has yielded abundant data, which are of great help for the division and correlation of the Neogene strata. The age data of the Xiejian Stage have led to a significant breakthrough in the Lunpola Basin in northern Xizang Autonomous Region. He et al. (2012) used SIMS U-Pb zircon dating to precisely date the bentonite at the lower/middle boundary of the Dingqing Fm. Analysis of 26 samples produced a highly reliable U-Pb age of  $23.5 \pm 0.2$  Ma ( $2\sigma$ , MSWD=1.1), located near the Oligocene/Miocene boundary (23.03 Ma), which demonstrates that the Dingqing Fm. includes parts of both the Oligocene and Miocene, which is consistent with the evidence obtained from mammalian fossils (Deng et al., 2012). In the lower part of the Dingqing Fm. in the Lunbori section, there are a thin brown layer of silty mudstone and a thin layer of tuffaceous sandstone. The volcanic ash age is 20.6–20.7 Ma (Mao et al., 2019), close to the lower boundary age of the Shanwangian Stage (20.44 Ma).

Diorite  $^{40}\text{Ar}$ - $^{39}\text{Ar}$  dating of the volcanic ash deposits in the

upper and middle parts of the Mangxiang Fm. in the Oiyug Basin yielded an age of  $15.10 \pm 0.49$  Ma, and the phlogopite dating result extracted from the overlying potassic lava sequence was  $15.03 \pm 0.11$  Ma (Spicer et al., 2003), similar to the lower boundary age of the Tungurian Stage.

At the Bhilomar site in the Siwalik area on the southern margin of the Tibetan Plateau, the Nagri Formation contains bentonites. The fission track age of the zircon phenocrysts is  $9.46 \pm 0.59$  Ma (Johnson et al., 1982), which is consistent with the age of the Bahean Stage of the Late Miocene indicated by mammalian fossils.

The late Cenozoic strata of the Zanda Basin have a thickness of 800 m, and were first called the Zhada Formation (Zhang et al., 1981). Later, these strata were renamed as the Zhada Group, including the Pliocene Tuolin Fm. and the Pleistocene Xiangzi Fm. (Qian, 1990). Zhu et al. (2008) limited the Tuolin Fm. to the Lower Pliocene and named the Upper Pliocene strata the Guge Fm. ESR dating at the bottom of the Xiangzi Fm. yielded an age of  $2.58 \pm 0.22$  Ma (Zhang et al., 2015b), representing the Neogene/Quaternary boundary.

## 6. Correlations of Neogene strata of the Tibetan Plateau

At the beginning of the Cenozoic, the Tibetan Plateau completed the conversion of the Tethys between ocean and continent as well as terrane amalgamation, becoming a unified landmass and entering a stage of intracontinental evolution. According to the tectonic evolution background and formation mechanism, tectonic geomorphic landscape, sedimentary filling sequence and sedimentary environment evolution process, the Cenozoic basins of the Tibetan Plateau and its adjacent areas are divided into five stratigraphic regions, the South Xinjiang-West Kunlun Region, the Qaidam-Qilian-West Qinling Region, the Qiangtang Region, the West Yunnan-West Sichuan Region, and the Gangdise-Himalaya-Siwalik Region, and can be further subdivided into stratigraphic subregions (Zhang et al., 2010). The boundaries of these stratigraphic regions are related to a series of large mountains with roughly east-west strike controlled by thrust faults. From south to north, they include the Himalayan, Gangdise, Tanggula, Kunlun, Altyn, and Qilian mountains. In the east of the Tibetan Plateau, they turn to strike roughly north-south. These boundaries do not apply to the sutures that divide the main blocks of the Tibetan Plateau (Tapponnier et al., 2001), because these sutures formed quite early. The youngest of these sutures, the Yarlung Zangbo suture, also formed in the early Cenozoic, and Cenozoic basins often developed in the valleys where the sutures pass; that is, a series of Cenozoic basins cross two blocks, such as the Bangong-Nujiang suture (Figures 3 and 4).

## 6.1 South Xinjiang-West Kunlun stratigraphic region

### 6.1.1 Tarim Basin

The Tarim Basin is a tectonic flexure and compression basin under a compressional background. The Paleogene, under the Neogene, mainly comprises shore and shallow-sea deposits formed in a semi-closed bay of the Neotethys Ocean, which transformed beginning in the Late Oligocene into a continental lake basin. There is a parallel unconformity or micro-angled unconformity between the Paleogene and Neogene deposits. The Neogene strata in the Tarim Basin from old to new are the Keziluo, Anju'an, Pakabrak and Artux formations, all of which are in conformable contact. Dating of this set of strata is mainly based on ostracods and a small number of foraminifera as age markers. The Keziluo Fm. belongs to the Xiejian and Shanwangian, and is composed of fine clastic rock that is mostly red with a small amount of grayish-green material. A thin layer of gypsum is present in the upper part. These deposits formed in saline shore and shallow lake environments of the offshore plain. The Anju'an Fm. belongs to the Tungurian and comprises variegated shore- and shallow-lake-facies fine clastic rocks. The Pakabrak Fm. belongs to the Bahean-Gaozhuanian, and is mainly interbedded with gray conglomerate and grayish red fine sandstone. The Artux Fm. belongs to the Maze-gouan, and is interbedded with gray conglomerate and light red fine sandstone, which formed in piedmont river-delta-brackish waterfront shallow lake depositional environments. The paleomagnetic age of the Neogene continental clastic rock strata in the Kuqa area at the northern margin of the Tarim Basin is 13.3–2.6 Ma, and these strata are overlain by the Quaternary Xiyu Conglomerate. From bottom to top, the Neogene strata are the Middle-Upper Miocene Jidike Fm., in which the three-toed horse *Hipparion chiai* (= *H. weihoense*) occurs, the Upper Miocene Kangcun Fm. and the Pliocene Kuqa Fm. (Sun et al., 2009). In the hinterland of the Tarim Basin, there is a nearly east-west-trending monoclinical mountain called Mazartag, which is the area with the best exposure of late Cenozoic strata in the basin. The terrestrial strata of the Mazartag section are 1100 m thick, and the paleomagnetic results show that deposition began at 9.7 Ma. The Upper Miocene consists of purplish-red lacustrine mudstone and fluvial fine sandstone, which are parallel to and unconformable with the underlying marine strata. The upper part deposited after 6 Ma is mainly Pliocene strata, which are composed of grayish-yellow eolian dust deposits mixed with pale yellow fluvial sandstone. Near the bottom, the Gaozhuanian subgenus *Hipparion* (*Plesiohipparion*) has been found (Sun et al., 2017).

### 6.1.2 West Kunlun-Karakoram mountains

Intermountain depression and fault basins formed with the rapid uplift of mountains developed in this area, and the

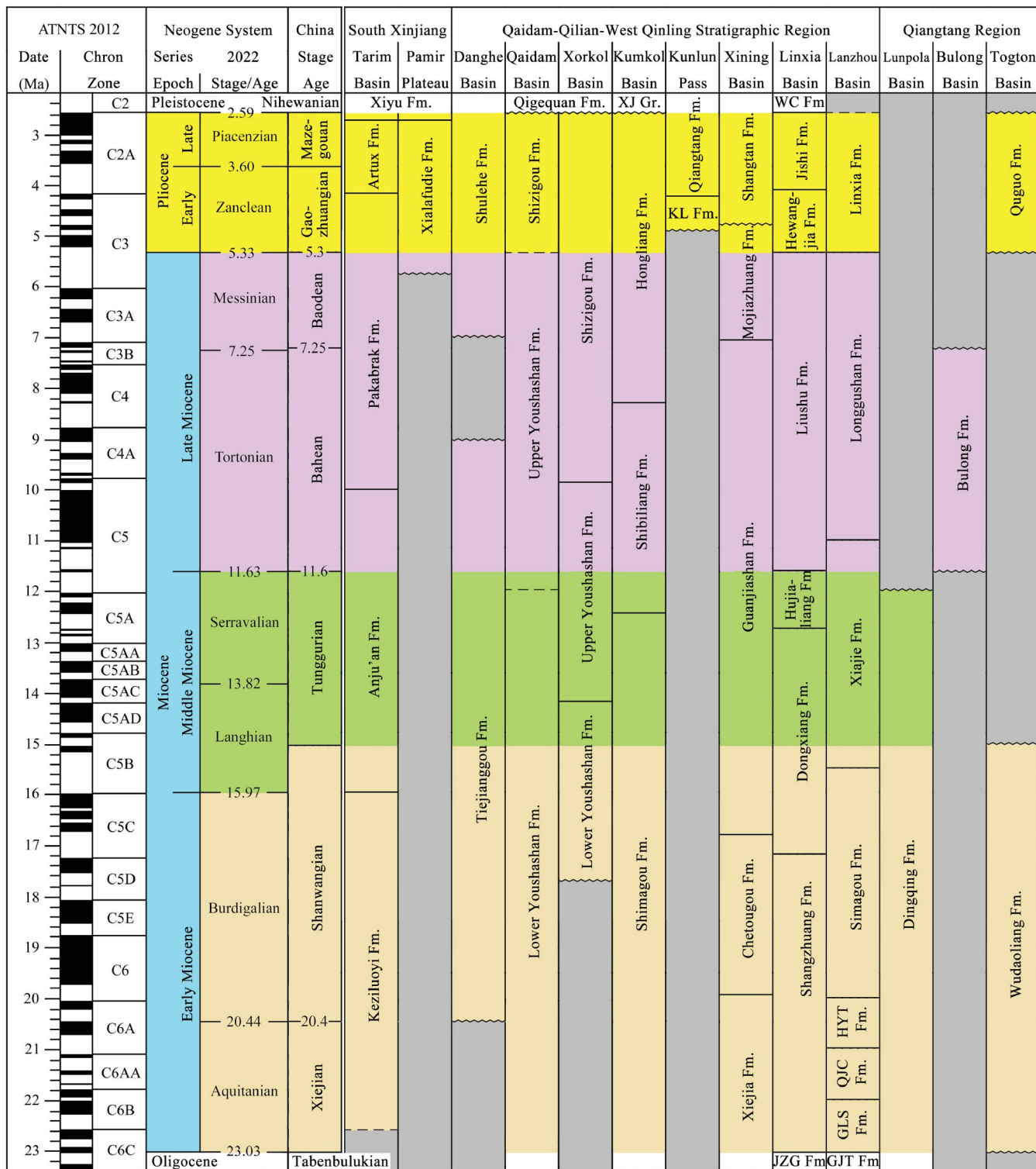


**Figure 3** Stratigraphic correlation of Neogene basins in the northern Tibetan Plateau. Abbreviations: Fm., Formation; GJT, Ganjiantan; GLS, Gaolanshan; Gr., Group; HYT, Huangyangtuo; JZG, Jiaozigou; KL, Kunlun; QJC, Qujiachuan; WC, Wucheng; XJ, Xinjiang.

Waqia area of Tashkurgan County in the Pamir Plateau can be regarded as a typical representative. The Xialafudie Fm. here is a set of fluvial and lacustrine brownish-yellow, grayish-green medium- or thin-layered silty mudstone and argillaceous siltstone deposits, unconformably overlying

Triassic deposits and overlain by the Xiyu Conglomerate. Its age was originally determined as Tertiary (Yang, 1998) and later revised to Lower Cretaceous (Yang et al., 2005). Liu et al. (2021) evaluated the geological age and paleoenvironment of the Xialafudie Fm. based on analysis of animal, plant

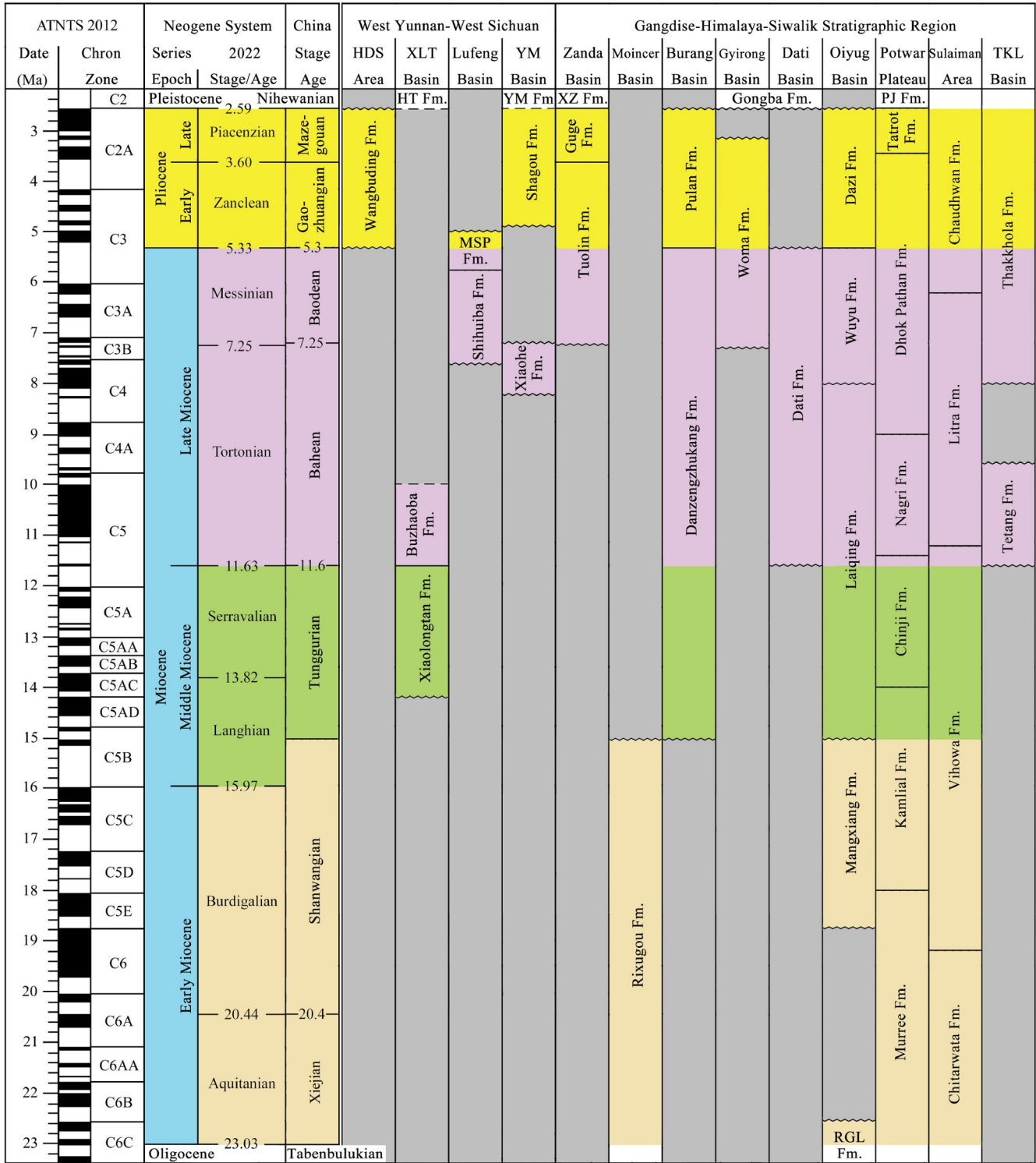


**Figure 4** Stratigraphic correlation of Neogene basins in the southern Tibetan Plateau. Abbreviations: Fm, Formation; HDS, Hengduanshan; HT, Hetou; MSP, Miaoshanpo; PJ, Pinjor; RGL, Rigongla; TKL, Thakkhola; XLT, Xiaolongtan; XZ, Xiangzi; YM, Yuanmou.

and sporopollen fossils. The plant fossils found in the Xiaolafudie Fm. are mainly *Salix*, *Potentilla*, *Poaceae*, *Caragana*, etc. Phylogenetic analysis of *Caragana* indicates that it first appeared on the Tibetan Plateau during the Middle Miocene and underwent accelerated differentiation in the late Late

Miocene. The fish fossils belong to the family Nemacheilidae, order Cypriniformes, and may be attributed to the genus *Triplophysa*. These fossils are found in the Gaozhuangian layers of the Qiangtang Formation in the Kunlun Pass Basin (Wang and Chang, 2012). Based on comprehensive evalua-

tion, the age of Xialafudie Fm. is judged to be Pliocene (Liu et al., 2021).

## 6.2 Qaidam-Qilian-West Qinling stratigraphic region

### 6.2.1 Qilian Mountains

A series of basins in the Qilian Mountains and their northern foothills, including the Danghe, Jiuquan-Zhangye, Ulanbulak, Har Lake, Suli and Wuwei basins from west to east, are jointly controlled by the Altyn Tagh, East Kunlun, and West Qinling tectonic belts (Yang et al., 2017). The Yindirte fauna discovered in the Tabenbuluk area of the Danghe Basin in western Gansu Province is the basis for the establishment of the Upper Oligocene Tabenbulukian Stage. This area has been a key site for the study of the Altyn Tagh strike-slip fault in recent decades. One reason is that this area has the only clear sequence controlled by mammalian ages in several piedmont basins on the northern edge of the Tibetan Plateau. There are at least three sets of sedimentary sequences in the Danghe Basin: the Late Eocene-Oligocene Paoniuan Formation, the Early-Late Miocene Tiejiaogou Fm. and the Late Miocene-Pliocene Shulehe Fm. A series of thrust faults cut off the bottom of each formation, and mammalian fossils have been found in each set of strata. The Xishuigou fauna in the lower part of the Tiejiaogou Fm. includes *Platybelodon dangheensis*, *Turcocerus halamagaiensis*, *Amphimoschus xishuiensis*, *Kinometaxia guangpui*, “*Kansupithecus*” and *Heterosminthus intermedius* (Wang X M et al., 2008, 2013a; Li Y K et al., 2022). Gilder et al. (2001) and Yin et al. (2002) established two independent paleomagnetic sections at Xishuigou, but both research groups incorrectly interpreted the paleomagnetic age because they were not familiar with the fossil localities of Bohlin (they included the Yindirte fauna in the Xishuigou section, resulting in downward extension of the entire section). After reinterpretation of the paleomagnetic age by Wang X M et al. (2013a), the age of the Xishuigou fauna is interpreted to be about 20–17 Ma; that is, Shanwangian. *Sayimys obliquidens*, *Litodonomys xishuiensis*, *Phyllotillon* sp., Cervidae indet. and Proboscidea indet. have been found in the middle part of the Tiejiaogou Fm. Comparison of these fossils with the Tiejiaogou paleomagnetic section of Sun et al. (2005) indicates that the age of this fauna is likely about 15.5–12 Ma. Fossils found in the Shulehe Fm. in the upper part of the Xishuigou section, such as *?Gazella*, *?Tragoreas* and Proboscidea indet., are relatively fragmentary. Their age may be between Late Miocene and Pliocene (Wang X M et al., 2003, 2008, 2013a; Wang B Y et al., 2003). The Hongyazi Basin developed between the South Danghe and Chahan'ebotu mountains has four sets of sedimentary sequences, which are, from early to late, unnamed Oligocene strata, the Middle Miocene Baiyanghe Fm., the Late Miocene Hongyazi Fm., and Quaternary accumulation. In addition to the Quaternary strata, mammal

fossils are found in the other three sets of strata. The unnamed Oligocene strata contain the Haltang fauna, represented by the *Desmatolagus-Karakoromys decessus* assemblage, which may be roughly equivalent in age to the Dingdangou fauna in the Tabenbuluk area. The Ebotu fauna occurs in the Baiyanghe Fm., represented by a typical Tunggurian small mammal assemblage of *Heterosminthus orientalis*, *Megacricetodon sinensis*, *Democricetodon lindsayi* and *Alloptox gobiensis*. In the Hongyazi Fm., there are common members of the Baodean *Hipparion* fauna of North China, including *Hipparion platyodus*, *Chilotherium* cf. *xizangensis*, *Palaeotragus microdon* and *Gazella* cf. *gaudryi* (Gu et al., 1988; Zhang and Xie, 1988; Li et al., 2013).

### 6.2.2 Qaidam Basin

The evolution of the Qaidam Basin has been jointly affected by the Qilian Mountains, Altyn Tagh, and East Kunlun tectonic belts. The Neogene accumulation in the basin is very thick and successive, with a thickness of nearly 4600 m. The stratigraphic structure is relatively simple, and the strata at the northern edge of the basin are well exposed. It is an ideal place to study the evolution of terrestrial mammals. Abundant Neogene mammal fossils have been found in the areas of Hurleg and Toson lakes, and at least four faunas can be identified: the Middle Miocene Olongbuluk fauna, the early Late Miocene Toson and Shengou faunas, and the Early Pliocene Huaitoutala fauna. The fossils of the Olongbuluk fauna are mainly found in the red mudstone and green sandstone near the axis of the two wings of the Hurleg anticline at the bottom of the section, and include *Hispanotherium matritense*, *Acerorhinus tsaidamensis*, *Lagomeryx tsaidamensis*, *Stephanocemas palmatus*, and possibly *Dicroceros*. The Toson fauna includes *Ictitherium*, *Eomellivora*, *Chalicotherium brevisrostris*, *Hipparion teilhardi*, Sivatherinae indet., *Dicroceros*, *Euprox*, *Olonbulukia tsaidamensis*, *Qurlignoria cheni*, *Tossunnoria pseudibex*, *Tsaiidamotherium hedini*, *Protoryx*, *Tetralophodon*, and the ostrich *Struthio* (Wang et al., 2007, 2011). The age represented by the Toson fauna is the time when some endemic species first appeared on the Tibetan Plateau. Bovids with plateau characteristics include *Ts. hedini*, *To. pseudibex*, *Q. cheni* and *O. tsaidamensis*; among these, *Q. cheni* is the ancestral type of the modern Tibetan antelope (*Pantholops*) (Tseng et al., 2022; Wang et al., 2023). The early Late Miocene Shengou fauna is most similar to the small mammal assemblage in the lower part of the Bahe Formation in Lantian, Shaanxi (Qiu and Li, 2008), in which the large mammals include *Ictitherium*, *Adcrocuta eximia*, *Plesiogulo*, *Promephitis parvus*, *Acerorhinus tsaidamensis*, *Dihoplus ringstroemi*, *Hipparion weihoense*, *H. teilhardi*, *Euprox*, *Gazella* and *Amebelodon*; small mammals include *Sinotamias*, *Sciurotamias* cf. *pusillus*, *Pliopetaurista*, Eomyidae indet., *Lophocricetus* cf. *xianensis*, *Protalactaga*, *Myocri-*

*cetodon lantianensis*, *Nannocricetus primitivus*, *Sinocricetus*, *Huerzelerimys exiguus*, *Pararhizomys*, *Ochotonomys primitiva*, and *Ochotona* (Qiu and Li, 2008). The Early Pliocene Hwaitoutala fauna is not rich in fossils, and includes only *Ochotona*, *Orientalomys/Chardinomys*, *Micromys* and *Pseudomeriones*.

### 6.2.3 Xorkol Basin

The formation and development of the Xorkol Basin is closely related to the Altyn Tagh fault, and the Neogene sedimentary succession is consistent with that of the Qaidam Basin on its east side (Li and Qi, 1982; Chen et al., 2003). Li et al. (2002) discussed the origin of the Xorkol corridor basin, and suggested that the basin was a special type of long-stripped strike-slip fault basin, formed during the strike-slip deformation of the Altyn Tagh fault as a result of the joint action of transformation compression and uplift. The discovery of *Yuomys altunensis* in the Xishuigou Fm. indicates that its stratigraphic age is late Middle Eocene or later (Wang, 2017). Li J X et al. (2014) proposed that the main Xorkol area was uplifted and denuded before 17.7 Ma, and that it generally did not receive sedimentation, except for a small amount of sedimentation at the junction of the north and east sides with the Qaidam Basin. At about 17.7 Ma, the basin began to subside again, and the main body of the basin began to receive sedimentation. A set of sedimentary strata (Lower Youshashan Fm.) dominated by proluvial fan and shore-shallow lake facies developed. The interval of 14.2–9.88 Ma was the main development period of the basin. The basin widely received sedimentation, mainly consisting of a large set of stable lacustrine sediments (Upper Youshashan Fm.). After about 9.88 Ma, the basin entered a shrinking period, and the sedimentary environment changed significantly. The water body became shallow, and the early semi-deep lake environment changed into unstable underwater fan-delta and diluvial fan facies, forming a thick succession of coarse clastic deposits (Shizigou Fm.) (Chang et al., 2001; Zhang et al., 2010).

### 6.2.4 Kumkol Basin

The Altyn Tagh Mountains, located at the junction of Xinjiang, Qinghai and Gansu provinces, form the northern boundary of the Tibetan Plateau (Chen et al., 2010). The Kumkol Basin, located between the Altyn Tagh and East Kunlun mountains, is one of the Tibetan Plateau basins with the most complete Cenozoic sedimentary successions preserved and developed in step with the plateau uplift (Zhang et al., 1996; Pan et al., 2013). This succession is closely related to the formation of the northern boundary of the Tibetan Plateau and the tectonic activity of the Altyn Tagh fault. The Cenozoic sediments in the basin are very thick, up to 7000 m. The stratigraphic exposures span from Oligocene to Pleistocene, and are divided from bottom to top into the

Shimagou, Shibiliang, and Hongliang formations, and the “Xinjiang Group” conglomerate. Abundant small mammal fossils have been found at the top of the Shimagou Fm., including *Erinaceus* cf. *mongolicus*, *Eptesicus*, *Spermophilinus kumkolensis*, *Myomimus maritsensis*, *Dipus nanus*, *Democricetodon lindsayi* and Ochotonidae (Li et al., 2020). Among them, the typical locality of *D. lindsayi* is the Middle Miocene Tunggur Fm. in Inner Mongolia, where this taxon persisted until the Bahean of the Late Miocene (Qiu, 1996; Qiu and Li, 2016). *Spermophilinus* has only one known representative species in the Late Miocene of central Inner Mongolia, *S. mongolicus*; *S. kumkolensis* of Kumkol is slightly less derived than this species. In addition to *Dipus nanus* of the early Late Miocene Shala locality in Inner Mongolia, small three-toed jerboas have similar representatives in the Late Miocene Dingshanyanchi Fm. in Junggar, Xinjiang, and in the Middle Miocene Shomyshtin Fm. in Kazakhstan (Kordikova et al., 2004; Wu et al., 2014). Through comparison with similar small mammal fossil assemblages in Inner Mongolia (Qiu et al., 2013; Qiu and Li, 2016), and based on the slightly more primitive characters of *Spermophilinus kumkolensis* compared with *S. mongolicus*, Li et al. (2020) inferred that the age of the small mammalian fauna of the Shimagou Fm. was latest Middle Miocene, which is consistent with the magnetostratigraphic age of 12.5 Ma (Lu et al., 2016).

### 6.2.5 Kunlun Pass Basin

The Kunlun Pass Basin, with an altitude of 4786–4923 m, is one of the highest places in the world with preserved vertebrate fossils. There are mammal fossils in the fluvial-lacustrine sediments in the lower part of the Qiangtang Formation in the basin, named the Yuzhu fauna, which include fossils of 16 mammal taxa (Wang X M et al., 2013a), as well as the fish fossils *Gymnocypris* and *Triplophysa* (Wang and Chang, 2010, 2012). The Yuzhu fauna is attributed to the Early and mid-Pliocene. *Vulpes qiuzhudingi*, cf. *Panthera blytheae*, aff. *Arctomeles* sp., *Qurlignoria hundesiensis*, *Aepyosciurus*, *Prosiphneus* and *Ochotona* can be compared with those of the Zanda fauna. *Prosiphneus*, *Mimomys*, *Orientalomys*, *V. qiuzhudingi*, aff. *Arctomeles* sp., *Proboscipparion pater* and *Qurlignoria* are the most important taxa chronostratigraphically, and mainly lived in the Early Pliocene of East Asia. *Orientalomys* and *Mimomys* were discovered in the Pliocene of North China. Regarding morphology, the cheek teeth of *Prosiphneus* and *Mimomys* in the Kunlun Pass Basin still had tooth roots, and their dentine tracts were quite low, which can be compared with members of the Early Pliocene Gaotege fauna in Inner Mongolia. In size and shape, *Prosiphneus* of the Qiangtang Fm. is similar to *Prosiphneus* cf. *eriksoni* of Bilike in Inner Mongolia, but it is more primitive than that of Gaotege and slightly more derived than that of the Zanda Basin. *Mimomys* of the Yuzhu



fauna is similar to *Aratomys bilikeensis* of Bilike, as represented by its smaller size, cheek teeth with roots, and lack of cement, but it is more similar to *Mimomys* of the lower layers of Gaotege, especially in terms of dentine tract height (Li Q et al., 2014). *Aepyosciurus* in the Kunlun Pass Basin can be compared with the fossils at the ZD1001 locality in the Zanda Basin, and the paleomagnetic age of the latter is 4.42 Ma (Wang X M et al., 2013b). Several carnivorans and the primitive *Qurlignoria* of the Tibetan Plateau have also been found in the Zanda Basin (Bohlin, 1937; Tseng et al., 2013, 2022; Wang X M et al., 2013b, 2014, 2023), strongly indicating that they have similar ages (Li Q et al., 2014). The late Cenozoic strata of the Kunlun Pass Basin are divided into three lithological units; from bottom to top, these are the Kunlun Fm., Qiangtang Fm., and Wangkun glacial moraine bed. Traditionally, the Qiangtang Fm., which has yielded *Hipparion* fossils, is considered as Nihewanian, and the underlying Kunlun Fm., which is a pluvial variegated sandy conglomerate 250 m thick, has a paleomagnetic age of 3.58–2.69 Ma; that is, Mazegouan (Song et al., 2005). Li Q et al. (2014) reinterpreted the paleomagnetic age of Song et al. (2005) according to the features of the Yuzhu fauna, and constrained the age of the late Cenozoic sediments in the Kunlun Pass Basin to ~4.9–0.5 Ma. The ages of the Kunlun Fm. and the lower Qiangtang Fm. are Gaozhuangian.

#### 6.2.6 Xining Basin

A series of intermountain basins are distributed in the east of Qinghai Province, such as the Guide, Minhe, Xunhua and Xining basins. The Cenozoic strata of the Xiejia section in Huangzhong County within the Xining Basin are the most representative; from bottom to top, these are the Mahalagou, Xiejia, Chetougou and Guanjiashan formations. The Xiejia Fm. is in conformable contact with the Mahalagou and Chetougou formations. The Xiejia fauna is mainly composed of small mammal fossils, including the lagomorph *Sinolagomys pachygnathus*, rodents *Cricetodon youngi*, *Parasminthus xinningensis*, *P. huangshuiensis*, *Litodonomys lajeensis*, *Yindirtemys suni*, *Y. xinningensis* and *Tachyorcyctoides kokonorensis*, the giant rhino *Turpanotherium elegans*, and the bovid *Sinopalaeceros xiejiaensis* (Qiu et al., 2013), which together are a representative fauna of the Xiejian. Characteristics of the sporopollen assemblage from the Xiejia section are generally consistent with those of sporopollen floras of the Early Miocene in China (Wang and Deng, 2009). The lower boundary of the Xiejian Stage is located within the continuous deposits of brownish-red massive mudstone in the lower part of the Xiejia Fm., 14 m from the bottom of this formation (Deng et al., 2019a). The bottom of Chetougou Fm. contains *Heterosminthus*, *Megacricetodon sinensis*, and *?Eumyarion* sp. (Qiu et al., 1981), indicating a Shanwangian age. Eight mammal fossils are found in the Guanjiashan Fm., *Alloptox chinghaiensis*, *Plesiodipus lei*,

*Gnathabelodon connexus*, *Protanancus? wimani*, *Kubanochoerus minheensis*, *Stephanocemas chinghaiensis*, *Micromeryx* sp. and *Turcocerus? noverca* (Qiu et al., 1981; Zhang et al., 2017), showing Tunggurian characteristics.

#### 6.2.7 Linxia Basin

The Linxia Basin is a subbasin of the Longzhong Basin; similar subbasins include the Tianshui Basin and others (Guo et al., 2002; Li et al., 2006). The Linxia Basin is located at the northeastern margin of the Tibetan Plateau, adjacent to the western Qinling Mountains and the Loess Plateau. Its northern, western and southern boundaries are defined by high-angle thrust faults. The basin is filled with late Cenozoic red deposits 700–2000 m thick, dominated by lacustrine siltstones and mudstones mixed with fluvial conglomerates and sandstones, with loess deposits 30–200 m thick at the top of the sequence (Fang et al., 2003). In the center of the basin, Cenozoic deposits overlie Caledonian granite, and from bottom to top are the Lower Oligocene Tala Formation, Upper Oligocene Jiaozigou Fm., Lower Miocene Shangzhuang Fm., Middle Miocene Dongxiang and Hujialiang formations, Upper Miocene Liushu Fm., Lower Pliocene Hewangjia Fm., Upper Pliocene Jishi Fm. and Lower Pleistocene Wucheng Fm. The giant rhino *Paraceratherium* fauna and true horse *Equus* fauna contained in Jiaozigou and Wucheng formations respectively well define the upper and lower boundaries of the Neogene strata (Deng et al., 2013b). The lower part of the Shangzhuang Fm. is yellowish-brown sandstone, and the upper part is brownish-red mudstone that contains the Shanwangian Sigou fauna. The Dongxiang Fm. consists of brownish-red mudstones intercalated with greenish-gray marl beds, containing the early Tunggurian Shinanu fauna. The Hujialiang Fm. comprises fluvial sandstones and conglomerates, and contains the late Tunggurian *Platybelodon* fauna. The Liushu Fm. is yellowish-brown silty mudstones, which are typical red clay deposits. This formation contains rich fossils of the Late Miocene *Hipparion* fauna that can be divided into four horizons. The lower three horizons belong to the Bahean, and the uppermost horizon belongs to the Baodean. The lower part of the Hewangjia Fm. consists of sandstone and conglomerate, and the upper part is yellowish-brown silty mudstone (red clay), which contains the Gaozhuangian *Hipparion* fauna. The Jishi Fm. is grayish-black conglomerate, and fossils of *Pliocrocuta perrieri*, *Lynx lynx* (Jiangzuo et al., 2023) and antelope *Antilospira* have been found in its mudstone lenses.

#### 6.2.8 Lanzhou Basin

The thickness of Mesozoic and Cenozoic terrestrial deposits in the Lanzhou Basin is more than 4000 m, and the strata are well exposed from Upper Cretaceous to Miocene. The white sandstone of the Xiejian Huangyangtuo Fm. contains the Zhangjiaping fauna (Xie, 2004), which is composed of the

main Xiejian taxa and a few surviving Oligocene members, including *Desmatolagus pusillus*, *Sinologomys kansuensis*, *S. ulunguensis*, *S. pachygnathus*, *Tataromys plicidens*, *Yindirtemys grangeri*, *Y. deflexus*, *Y. ambiguus*, *Boumymys*, *Prodistylomys*, *Tachyoryctoides* cf. *kokonorensis*, *Sayimys*, *Ansomys*, *Anomoemys*, *Parasminthus asiae-orientalis*, *P. tangingoli*, *Heterosminthus orientalis*, *Protalactaga*, *Crice-todon*, *Democricetodon*, *Atlantoxerus*, *Sinotamias*, *Hyaenodon weilini*, *?Ictiocyon* cf. *socialis*, *Turpanotherium elegans*, *Aprotodon lanzhouensis*, and *Phyllotillon huangheensis*. The Duitingou fauna in the sandstone and red mudstone of the Simagou Fm. includes Shanwangian taxa: *?Metexallerix*, *Sinologomys*, *Alloptox minor*, *Bellatona forsythmajori*, *Megacricetodon*, *Democricetodon*, *Heterosminthus*, *Protalactaga grabau*, *Prodistylomys*, and *Stephanocemas* (Qiu et al., 2013). The Tunggurian Xiajie Fm. contains the Quantougou fauna, including *Mioechinus?* *gobiensis*, *Microdyromys wuae*, *Heterosminthus orientalis*, *Protalactaga grabau*, *P. major*, *Mellalomys gansus*, *Myocricetodon plebius*, *Plesiodipus leei*, *Megacricetodon sinensis*, *Ganocricetodon cheni*, *Paracricetulus schaubi*, Ochotonidae, *Kubanochoerus gigas*, and *Protanancus?* *wimani* (Qiu, 2000, 2001a, 2001b). The Late Miocene red siltstone and sandstone of the Longgushan Fm. contain the Xingjiawan fauna, including *Adrococuta eximia*, *Yoshi yongdengensis*, *Y. faie*, *Paramachaerodus schlosseri*, *P. yingliangi*, *Stegodon*, *Chilotherium habereri*, *Hipparion*, *Chleuastochoerus stehlini* and abundant deer (Zhang, 1993; Jiangzuo et al., 2022b).

### 6.3 Qiangtang stratigraphic region

#### 6.3.1 Lunpola Basin

The Bangong-Nujiang suture zone in the center of the Tibetan Plateau is characterized by many Cenozoic basins (Luo et al., 1996), and the Lunpola Basin, which is developed on the Yanshanian fold basement, is a typical representative (Lei et al., 1996). The Cenozoic deposits in the Lunpola Basin are more than 4000 m thick and consist of the Niubao Fm. in the lower part and the Dingqing Fm. in the upper part. The Dingqing Fm. is widely distributed in the east and central parts of the Lunpola Basin. This formation is a set of greenish-gray shales intercalated with sandstone and oil shale, with a thickness of 300–1100 m. It is rich in animal and plant fossils, including mammals, fish, ostracods, gastropods, insects and sporopollens (Sun J M et al., 2014, 2023; Deng et al., 2021c). The hornless rhino *Plesiaceratherum*, a first appearing and characteristic genus of the Shanwangian, has been found in the upper part of the Dingqing Fm. (Deng et al., 2012). *Plesiaceratherum* is also found in the Shanwang Fm. in Linqu County, Shandong Province, and the Jiulongkou Fm. in Cixian County, Hebei Province (Qiu et al., 2013); thus, this taxon indicates that the upper part of the Dingqing Fm. entered the Miocene. Small mammal fossils in

this formation include *Plesiosciurus sinensis*, *Heterosminthus* cf. *juncundus*, *Sayimys* cf. *sihongensis* and *Sinologomys kansuensis*. The squirrel *Plesiosciurus sinensis* can be directly compared with the Early Miocene *P. sinensis* in Sihong County, Jiangsu Province. *Heterosminthus jucundus* is most similar to that of the Middle Miocene Sarybulak Fm. in the Zaisan Basin, Kazakhstan, but its body size is obviously small, indicating that it was likely more primitive. The mole rat *Sayimys* cf. *sihongensis* can be compared with the Early Miocene *S. sihongensis* in Sihong, Jiangsu, but the body is smaller. Both the cheek tooth size and p3 shape of the pika are consistent with *Sinologomys kansuensis*, and the age distribution of this species is mainly Late Oligocene to Early Miocene. According to the mammalian fossils and isotopic dating data, the Oligocene and Miocene boundary is located in the lower part of the Dingqing Fm. (Deng et al., 2019c). Mao et al. (2019) and Sun J M et al. (2023) measured in different exposures to show that the upper part of the Dingqing Fm. is about 13 and 12 Ma, respectively, which is at the end of the Middle Miocene, but the dated exposures did not reach the top of this formation.

#### 6.3.2 Bulong Basin

The Cenozoic fluvial strata of the Bulong Basin in Biru County, Xizang Autonomous Region at the southern foot of the Tanggula Mountains are partially exposed, distributed along the Cuoshang River, and most of them are covered by alpine meadows. The Bulong Fm. is mainly composed of gray mudstone with interbedded black mudstone and grayish-black mudstone, underlain by pre-Cenozoic gray papery shale, and overlain by a Quaternary gravel layer, both with unconformable contacts. Mammalian fossils found in the Bulong Fm. include *Brachyrhizomys naquensis*, *Dinocrococuta xizangensis*, *Leptofelis* sp., *Metailurus* sp., *Subchilotherium intermedium*, *Hipparion xizangense*, *Samotherium* sp. and *Gazella* sp. (Huang W B et al., 1980; Zheng, 1980; Deng, 2006b). Zheng (1980) suggested that *Brachyrhizomys* from Bulong was most similar to *Rhizomyoides punjabiensis* in the Chinji Fm. in the Siwalik region, Pakistan. Qiu et al. (1987) considered *Hipparion* (*Hippotherium*) *xizangense* from Bulong to be obviously primitive, possibly more primitive than the three-toed horses of the Bahe Fm. in the Lantian area. Zhang (2005) proposed that *Dinocrococuta* from Bulong may be the same species as *D. senyureki* in Sinap, Turkey as an ancestral type of *D. gigantea*. Based on fossil evidence, the Bulong Fm. belongs to the Bahean of the Upper Miocene.

#### 6.3.3 Hoh Xil-Togton River Basin

The sedimentary strata developed in this area are mainly the Tuotuohe, Yaxicuo, Wudaoliang, Quguo, and Kunlun formations. The Wudaoliang Fm. is 399.4 m thick, and comprises light grayish-green marl with gypsum layers, purplish-

red fine sandstone and light gray mudstone of saline lacustrine facies. These deposits contain plant fossils of *Berberis* cf. *asiatica* (Sun et al., 2015) and ostracods including *Eucypris qaiweigouensis*, *Limnocythere limbosa*, *Candoniella marcida*, *Mandelstam*, *Cycloocypris* and *Darwinula nadiniae*, and the age is Miocene. The thickness of the Quguo Fm. is 1070–2283 m, and its lower part is grayish-brown conglomerate, siltstone and thin mudstone with lithic sandstone; the upper part is grayish and grayish-brown thin-layered packstone and mudstone mixed with siltstone, belonging to fan-delta and lacustrine deposits. This formation has yielded the stonewort *Charites*, gastropod *Galba* and ostracods such as *Candona*, *Cycloocypris*, *Ilyocypris*, *Eucypris*, *Leucocythere* aff. *tropis* and *Candoniella formosa*. The age of the Quguo Fm. is Pliocene (Zhang et al., 2010).

## 6.4 Western Yunnan-Western Sichuan stratigraphic region

### 6.4.1 Hengduan Mountains

A series of Cenozoic fault basins are distributed in the Hengduanshan area, containing vertebrate fossils, especially of mammals. The deposits are characterized by dark lacustrine coal-bearing facies. Wangbuding is located in Dege County, Ganzi Prefecture, Sichuan Province, on a cliff of Paleozoic black slate along the east bank of the Jinsha River, with an altitude of more than 3700 m. The Wangbuding Formation is a typical riverbed accumulation, which gradually transitions from the bottom coarse gravel layer to fine gravel and sandy clay interlayers, with a total thickness of less than 16 m. It contains rich mammal fossils, including *Ochotona hengduanshanensis*, *Miomys* cf. *hengduanshanensis*, *Ursus* cf. *thibetanus*, *Martes* cf. *pachygnatha*, *Meles chiai*, *Pachycrocuta licenti*, *Metailurus hengduanshanensis*, *Homotherium hengduanshanensis*, *Lynx shansius*, *Sivapanthera* sp., *Hengduanshanhyrax tibetensis*, *Muntiacus lacustris*, *M. hengduanshanensis*, *Gazella* sp. and *Ovis* cf. *shantongensis*? (Zong et al., 1996). The Wangbuding Fm. was originally interpreted to be no younger than Early Pleistocene based on its mammalian fossils, and was later determined to be Pliocene (Chen, 2003; Qiu et al., 2013). Located in Yanyuan County, Liangshan Prefecture, Sichuan Province, the Yanyuan Basin is surrounded by mountains with altitudes of more than 3000 m, and received different types of sediments throughout the Neogene. The Yanyuan Fm. comprises shale and sandstone containing lignite, and has yielded fossils of *Sinomastodon yanyuanensis*, *Stegodon elephantoides*, *Axis*, and *Cervavitus*; the age is Pliocene, and the overlying strata are Pleistocene. The Yongren Basin is located in Yongren County, Yunnan Province. The Tangguanyao Fm., which overlies the Cretaceous Zhaojiadian Fm., is a set of clastic deposits of fluvial, lacustrine and swamp facies, and contains mammalian fossils such as *Stegodon*

*elephantoides*, *Stegolophodon officinalis*, *Tapirus* cf. *teillardii*, and *Gazella*; its age is Pliocene. The Baoshan Basin is located on the east side of the Gaoligong Mountains in western Yunnan. The Yangyi Fm. overlies the Upper Paleozoic and comprises lacustrine coal-bearing strata in which *Stegodon* cf. *zdanskyi*, *Stegolophodon officinalis*, *Sinomastodon*, *Cervavitus* and other mammal fossils have been found; the age is Pliocene (Zong et al., 1996).

### 6.4.2 Xiaolongtan Basin

The basement of the Xiaolongtan Basin in Kaiyuan County, Yunnan Province is strata dominated by Middle and Upper Triassic limestone, overlain by Cenozoic fluvial-lacustrine deposits containing rich lignite beds, called the Xiaolongtan Fm. This formation is divided into three members, the lower conglomerate, the middle lignite clay and the upper marlstone, with a total thickness of 50–1070 m. The upper marlstone is 150–180 m thick, and some researchers still use its original name, the Buzhaoba Fm. (Li C X et al., 2021). The Xiaolongtan Fm. is characterized by the discovery of *Lufengpithecus keiyuanensis* (Wu et al., 1989), as well as specimens of *Tetralophodon xiaolongtanensis*, *Stegolophodon latidens*, *Zygalophodon chinjiensis*, *Tapirus* cf. *yunnanensis*, *Parachleuastocoeris sinensis*, *Propotamochoerus parvulus*, *Hippopotamodon hyotherioides* and *Euprox* sp. Among these, *L. keiyuanensis*, *Tetralophodon*, *Zygalophodon*, *Tapirus*, *Parachleuastocoeris*, *Hippopotamodon* and *Euprox* have age significance, together indicating that the Xiaolongtan Fm. belongs to the Tunggurian, Middle Miocene; the paleomagnetic interpretation is consistent with this result (Li et al., 2015; Zhang et al., 2019). However, Li C X et al. (2021) suggested that the age of the fossiliferous layer of this formation may be early Late Miocene, namely the Bahean. In the Hetou Fm. overlying the Xiaolongtan Fm., *Stegodon*, *Sus*, *Hexaprotodon*, *Rusa* cf. *unicolor* and other mammal fossils of the Early Pleistocene have been found (Dong and Qi, 2013).

### 6.4.3 Lufeng Basin

The Shihuiba Formation in the Lufeng Basin, Yunnan Province mainly covers the fronts of the hills composed of the Precambrian Kunyang Group. It is a set of sand, gravel, sandy clay, clay and lignite deposits of lacustrine-swamp facies, and its top is covered by Quaternary purplish-red weathering crust and a brownish-yellow terrace gravel layer. The lignite layers are rich in mammal fossils, including *Lufengpithecus*, *Laccopithecus*, *Prodendrogale yunnanica*, *Yunosaptor scalprum*, *Heterosorex wangi*, *Sciurotamias wangi*, *Platacanthomys dianensis*, *Miorhizomys tetracharax*, *Kowalskia hanae*, *Alilepus longisnuosus*, *Amphimachairodus horribilis*, *Indarctos atticus*, *Ailurarctos lufengensis*, *Ursavus sylvestris*, *Sivaonyx bathygnathus*, *Cernictis lufengensis*, *Gomphotherium*, *Zygalophodon*, *Hipparion*

*theobaldi*, *H. lufengense*, *Tapirus*, *Anisodon yuanmouensis*, *Acerorhinus lufengensis*, *Shansirhinus* cf. *ringstroemi*, *Yunnanochoerus*, *Euprox*, *Muntiacus*, *Paracervulus* and *Sele-noportax* (Deng and Qi, 2009; Sun, 2013; Dong and Qi, 2013; Chen et al., 2016). Among them, the rabbit *Alilepus* and the rhinoceros *Shansirhinus* are first appearing genera, and the bear *Indarctos* is a last appearing genus of the Baodean (Qiu et al., 2013). The co-existence of these genera indicates that the age of the Shihuiba Fm. is the Late Miocene Baodean. The three-toed horse *H. theobaldi* is also distributed in Siwaliks and Myanmar (Woodburne et al., 1996) on the southern edge of the Tibetan Plateau, which also shows that the Tibetan Plateau had risen to a certain height during this period, blocking the migration of animals on the southern side of the Himalayas to the northeast, such that they could only live and migrate along the Himalayas.

#### 6.4.4 Yuanmou Basin

The Yuanmou Basin is a fault basin located on the southern bank of the Jinsha River in central Yunnan Province. It is about 45 km long from north to south and 18 km wide from east to west. Mesozoic predominantly red clastic deposits are exposed on the eastern and southern edges of the Yuanmou Basin, the Precambrian Kunyang and Jinning groups are exposed on the western edge, and the Kunyang Group and Cretaceous red beds are exposed on the northern edge. The basement of the basin is mainly the Kunyang Group, and the basin is filled with late Cenozoic clastic deposits. The Late Miocene Xiaohe Formation contains ancient ape fossils. The entire mammalian fauna includes 110 species in 41 families and 9 orders. Fossils with biostratigraphic significance include *Lufengpithecus*, *Indraloris*, *Sinoadapis*, *Prodontrogale yunnanica*, *Yunosaptor scalprum*, *Heterosorex wangi*, *Sciurotamias wangi*, *Platacanthomys dianensis*, *Miorhizomys tetracharax*, *M. blacki*, *Kowalskia hanae*, *Arctamphicyon* aff. *lydekkeri*, *Pseudarctos* aff. *bavaricus*, *Indarctos*, *Ailurarctos yuanmouensis*, *Sivaonyx bathygnathus*, *Amphimachairodus*, *Longchuansmilus xingyongi*, *Tetralophodon*, *Mammut*, *Tapirus*, *Acerorhinus yuanmouensis*, *Yunnanochoerus*, *Molarochoerus yuanmouensis*, *Euprox*, *Muntiacus* and *Paracervulus* (Dong and Qi, 2013; Sun et al., 2022; Jiangzuo et al., 2022a); the small mammals of this assemblage are slightly earlier than those of the Lufeng fauna. The rodent *Kowalskia* is a first appearing genus of the Bahean (Ni and Qiu, 2002; Qiu et al., 2013); therefore, the Xiaohe fauna has been attributed to the Bahean. Among the large mammals, the carnivorans *Arctamphicyon* aff. *lydekkeri* and *Pseudarctos* aff. *bavaricus* are surviving genera and species of the Middle Miocene, and *Indarctos* is a first appearing genus of the Bahean and a characteristic genus of the Late Miocene; *Tapirus* is a first appearing genus, *Tetralophodon* is an index fossil, and *Euprox* is a last appearing genus of the Bahean (Qiu et al., 2013). Their combination further con-

firms that the Xiaohe fauna belongs to the Bahean. The stratum overlying the Xiaohe Fm. is the Shagou Fm., where mammals such as *Rhizomys*, *Miorhizomys blacki*, *Enhydridon* cf. *falconeri*, *Stegolophodon stegodontoides*, *Stegodon yuanmouensis*, *S. elephantoides*, *S. zhaotongensis*, *Rhinoceros*, *Muntiacus nanus* and *Cervus* have been reported (Qian et al., 1991), of which *Muntiacus* is a first appearing genus and *Stegodon* is a characteristic genus of the Gaozhuangian (Qiu et al., 2013), indicating Pliocene attribution of the Shagou fauna. The Early Pleistocene Yuanmou Fm. above the Shagou Fm. contains *Homo erectus* fossils of Yuanmou Man.

## 6.5 Gangdise-Himalaya-Siwalik stratigraphic region

### 6.5.1 Zanda Basin

During the late Cenozoic, with nearly east-west extensional deformation in the interior of the Tibetan Plateau, a series of nearly north-south to north-east rift basins developed in the southern Tibetan Plateau and its adjacent areas, with relatively complete late Cenozoic strata. The Zanda Basin is located at the western end of this series of basins, at the northern foot of the western Himalayas with faults as boundaries; the exposed fluvial-lacustrine deposits are more than 800 m thick, and overlie the Mesozoic Tethys sedimentary basement (Wang S F et al., 2008; Kempf et al., 2009; Saylor et al., 2009). The upper Cenozoic of the Zanda Basin was first called the Zhada Fm. (Zhang et al., 1981), and later was further divided into the Pliocene Tuolin and Guge formations and the Pleistocene Xiangzi Fm. (Qian, 1990; Zhu et al., 2008). The division of these formations is based on perceived depositional hiatuses, which were later shown to be false (Wang S F et al., 2008; Saylor et al., 2009). Therefore, the entire set of late Cenozoic strata continues to sometimes be called the Zanda Fm. (Wang X M et al., 2013a, 2013b). Fossils such as *Palaeotragus microdon* (Zhang et al., 1981) and *Hipparion (Plesiohipparion) zandaense* (Li and Li, 1990) have previously been found here. In recent years, mammal and fish fossils have been found throughout the entire section except the top and bottom conglomerate beds; the small mammal fossils found in the lower two localities of the section in particular have important age significance (Wang X M et al., 2013a). The mammalian fossils contained in the Tuolin Fm. and Guge Fm. are mainly Pliocene in age, including *Nyctereutes* cf. *tingi*, *Vulpes qiuzhudingi*, *Sinicuon* cf. *dubius*, *Chasmaporthetes gangriensis*, *Pliocrocota perrieri*, *Panthera blytheae*, *Hipparion zandaense*, *Coelodonta thibetana*, *Cervavitus*, *Protovis himalayensis*, *Antilospiral Spirocercus*, *Qurlignoria hundesiensis*, *Aepyosciurus*, *Nannocricetius qiui*, *Aepyocricetus liuae*, *Prosiphneus* cf. *eriksoni*, *Mimomys (Aratomys) bilikeensis*, *Apodemus*, *Trischizolagus* cf. *mirificus*, *T. cf. dumitrescuae* and *Ochotona* (Deng et al., 2021b; Wang et al., 2023). *Nyctereutes* and

*Trischizolagus* are first appearing and characteristic genera; *Chasmaporthetes*, *Pliocrocota*, *Coelodonta* and *Antilospira* are first appearing genera; *Hipparion* (*Plesiohipparion*) and *Mimomys* (*Aratomys*) are first appearing subgenera and characteristic fossils; and *Nannocricetus* is a last appearing genus of the Gaozhuangian. The combination of these taxa shows distinctive characteristics of the Early Pliocene. Taking this fauna as a constraint condition, the paleomagnetic results indicate that the time span of the late Cenozoic deposits in the Zanda Basin is from the Baodean of the Upper Miocene to the Quaternary, beginning at 6.4 Ma (Wang X M et al., 2013b).

#### 6.5.2 Moincer Basin

The Moincer Basin is located in Ngari, Xizang Autonomous Region. It is separated from the Zanda Basin by the Ayirariju Mountains in the southwest and borders the Gangdise Mountains in the north. Moincer is also roughly located in the watershed between the Gar Zangbo, a tributary of the upper reaches of the Sengge Zangbo (Shiquan River), and the Moincer River, a tributary of the upper reaches of the Langqen Zangbo (Xiangquan River). The strata of the Moincer Basin were first established as the Upper Cretaceous-Eocene Menshi Fm., Miocene Yemagou Fm. and Pliocene Rixugou Fm. The Menshi Formation is more than 1000 m thick, with sandy conglomerate in the lower part, shale and mudstone mixed with coal seams in the middle, containing mainly *Eucalyptus* plant fossils, and tuff in the upper part. The Yemagou Fm. is 600 m thick; the upper part is grayish-green and grayish-purple sandstone and mudstone, and the lower part is thick sandstone with sandy conglomerate; there are plant fossils mainly belonging to *Populus*, *Salix*, *Albizia* and *Sophora* of the Leguminosae. The Rixugou Fm. is 500 m thick; the upper part is mainly composed of purplish-red, yellowish-brown and grayish-green mudstones, and the lower part is composed of sandstone and pebbly sandstone (Geng and Tao, 1982). The upper part of the basin comprises Pleistocene sand and gravel layers containing *Equus* fossils (Li et al., 2011). The Yemagou Fm. has been compared with the Eocene Qiuwu Fm., and the Rixugou Fm. has been compared with the Late Oligocene-Early Miocene Dazhuka Fm. (Zhang et al., 2010).

#### 6.5.3 Burang Basin

The Burang Basin is located at the foot of Mount Naimonyi in Ngari, Xizang Autonomous Region, with a length of 40 m and a width of 12 km. The east and west sides are bounded by steep to moderately inclined brittle normal faults. The Cenozoic strata unconformably overlie the Tethys sedimentary sequence. The Miocene Danzengzhukang Fm. is 894 m thick in the west of Mount Kangrinboqe, where its name originates; the lithology is mainly grayish-yellow, grayish-white conglomerate, sandy conglomerate, felds-

pathic lithic sandstone and muddy siltstone, and it is in angular unconformable contact with the underlying Paleogene or Cretaceous strata; however, its thickness in the south of Burang county town is only about 272 m, without an exposed bottom (Zhang et al., 2015a). Murphy et al. (2002) divided the Pulan Fm. of the Burang Basin into three parts; the lower part is composed of white to yellowish-brown sandstone and siltstone interbedding, and contains a small amount of conglomerate lenses, with a total thickness of more than 100 m and no exposed bottom; the middle part is white to yellowish-brown sandstone, siltstone and boulder conglomerate sequences that coarsen upward, with a thickness of 200 m; the upper part is a boulder conglomerate sequence about 100 m thick. According to comparison, the current Danzengzhukang Fm. is equivalent to the lower and middle parts of the Pulan Fm. The sporopollen and ostracod fossils of the lignite outcrop in the Burang Basin, which is equivalent to the upper part of the Danzengzhukang Fm., were analyzed previously, and it was suggested that the strata in this section belong to the Pliocene (Cao, 1982). Recently, based on sporopollen fossils and regional tectonic evolution, it has been argued that the formation age of the Danzengzhukang Fm. is Middle-Late Miocene, and that the upper strata of the original Pulan Fm. are Pliocene deposits (Zhang et al., 2015a).

#### 6.5.4 Gyirong Basin

The Gyirong Basin is located at the northern foot of Mount Xixabangma, and is a fault basin with an altitude of 4100–4400 m. The thickness of the Cenozoic fluvial-lacustrine Woma Fm. in the basin is more than 450 m, and this formation unconformably overlies Jurassic marine strata and underlies the Early Pleistocene Gongba sandstone and conglomerate. The lower layers of the lower part of the Woma Fm. are composed of greenish-gray carbonaceous mudstone and yellowish-gray sandy mudstone. There are fossils of the *Hipparion* fauna, including *Plesiodipus tibetensis*, *Himalayactaga liui*, *Ochotona guizhongensis*, *Hipparion forstenae*, *Chilotherium xizangensis*, *Palaeotragus microdon*, *Metacervulus capreolinius*, *Gazella gaudryi*, *Adcrocuta* and *Heterosminthus*. In the middle part, gray conglomerate, yellow sandstone and gray sandstone occur alternately. The upper part is light-yellow mudstone with a thickness of 40–80 m (Huang W B et al., 1980; Ji et al., 1980). *Hipparion forstenae* is a biostratigraphic marker of the lower boundary of the Baodean (Deng et al., 2019a).

#### 6.5.5 Dati Basin

The Dati Basin is located in the south of the Nienixiongla platform, 45 km north of Nyalam County, Xizang Autonomous Region. The lacustrine strata are distributed at altitudes of 4750–4980 m, with a visible thickness of about 500 m, and unconformably overlie the Early Pleistocene Gongba

conglomerate. The upper part of the Dati Formation is relatively loose grayish-white and grayish-yellow coarse sand and fine conglomerate; the middle part is sandwiched with multiple layers of ferruginous sandstones, and has yielded *Hipparion forstenae* fossils; the lower part is interbedded with grayish-yellow and bluish-gray silty sand and clay (Huang C X et al., 1980). *H. forstenae* was previously found in Baode and Huoxian in Shanxi Province, Linxia in Gansu Province, and Gyirong in Xizang Autonomous Region. Precise paleomagnetic dating has been performed for the *Hipparion* horizons in Baode and Gyirong, both with an age of 7.0 Ma (Chron C3Bn) (Yue et al., 2004a, 2004b), and the first appearance of *H. forstenae* is therefore regarded as a biostratigraphic marker of the lower boundary of the terrestrial Baodean in China, corresponding to the marine Messinian (Deng et al., 2013a). The horizon in the Dati Basin containing *H. forstenae* is therefore equivalent to the Baodean strata, and the Dati Fm. represents Late Miocene deposits (Deng et al., 2015b).

#### 6.5.6 Oiyug Basin

Cenozoic sedimentary basins are developed only in the south of the Gangdise Mountains, represented by the Oiyug Basin. This basin is one of the larger Cenozoic relict intermountain basins in the south of the Tibetan Plateau. It is located in Namling County, Xizang Autonomous Region, north of the Yarlung Zangbo River and between the Gangdese and the Nyainqentanglha mountains, with altitudes of 4200–4800 m. The Cenozoic deposits in the Oiyug Basin are well developed and rich in plant and sporopollen fossils, but the stratigraphic age is mainly determined by isotopic dating (Spicer et al., 2003; Chen et al., 2008). The lithostratigraphic division of the Oiyug Basin is very complex. This paper adopts a newer and more widely used comprehensive scheme. The basement of the basin is the Linzizong Group, which ranges from Upper Cretaceous to Eocene. The overlying Rigongla Formation consists of the purplish-red terrestrial coarse sandstone, fine sandstone, siltstone, pebbly sandstone, conglomerate and acid tuff with a small amount of alkaline lava, and the top part contains sporopollen fossils. The Lower-Middle Miocene Mangxiang Fm. is mainly composed of gray clastic rocks (mudstone, sandstone and conglomerate) bearing coal, with volcanoclastic rocks (tuff, tuffaceous sandstone and conglomerate), often with oil shale. The Middle-Upper Miocene Laiqing Fm. is andesite and pyroclastic rock (andesitic tuff and andesitic volcanic breccia). The Upper Miocene Wuyu Fm. is composed of coal strata. The Pliocene Dazi Fm. is characterized by sandstone and conglomerate facies (Liu and Li, 2016).

#### 6.5.7 Potwar Plateau

The Siwalik Group of the South Asian subcontinent includes fluvial strata from the Miocene to Pleistocene. This group

was deposited in a series of basins in Pakistan, India and Nepal on the southern edge of the Tibetan Plateau. Its lithology includes sandstone, siltstone, mudstone and small amounts of conglomerate and marl. It has an immense thickness, rich fossils, and high diversity of terrestrial and aquatic vertebrates. It has been studied for more than 180 years. The underlying strata are Eocene marine deposits (Flynn et al., 2013). The Potwar Plateau is located in the north of Pakistan. The study of the well-developed and well-exposed Siwalik Group strata has greatly affected the interpretation of biostratigraphy in the foothills of the Himalayas in Pakistan (Pilgrim, 1912; Raza and Meyer, 1984). The Neogene strata of this group are continuous and complete, and have reliable paleomagnetic dating (Johnson et al., 1985; Barry et al., 2002). They are divided into the Early Miocene Murree Fm., Early-Middle Miocene Kamlial Fm., Middle Miocene Chinji Fm., Late Miocene Nagri Fm., Late Miocene-Early Pliocene Dhok Pathan Fm., and Late Miocene Tatrot Fm. In the Murree Fm., the rodents *Prosayimys*, *Primus*, *Democricetodon*, *Sayimys intermedius* and *Prokanisamys arifi*, the elephant *Prodeinotherium* and the pig *Listriodon guptai* first appeared. The Kamlial Fm. is mainly sandstone, and the amount of red siltstone increases upward; the rodents *Kochalia gespei* and *Sayimys sivalensis* and the pig *Listriodon pentapotamiae* appeared for the first time. The Chinji Fm. is mainly composed of red silt and clay mixed with paleosol, as well as gray cross-bedded sandstone; the rodents *Myomimus*, *Sayimys chinjiensis* and *Progonomys hussaini* first appeared. The Nagri Fm. is characterized by massive and multi-layered greenish-gray sands, containing small amounts of red silt; the three-toed horse *Hippotherium* and the bovid *Selenoportax* first appeared in these strata. Light-yellow sand bodies frequently appear in the Dhok Pathan Fm., which contains mudstone and a small amount of gray sand; the giraffe *Giraffa punjabiensis*, the porcupine *Hystrix sivalensis*, the rabbit *Alilepus* and the hippopotamus *Hexaprotodon sivalensis* first appeared. The Tatrot Fm. is characterized by gravel deposits, and the elephant *Elephas planifrons* first appeared (Barry et al., 2013; Flynn et al., 2013).

#### 6.5.8 Sulaiman area

The Sulaiman Mountains trend south-north, have altitudes 1000–3400 m above sea level, are located between Pakistan's Balochistan and Punjab provinces, and extend northward to the North-West Frontier Province. The late Mesozoic and Cenozoic deposits are mainly Tethys marine strata, although there are relatively thick and well-exposed middle Cenozoic sea-land transitional deposits on the eastern side of the Sulaiman Mountains, closely related to the uplift of the Himalayas and the closure of the Tethys Sea under the background of Indo-Eurasian collision (Beck et al., 1995; Clift et al., 2001). This set of strata is most typical in the

Bugti Hills and the Zinda Pir area of the Sulaiman Mountains, and is rich in vertebrates, especially Miocene-Pleistocene mammal fossils in fluvial deposits. The middle and lower parts of the Chitarwata Fm. are Oligocene; the upper part, 50–200 m thick, comprises the Early Miocene Xiejian strata, which contain first appearing rodents in the region such as *Eumyarion*, *Democricetodon*, *Spanocricetodon*, *Primus*, *Prokanisamys* and *Prosayimys*, the carnivoran *Amphicyon*, the elephants *Prodeinotherium* and *Gomphotherium*, the artiodactyls *Listriodon*, *Telmatodon*, *Hemimeryx*, *Dorcatherium*, *Eotragus* and *Bugtimeryx*, and the perissodactyls “*Chalicotherium*”, *Phyllotillon*, *Protaceratherium*, *Mesaceratherium*, *Pleuroceros*, *Plesiaceratherium*, *Brachypotherium*, *Prosantorhinus*, *Gaiotherium* and *Bugtirhinus*. The Vihowa Fm. is 100–200 m thick, and its lower part is Shanwangian, with first appearing rodents in the region such as *Megacricetodon*, *Myocricetodon*, *Sayimys intermedius* and *Diatomys*, the creodonts *Pterodon* and *Hyanailouros*, the carnivoran *Megamphicyon*, the proboscideans *Protanancus* and *Choerolophodon*, the artiodactyls *Listriodon guptai*, *Dorcabune* and *Progiraffa*, and the perissodactyls *Rhinoceros* sp. and *Brachypotherium perimense*. The upper part of this formation is Tunggurian and contains *Deinotherium*, *Listriodon pentapotamiae*, cf. *Elachistoceras* and *Anisodon*. The Litra Fm. is up to 1700 m thick, and was deposited in the Late Miocene; the three-toed horses first appeared in this formation, including *Cormohipparion (Sivalhippus) theobaldi* and *Hippotherium* sp. (Antoine et al., 2003), accompanied by the first appearances of *Parachleuastochoerus*, ? *Propotamochoerus*, ? *Bramatherium*, *Hispanodorcas*, *Prostrepsiceros*, *Alicornops compatrium* and *Rhinoceros* aff. *sivalensis*, and the last appearance of *Listriodon* in this region, corresponding to the Bahean. The thickness of the Chaudhwan Fm. is about 1500 m at most, and its age is Pliocene-Pleistocene (Antoine et al., 2013).

#### 6.5.9 Thakkhola Basin

The Thakkhola Basin, also known as the Mustang Basin, is a graben basin located in the north-central part of Nepal on the southern edge of the Tibetan Plateau, between the southern Tibetan detachment system and the Yarlung Zangbo suture. Its west side is defined by Miocene leucogranites, and its east side is defined by Paleozoic and Mesozoic deposits and leucogranites. The Neogene deposits of the basin are composed of upper and lower sets of strata separated by an angular unconformity, and contain plant and ostracod fossils; these deposits are overlain by Quaternary strata. The lower Tetang Formation is mainly exposed in the southeast of the basin, with a thickness of about 230 m, and transitions from fluvial to lacustrine facies. The paleomagnetic results show that deposition of the bottom sediments began at about 11.6 Ma, and the paleomagnetic age at the top is 9.6 Ma. The Thakkhola Fm., which has a thickness of about 1000 m in the

upper part, is exposed across the entire basin. It comprises alluvial fan deposits in the west and fluviolacustrine deposits in the middle and east. Its age is from 8 to 2 Ma (Adhikari and Wagreeich, 2013). The vegetation reconstructed according to the stable carbon isotopes of paleosol carbonate in the Thakkhola Fm. shows the presence of C<sub>4</sub> plants, which also provides an age constraint of less than 7 Ma (Garzzone et al., 2000a). Paleocurrent reconstruction indicates a southward main stream since the deposition of the Thakkhola Fm. In the later period, Kali Gandaki valley incised more than 1000 m in the basin deposits, reaching the Cretaceous Tethys Ocean sedimentary rock series of the basement (Garzzone et al., 2000b).

## 7. Climatic and environmental changes on the Tibetan Plateau during the Neogene

The Neogene in China is mainly represented by terrestrial strata. Although stable carbon and oxygen isotope analysis of carbonates in deposits and tooth enamel of mammalian fossils has been conducted in many sections, the continuity of these data is poor, and the sedimentary carbonate is greatly affected by diagenesis. Therefore, the interpretation for these data on the Neogene climate and environmental changes must be further improved in terms of its accuracy and reliability. In addition, because the stable carbon and oxygen isotope data of different types of sediments show some fractionation differences, it may be difficult to compare these data between different regions. This paper summarizes the carbon and oxygen isotope data of the northern and southern edges of the Tibetan Plateau. Because of the large amount of data, the diversity of sample types and systematic deviation in isotope testing, the overall distribution of the data will weaken the trend of change in each region, but it can be used for large-scale north-south comparison.

### 7.1 Northern Tibetan Plateau

In the Tibetan Plateau, the Neogene deposits in the Linxia Basin are continuous, and the results of chemical stratigraphic research can be interpreted as representative of this area (Figure 5). From 25 Ma onward, the  $\delta^{13}\text{C}$  values indicate that a clear C<sub>4</sub> plant signal did not appear in the Linxia Basin until the Quaternary, revealing that the vegetation type in this area was dominated by C<sub>3</sub> plants in the Neogene (Wang and Deng, 2005; Biasatti et al., 2010). Carbon isotope analysis of carbonate in deposits from the Maogou and Wangjiashan sections also shows that the  $\delta^{13}\text{C}$  values were very stable, with no obvious signal that the vegetation changed from C<sub>3</sub> to C<sub>4</sub> (Dettman et al., 2003; Fan et al., 2007). This forms a sharp contrast with the rapid expansion of C<sub>4</sub> vegetation in Pakistan and Nepal on the southern margin of the Tibetan

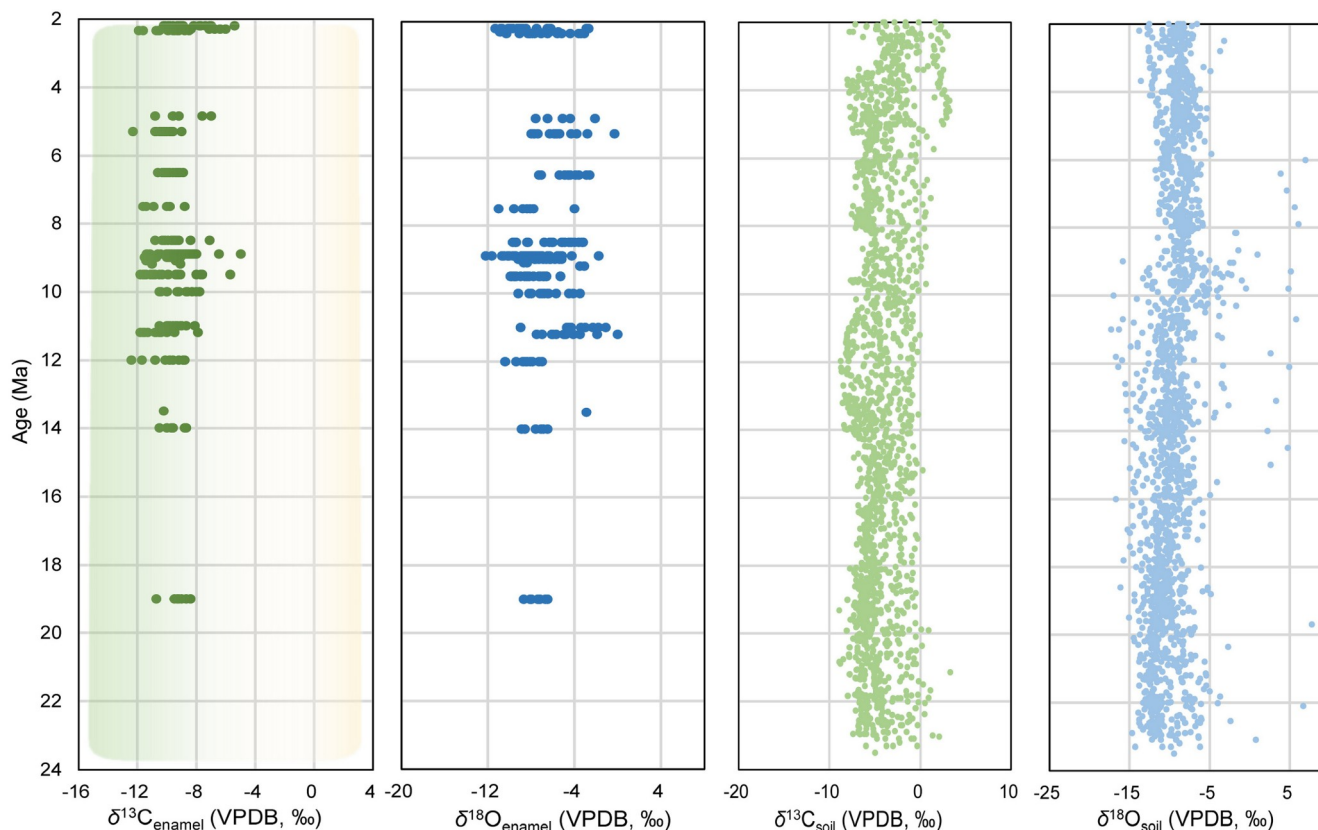


**Figure 5** Neogene stable carbon and oxygen isotope variation trends in the northern Tibetan Plateau. Enamel carbon and oxygen isotope data were collected from the Linxia Basin (Wang and Deng, 2005; Biasatti et al., 2010, 2012;  $n=145$ ), Qaidam Basin (Zhang et al., 2012;  $n=43$ ), Kunlun Pass Basin (Wang Y et al., 2008b;  $n=27$ ) and Xunhua Basin (Hu et al., 2021;  $n=56$ ) (271 samples in total; because of the large amount of data, only the overall sampling data were selected; only carbon isotope data were available for some samples). Paleosol carbon and oxygen isotope data were mainly collected from the Linxia Basin, Lanzhou Basin, Zhuanglang Basin, Subei Basin, Hexi Corridor, Xunhua Basin, Qaidam Basin, and Tarim Basin (Dettman et al., 2003; Kent-Corson et al., 2009; Hough et al., 2011; Zhuang et al., 2011; Li B F et al., 2016; Li L et al., 2016; Dong et al., 2018). There were 1859 samples in total, but only carbon isotope data were available for some samples).

Plateau, as well as in Africa and America during the Late Miocene, as indicated by the positive drift of  $\delta^{13}\text{C}$  in mammalian enamel and paleosol deposits (Quade et al., 1989; Cerling et al., 1997).

The Qaidam Basin also hosts an abundant and continuous Neogene mammal fossil record. In the stable isotope analysis of tooth enamel of herbivore fossils from the Late Miocene to Early Pliocene, it was found that  $\delta^{13}\text{C}$  values reflect ecological habits dominated by consumption of  $\text{C}_3$  vegetation, indicating that the vegetation types in this basin were similar to those in the Linxia Basin (Zhang et al., 2012). However, a few Late Miocene and Early Pliocene samples from the Qaidam Basin had  $\delta^{13}\text{C}$  values higher than  $-8\text{‰}$ , which may indicate that a small amount of  $\text{C}_4$  vegetation was distributed in the Qaidam Basin at this time. In the adjacent Xunhua Basin, the fossil enamel of the *Hipparion* fauna at about 9 Ma had  $\delta^{13}\text{C}$  values distributed between  $-11.4\text{‰}$  and  $-5\text{‰}$  (Hu et al., 2021), which is similar to the data of contemporary fauna in the Qaidam Basin; both show wider distributions and higher averages comparable with the values ( $\delta^{13}\text{C}$ :  $-11.6\text{‰}$  to  $-9.1\text{‰}$ ) of the Dashengou fauna that lived

at the same time in the Linxia Basin.

At a high altitude (about 4700 m) in the Kunlun Pass Basin, south of the Qaidam Basin, the  $\delta^{13}\text{C}$  values ranged from  $-14.8\text{‰}$  to  $-10.6\text{‰}$ , which conforms to the ecological habit of feeding purely on  $\text{C}_3$  vegetation and is consistent with the situation of local modern vegetation (Wang Y et al., 2008b). However, Pliocene fossil enamel of members of the Equidae, Rhinocerotidae and Artiodactyla has  $\delta^{13}\text{C}$  values higher than those of modern mammals ( $-5.4\text{‰}$  to  $-10.2\text{‰}$ ) (the age of fossil materials in the original text was corrected by Wang et al., 2015 as 4.2–3.6 Ma), reflecting an obvious  $\text{C}_4$  signal. This difference indicates that the Pliocene ecosystem of the Kunlun Pass Basin may have contained a small amount of  $\text{C}_4$  vegetation, which is different from the cold and harsh environment in the same area today. The Kunlun Pass Basin was warm and moist in the Pliocene; thus, it may not yet have reached its current height (Wang Y et al., 2008b; Wang et al., 2015).

On the whole, the Neogene paleoenvironmental changes at the northern margin of the Tibetan Plateau, as reflected by carbon isotopes, differed from those in the Loess Plateau and



the North China Plain. The latter two regions had the same rhythm of global  $C_4$  expansion. A large number of studies have found that this event occurred in many areas in northern China from the end of the Miocene to the Early Pliocene (Ding and Yang, 2000; Passey et al., 2009; Zhang et al., 2009; Shen et al., 2018; Lu et al., 2020). This difference can be attributed to the complex geological conditions and frequent tectonic activity at the northeastern margin of the Tibetan Plateau, which led to distinct differences from other regions in the paleoclimate and paleoenvironment. In addition, although there is still a small amount of  $C_4$  vegetation on the Tibetan Plateau (the highest record is about 4500 m above sea level, Wang L et al. (2004), the existing vegetation is mainly dominated by  $C_3$  plants (Deng and Li, 2005; Wang Y et al., 2008a; Xu et al., 2010). The differences between fossil records and living environments reveal important information related to the uplift history of the plateau, and also reflect the high regional diversity of the paleoenvironment at the northern margin of the Tibetan Plateau in the Neogene, when tectonic activity was frequent.

Different from the regional particularity revealed by carbon isotopes, the Neogene oxygen isotope sequence in the northern part of the Tibetan Plateau clearly reflects important signals related to global climate change.

The tooth enamel  $\delta^{18}O$  values of herbivores in the Linxia Basin show that there were several significant climate change events in the Cenozoic; at about 9.7, 7 and 2.5 Ma,  $\delta^{18}O$  underwent obvious positive drift, and the transition near 7 Ma was the most prominent (Wang and Deng, 2005). This can be compared with the analysis results in Pakistan and Nepal based on soil carbonate  $\delta^{18}O$  drift (Quade et al., 1989, 1995), indicating that the changes of climate conditions occurred simultaneously on both sides of the Tibetan Plateau. The  $\delta^{18}O$  values of deposits in the Linxia Basin since 29 Ma drifted rapidly and positively at 12 Ma, and their fluctuation increased after the Pliocene (Dettman et al., 2003). Subsequent oxygen isotope analysis of deposits in the Maogou and Wangjiashan sections also revealed that the climate in the Linxia Basin was gradually becoming more arid, and fluctuation intensified after the Pliocene (Fan et al., 2007).

Isotopic analysis of deposits in the Qaidam, Xunhua, Tarim, and Lanzhou basins and other sites in the northern Tibetan Plateau also revealed that the Late Miocene rapid positive drift of  $\delta^{18}O$  reflects aridity of the global climate and the expansion of grassland environments after the Late Miocene (Kent-Corson et al., 2009; Hough et al., 2011; Zhuang et al., 2011; Li B F et al., 2016; Li L et al., 2016; Dong et al., 2018). Although cross-regional diachronic data comparison cannot easily and clearly reflect the fluctuation of data relative to comparison based on a single site, the  $\delta^{18}O$  values of mammals and deposits in Figure 5 can still show the general positive drift trend after 10 Ma.

However, the  $\delta^{18}O$  values did not increase uniformly with

time; their variation range had a significant increasing trend starting in the Early Pliocene, reflecting the generally intensified aridity in this region. The mammalian  $\delta^{18}O$  values in the Linxia and Qaidam basins showed a negative drift trend at about 11 Ma (Wang and Deng, 2005; Biasatti et al., 2010; Zhang et al., 2012), which is consistent with the cooling event indicated in the marine records of the same period. The background of this phenomenon is related to the change of the tectonic background of the Tibetan Plateau. The violent uplift in the Neogene prevented the flow of warm and humid air from the Indian Ocean and the Bay of Bengal to travel to the north of the Tibetan Plateau (Zhang et al., 2012). The higher  $\delta^{18}O$  values of enamel samples from after the Pliocene indicate obvious variations of  $\delta^{18}O$  in the regional atmospheric precipitation. According to calculation, since the Pliocene, the annual  $\delta^{18}O$  value of precipitation has increased by 3.2‰, and its driving factor is likely to originate from the regional water cycle affected by tectonic and climate changes. The fossil  $\delta^{18}O$  values of fish teeth and bones and gastropod shells indicate that the Kunlun Pass Basin was occupied by freshwater lakes in the Late Pliocene (Wang Y et al., 2008b).

In addition, the results of carbon and oxygen isotope serial sampling in mammalian enamel can be used to indicate the seasonal changes of climate. Serial sampling of three-toed horses, rhinoceroses and proboscideans from the Late Miocene and Early Pliocene in the Qaidam Basin reflects seasonal changes in climate and vegetation (Zhang et al., 2012). The serial data of carbon and oxygen isotopes of bovids of the Longdan fauna in the Linxia Basin show a significant negative correlation trend, which is jointly influenced by summer monsoon rainfall and the emergence of seasonal  $C_4$  vegetation (Biasatti et al., 2010). These studies indicate that since at least the Late Miocene, the East Asian summer monsoon has had a significant impact on the climate of the area east of the Qaidam Basin (An et al., 2001).

In summary, the climatic and environmental background and vegetation development characteristics on the northern Tibetan Plateau in the Cenozoic are not only related to global change, but also have regional features.

## 7.2 Southern Tibetan Plateau

Different from the complex carbon isotope distribution in the northern Tibetan Plateau, the expansion history of  $C_4$  vegetation in the southern Tibetan Plateau, especially in the Siwalik region, is very obvious. As shown in Figure 6, a large number of carbon isotope data of enamel and deposits in the southern Tibetan Plateau recorded the significant transformation of the vegetation system from  $C_3$  to  $C_4$  at about 9–6 Ma, and oxygen isotopes also recorded a positive drift in the same period (Quade et al., 1989, 1992; Sanyal et al., 2004). As shown in Figure 6, carbon isotope changes since the Late Miocene in northern India, Pakistan, Nepal, and Myanmar

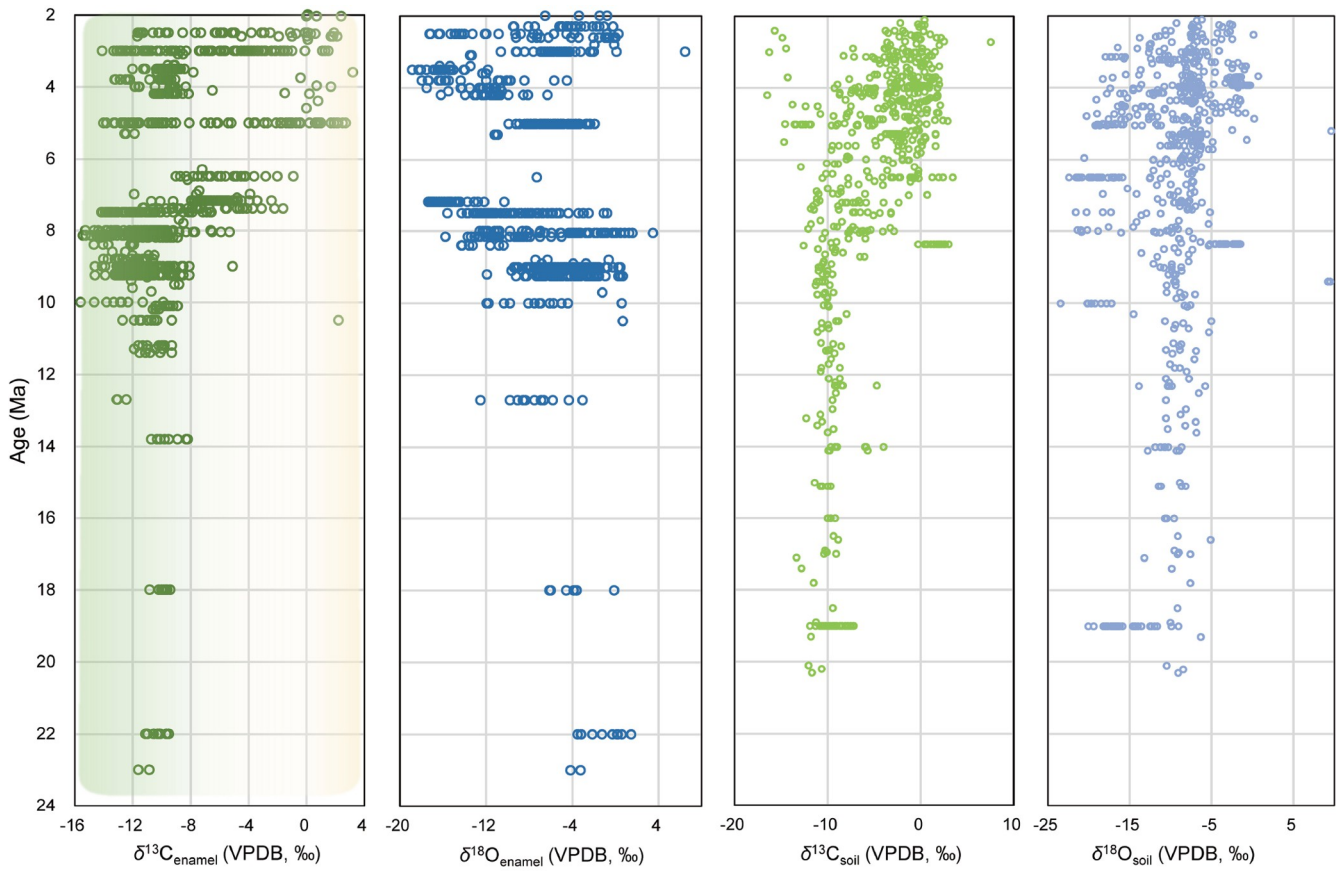


**Figure 6** Neogene stable carbon and oxygen isotope variation trends on the southern Tibetan Plateau. The carbon and oxygen isotope data of enamel were collected from the Gyirong Basin (Wang et al., 2006;  $n=46$ ), Zanda Basin (Wang Y et al., 2013;  $n=74$ ), Yunnan (Biasatti et al., 2012;  $n=154$ ), Myanmar (Zin-Maung-Maung-Thein et al., 2011, 2021;  $n=151$ ) and Siwaliks (including India, Pakistan and Nepal; Quade et al., 1992; Morgan et al., 1994; Stern et al., 1994; Cerling et al., 1999; Bibi, 2007; Nelson, 2007; Badgley et al., 2008; Morgan et al., 2009; Martin et al., 2011; Kimura et al., 2013; Patnaik et al., 2014, 2019; Khan et al., 2020; Waseem et al., 2021a, 2021b; Singh et al., 2023;  $n=859$ ). Because of the large amount of data, only bulk sampling data were selected; only carbon isotope data were available for some samples. Paleosol carbon and oxygen isotope data were mainly collected from Liuqu and Zanda in Xizang Autonomous Region, China as well as India, Nepal, Pakistan, and other regions, with a total of 665 data points. Only carbon isotope data were available for some samples (Quade and Cerling, 1995; Quade et al., 1995; Quade and Roe, 1999; Garzzone et al., 2000a; Sanyal et al., 2005; Saylor et al., 2009; Leary et al., 2017; Vögeli et al., 2017).

have been very obvious. The significance of this carbon isotope drift is that the  $C_4$  savanna in South Asia replaced  $C_3$  forest and woodland in the Late Miocene, resulting in changes of mammal faunas. Most fruit-eating and leaf-eating mammals in forests disappeared, and their ecological niches have been filled by other herbivores that feed on large amounts of  $C_4$  plants. This process of vegetation conversion lasted for more than one million years. A few lineages that persisted through the process of vegetation transformation show that, over time, the  $\delta^{13}C$  values increased. These results are evidence that the vegetation structure and mammalian ecological diversity within the subcontinent were driven by climate for a long time (Barry et al., 2002; Badgley et al., 2008).

In the Himalayan region, carbon and oxygen isotope characteristics are similar to those of Siwaliks at the southern margin of the Tibetan Plateau. Fossil enamel isotopes of the *Hipparion* fauna from about 7 Ma in the Gyirong Basin show that  $\delta^{13}C$  differed from the local modern vegetation characterized by  $C_3$  plants (Deng and Li, 2005), but showed nu-

merous  $C_4$  plant signals. The enamel  $\delta^{13}C$  values of the *Hipparion* fossils in the Gyirong Basin ranged from  $-2.4\%$  to  $-8.0\%$ , and the average value was  $-6.0\% \pm 1.1\%$ , indicating a mixed feeding habit of  $C_3$  and  $C_4$  plants, and thus an ecological environment characterized by sparse forests. In the Tuolin Fm. in the Zanda Basin, enamel  $\delta^{13}C$  values from 4.2 to 3.1 Ma were  $-9.6\% \pm 0.8\%$ , indicating that these mid-Pliocene mammals, like modern herbivores in the region, only ate  $C_3$  plants (Wang X M et al., 2013b). Related to  $\delta^{13}C$ , the enamel  $\delta^{18}O$  of this fauna in the Zanda Basin showed another significant positive drift after about 4–3 Ma in the mid-Pliocene, indicating a more arid climate. The trend of late aridity was also recorded in mammals at several localities during the late Neogene in Yunnan, but only  $C_4$  vegetation signals were found in Early Pleistocene fossil samples from Shangri-La and Yuanmou (Biasatti et al., 2012).

Because of the impact of the strong uplift of the Tibetan Plateau, the Late Miocene climate change characteristics detected in the Siwalik area on the southern margin and the

Linxia Basin on the northern margin of the plateau seem to be a regional response to global change. In addition, the strong uplift of the Tibetan Plateau in the Late Miocene strengthened the thermal contrast between sea and land, thus strengthening the monsoon circulation and leading to the expansion of C<sub>4</sub> vegetation (Quade et al., 1989, 1995; Quade and Cerling, 1995; Kutzbach et al., 1993; Prell and Kutzbach, 1992). The Linxia Basin still lacked C<sub>4</sub> plants in the Neogene, showing that the East Asian summer monsoon, which can bring atmospheric precipitation and a climate suitable for C<sub>4</sub> plants to northern China, was not enough to affect the northern Tibetan Plateau. The lack of C<sub>4</sub> plants during the Neogene in the Linxia Basin may be related to the fact that the early humid period in the basin and the later rapid cooling inhibited the growth of C<sub>4</sub> plants associated with dry and hot climates (Wu et al., 2022) (Figure 5).

## 8. Problems and prospects

The Neogene was an important period for the uplift of the Tibetan Plateau, and the Neogene strata of the plateau and surrounding areas have received extensive attention, because research in different directions of related disciplines requires a unified and accurate time scale. There has been a relatively complete and well-determined scheme for the division of the Neogene around the world; however, not only are marine strata taken as the standard, but also the selected stratotype sections are in the Mediterranean region. Thus, it is difficult to compare these standards with the Tibetan Plateau and its surrounding areas, which are dominated by terrestrial strata. Although terrestrial strata and the mammalian fossils they contain have different characteristics from marine successions, we generally try our best to keep the boundaries consistent between them. However, two Neogene GSSPs have not yet been established, those of the Burdigalian and Langhian stages; these awaited international standards will be useful in stratigraphic work on the Tibetan Plateau. In addition, the GSSPs of various stages of the Neogene system are defined by paleomagnetism (Hilgen et al., 2012), which can build a bridge between sea and land. Foraminifera and calcareous nannofossils are important biostratigraphic markers in marine strata, whereas mammals and ostracods in terrestrial strata have good stratigraphic division and correlation significance, especially small mammals such as rodents.

When paleomagnetism is used for absolute dating, a reasonable interpretation scheme can be obtained by matching with the ages determined based on mammalian fossils, and the results will be more reliable if isotopic dating results are used as constraints. However, similar to the Neogene strata in the entire East Asia region, the Neogene in the Tibetan Plateau also lacks isotopic absolute ages because of the scarcity of materials such as volcanic ash that can be used for

isotopic dating. Additional field work is needed to find volcanic rock interbeds, and other laboratory methods are needed to develop different dating approaches. Mammal fossils, especially small mammal fossils, have the characteristics of rapid evolution, wide distribution, and large quantities, but only compared with other mammalian groups; they are not comparable with foraminifera or other microfossils in terms of the above three characteristics. Therefore, much work still remains to be done in the division and correlation of Neogene strata in the Tibetan Plateau; for example, no mammal fossils have been found in the Burang and Thakkhola basins. Even in the Linxia Basin, which has the most abundant Neogene mammal fossils in Eurasia, poor continuity and difficulty in accurate calibration of taxon range zones remain persistent problems (Deng et al., 2013b).

Cenozoic terrestrial strata are mainly composed of lake and river deposits. Compared with marine deposits, they have small horizontal distribution ranges, are mostly isolated from each other, change rapidly in lithofacies, have many sedimentary discontinuities, and are often lacking in widely distributed marker beds. Without the help of other means, correlation between different sedimentary areas is often very difficult. However, since the Jurassic, especially in the Cenozoic, the share of terrestrial strata on land has increased rapidly, and by the Neogene, it far exceeded the share of marine strata, especially in Asia and North America. The global standard chronostratigraphy and geological chronology system established based on marine facies has been greatly limited at the stage/age level in the Cenozoic, especially in the Neogene (Qiu et al., 2013). China has widely developed Neogene terrestrial strata and abundant mammalian fossils, especially in the Linxia Basin on the northeastern margin of the Tibetan Plateau. Therefore, the establishment and improvement of the Chinese Neogene terrestrial stages based on mammalian fossils and marked by paleomagnetic dating methods have been widely recognized and adopted by international peers (Qiu et al., 2013). In the future, this work will also play a greater role in establishing the Neogene regional geological chronology of Asia, especially in the middle and high latitudes of the Asian continent.

**Acknowledgements** We thank Prof. Zhanxiang QIU, Prof. Zhuding QIU, Prof. Banyue WANG, Prof. Xijun NI of Institute of Vertebrate Paleontology and Paleoanthropology, Chinese Academy of Sciences, Prof. Xiaoming WANG of Natural History Museum of Los Angeles County, Dr. Lawrence FLYNN of Harvard University, and Prof. Chenglong DENG of Institute of Geology and Geophysics, Chinese Academy of Sciences for their guidance and help in the fieldwork and research. We thank Sara J. MASON for her editing the English text. The two reviewers are kindly acknowledged for their constructive comments on the manuscript. This work was supported by the Second Comprehensive Scientific Expedition on the Tibetan Plateau (Grant No. 2019QZKK0705), the Strategic Priority Research Program of the Chinese Academy of Sciences (Grant Nos. XDB26030000, XDA20070203), and the National Natural Science Foundation of China (Grant Nos. 41872005, 41872006).

**Conflict of interest** The authors declare that they have no conflict of interest.

## References

- Adhikari B R, Wagneich M. 2013. Microfacies analysis and paleoenvironmental significance of palustrine carbonates in the Thakkhola-Mustang Graben (Nepal Himalaya). *J Asian Earth Sci*, 77: 117–126
- An Z S, Kutzbach J E, Prell W L, Porter S C. 2001. Evolution of Asian monsoons and phased uplift of the Himalaya-Tibetan Plateau since Late Miocene times. *Nature*, 411: 62–66
- Antoine P O, Duranthon F, Welcomme J L. 2003. *Alicornops* (Mammalia, Rhinocerotidae) dans le Miocène supérieur des Collines Bugti (Balouchistan, Pakistan): Implications phylogénétiques. *Geodiversitas*, 25: 575–603
- Antoine P O, Métais G, Orliac M J, Crochet J Y, Flynn L J, Marivaux L, Rajpar A R, Roohi G, Welcomme J L. 2013. Mammalian Neogene biostratigraphy of the Sulaiman Province, Pakistan. In: Wang X M, Flynn L J, Fortelius M, eds. *Fossil Mammals of Asia: Neogene Biostratigraphy and Chronology*. New York: Columbia University Press. 400–422
- Badgley C, Barry J C, Morgan M E, Nelson S V, Behrensmeyer A K, Cerling T E, Pilbeam D. 2008. Ecological changes in Miocene mammalian record show impact of prolonged climatic forcing. *Proc Natl Acad Sci USA*, 105: 12145–12149
- Barry J C, Behrensmeyer A K, Badgley C E, Flynn L J, Peltonen H, Cheema I U, Pilbeam D, Lindsay E H, Raza S M, Rajpar A R, Morgan M E. 2013. The Neogene Siwaliks of the Potwar Plateau, Pakistan. In: Wang X M, Flynn L J, Fortelius M, eds. *Fossil Mammals of Asia: Neogene Biostratigraphy and Chronology*. New York: Columbia University Press. 374–399
- Barry J C, Morgan M E, Flynn L J, Pilbeam D, Behrensmeyer A K, Raza S M, Khan I A, Badgley C, Hicks J, Kelley J. 2002. Faunal and environmental change in the late Miocene Siwaliks of northern Pakistan. *Paleobiology*, 28: 1–71
- Beck R A, Burbank D W, Sercombe W J, Riley G W, Barndt J K, Berry J R, Afzal J, Khan A M, Jurgen H, Metje J, Cheema A, Shafique N A, Lawrence R D, Khan M A. 1995. Stratigraphic evidence for an early collision between northwest India and Asia. *Nature*, 373: 55–58
- Biasatti D, Wang Y, Deng T. 2010. Strengthening of the East Asian summer monsoon revealed by a shift in seasonal patterns in diet and climate after 2–3 Ma in northwest China. *Palaeogeogr Palaeoclimatol Palaeoecol*, 297: 12–25
- Biasatti D, Wang Y, Gao F, Xu Y, Flynn L. 2012. Paleocologies and paleoclimates of late Cenozoic mammals from Southwest China: Evidence from stable carbon and oxygen isotopes. *J Asian Earth Sci*, 44: 48–61
- Bibi F. 2007. Dietary niche partitioning among fossil bovids in late Miocene C<sub>3</sub> habitats: Consilience of functional morphology and stable isotope analysis. *Palaeogeogr Palaeoclimatol Palaeoecol*, 253: 529–538
- Bohlin B. 1937. Eine Tertiär Saugetier-Fauna aus Tsaidam. *Palaeont Sin Ser C*, 14:1–111
- Bohlin B. 1942. The fossil mammals from the Tertiary deposit of Tabenbuluk, western Kansu. Part I: Insectivora and Lagomorpha. *Palaeont Sin New Ser C*, 8a: 1–113
- Bohlin B. 1946. The fossil mammals from the Tertiary deposit of Tabenbuluk, western Kansu. Part II: Simplicidentata, Carnivora, Artiodactyla, Perissodactyla, and Primates. *Palaeont Sin New Ser C*, 8b: 1–259
- Cao L. 1982. Pliocene palynological flora in Disong of Burang, Xizang (Tibet) (in Chinese). *Acta Palaeont Sin*, 21: 469–483
- Castradori D, Rio D, Hilgen F J, Lourens L J. 1998. The Global Standard Stratotype-section and Point (GSSP) of the Piacenzian Stage (Middle Pliocene). *Episodes*, 21: 88–93
- Cerling T E, Harris J M, Leakey M G. 1999. Browsing and grazing in elephants: The isotope record of modern and fossil proboscideans. *Oecologia*, 120: 364–374
- Cerling T E, Harris J M, MacFadden B J, Leakey M G, Quade J, Eisenmann V, Ehleringer J R. 1997. Global vegetation change through the Miocene/Pliocene boundary. *Nature*, 389: 153–158
- Chang H, Fang X M, An Z S, Song C H, Qiang X K. 2001. Miocene-Pliocene strata features in the Suerkal Basin and the paleo-environment significance (in Chinese). *Mar Geol Quat Geol*, 21: 107–111
- Chen G F. 2003. A new genus of Pliohyracinae (Hyracoidea, mammalia) from the Late Pliocene of Dege, Sichuan, China (in Chinese). *Vert Palasiat*, 41: 240–248
- Chen H H, Han J T, Ding Z L, Sun H G, Guo Z F. 2008. Chronological dating and tectonic implications of late Cenozoic volcanic rocks and lacustrine sequence in Oiyug Basin of southern Tibet. *Sci China Ser D-Earth Sci*, 51: 275–283
- Chen S K, Pang L B, Deng T, Qi G Q. 2016. Chalicotheriidae (Mammalia, Perissodactyla) from the *Lufengpithecus* locality of Lufeng, Yunnan Province, China. *Historical Biol*, 28: 270–279
- Chen X H, Dang Y Q, Yin A, Wang L Q, Jiang W M, Jiang R B, Zhou S P, Liu M D, Ye B Y, Zhang M, Ma L X, Li L. 2010. The Coupling and Tectonics Evolution of Qaidam Basin and Its Surrounding Mountains (in Chinese). Beijing: Geological Publishing House. 1–365
- Chen Z L, Bai Y F, Chen B L, Wang X F, Chen X H, Liu J. 2003. Sedimentation and tectonic evolution of the north Xorkol Basin in the Altyn Tagh Range (in Chinese). *Geol Bull China*, 33: 405–411
- Chiu C S, Li C K, Chiu C T. 1979. The Chinese Neogene: A preliminary review of the mammalian localities and faunas. *Ann Geol Pays Hellen, Hors Serie*, 1: 263–272
- Clift P D, Shimizu N, Layne G D, Blusztajn J. 2001. Tracing patterns of erosion and drainage in the Paleogene Himalaya through ion probe Pb isotope analysis of detrital K-feldspars in the Indus Molasse, India. *Earth Planet Sci Lett*, 188: 475–491
- Deng T. 2003. New material of *Hispanotherium matritense* (Rhinocerotidae, Perissodactyla) from Laogou of Hezheng County (Gansu, China), with special reference to the Chinese Middle Miocene elasmotheres. *Geobios*, 36: 141–150
- Deng T. 2006a. Chinese Neogene mammal biochronology. *Vert Palasiat*, 44: 143–163
- Deng T. 2006b. A primitive species of *Chilotherium* (Perissodactyla, Rhinocerotidae) from the Late Miocene of the Linxia Basin (Gansu, China). *Cain Res*, 5: 93–102
- Deng T, Hou S K. 2014. The Neogene terrestrial chronostratigraphic sequence of China. In: Rocha R, Pais J, Finney S, Kullberg J C, eds. *STRATI 2013: First International Congress on Stratigraphy at the Cutting Edge of Stratigraphy*. Cham: Springer. 1009–1012
- Deng T, Hou S K, Shi Q Q. 2015a. Selection of the lower boundary stratotype of the terrestrial Upper Miocene Bahean Stage in China (in Chinese). *Acta Geosci Sin*, 36: 523–532
- Deng T, Hou S K, Shi Q Q, Chen S K, He W, Chen S Q. 2011a. Terrestrial Mio-Pliocene boundary in the Linxia Basin, Gansu, China. *Acta Geol Sin-Engl Ed*, 85: 452–464
- Deng T, Hou S K, Wang N, Lu X K, Li Y K, Li Y. 2015b. *Hipparion* fossils of the Dati Basin in Nyalam, Tibet, China and their paleoecological and paleoaltimetry implications (in Chinese). *Quat Sci*, 35: 493–501
- Deng T, Hou S K, Wang S Q. 2019a. Neogene integrative stratigraphy and timescale of China. *Sci China Earth Sci*, 62: 310–323
- Deng T, Hou S K, Xie G P, Wang S Q, Shi Q Q, Chen S K, Sun B Y, Lu X K. 2013a. Chronostratigraphic subdivision and correlation of the Upper Miocene of the Linxia Basin in Gansu, China (in Chinese). *J Stratigr*, 37: 417–427
- Deng T, Li Y M. 2005. Vegetational ecotype of the Gyirong Basin in Tibet, China and its response in stable carbon isotopes of mammal tooth enamel. *Chin Sci Bull*, 50: 1225–1229
- Deng T, Lu X K, Wang S Q, Flynn L J, Sun D H, He W, Chen S Q. 2021a. An Oligocene giant rhino provides insights into *Paraceratherium* evolution. *Commun Biol*, 4: 639
- Deng T, Qi G Q. 2009. Rhinocerotids (Mammalia, Perissodactyla) from *Lufengpithecus* site, Lufeng, Yunnan (in Chinese). *Vert Palasiat*, 47: 135–152
- Deng T, Qiu Z X, Wang B Y, Wang X M, Hou S K. 2013b. Late Cenozoic

- biostratigraphy of the Linxia Basin, northwestern China. In: Wang X M, Flynn L J, Fortelius M, eds. *Fossil Mammals of Asia: Neogene Biostratigraphy and Chronology*. New York: Columbia University Press. 243–273
- Deng T, Wang S Q, Xie G P, Li Q, Hou S K, Sun B Y. 2012. A mammalian fossil from the Dingqing Formation in the Lunpola Basin, northern Tibet, and its relevance to age and paleo-altimetry. *Chin Sci Bull*, 57: 261–269
- Deng T, Wang X M. 2004a. New material of the Neogene rhinocerotids from the Qaidam Basin in Qinghai, China (in Chinese). *Vert Palasiat*, 43: 216–229
- Deng T, Wang X M. 2004b. Late Miocene *Hipparion* (Equidae, Mammalia) of eastern Qaidam Basin in Qinghai, China (in Chinese). *Vert Palasiat*, 43: 316–333
- Deng T, Wang X M, Fortelius M, Li Q, Wang Y, Tseng Z J, Takeuchi G T, Saylor J E, Säilä L K, Xie G P. 2011b. Out of Tibet: Pliocene woolly rhino suggests high-plateau origin of Ice Age megaherbivores. *Science*, 333: 1285–1288
- Deng T, Wang X M, Ni X J, Liu L P, Liang Z. 2004. Cenozoic stratigraphic sequence of the Linxia Basin in Gansu, China and its evidence from mammal fossils (in Chinese). *Vert Palasiat*, 42: 45–66
- Deng T, Wang X M, Wu F X, Wang Y, Li Q, Wang S Q, Hou S K. 2019b. Review: Implications of vertebrate fossils for paleo-elevations of the Tibetan Plateau. *Glob Planet Change*, 174: 58–69
- Deng T, Wu F X, Su T. 2021b. Cenozoic Paleontological Expedition Report on the River and Lake Sources in the Tibetan Plateau (in Chinese). Beijing: Science Press. 1–378
- Deng T, Wu F X, Wang S Q, Su T, Zhou Z K. 2019c. Significant shift in the terrestrial ecosystem at the Paleogene/Neogene boundary in the Tibetan Plateau (in Chinese). *Chin Sci Bull*, 64: 2894–2906
- Deng T, Wu F X, Wang S Q, Su T, Zhou Z K. 2021c. Major turnover of biotas across the Oligocene/Miocene boundary on the Tibetan Plateau. *Palaeogeogr Palaeoclimatol Palaeoecol*, 567: 110241
- Dettman D L, Fang X M, Garzzone C N, Li J J. 2003. Uplift-driven climate change at 12 Ma: A long  $\delta^{18}\text{O}$  record from the NE margin of the Tibetan Plateau. *Earth Planet Sci Lett*, 214: 267–277
- Ding L, Maksatbek S, Cai F L, Wang H Q, Song P P, Ji W Q, Xu Q, Zhang L Y, Muhammad Q, Upendra B. 2017. Processes of initial collision and suturing between India and Asia. *Sci China Earth Sci*, 60: 635–651
- Ding Z L, Yang S L. 2000.  $\text{C}_3/\text{C}_4$  vegetation evolution over the last 7.0 Myr in the Chinese Loess Plateau: Evidence from pedogenic carbonate  $\delta^{13}\text{C}$ . *Palaeogeogr Palaeoclimatol Palaeoecol*, 160: 291–299
- Dong J B, Liu Z H, An Z S, Liu W G, Zhou W J, Qiang X K, Lu F Y. 2018. Mid-Miocene  $\text{C}_4$  expansion on the Chinese Loess Plateau under an enhanced Asian summer monsoon. *J Asian Earth Sci*, 158: 153–159
- Dong W, Qi G Q. 2013. Hominoid-producing localities and biostratigraphy in Yunnan. In: Wang X M, Flynn L J, Fortelius M, eds. *Fossil Mammals of Asia: Neogene Biostratigraphy and Chronology*. New York: Columbia University Press. 293–309
- Falconer H. 1868. On the fossil rhinoceros of central Tibet and its relation to the recent upheaval of the Himalayahs. In: Murchison C, ed. *Paleontological Memoirs and Notes of the Late Hugh Falconer*, Vol. I. London: R Hardwicke. 173–185
- Fan M J, Dettman D L, Song C H, Fang X M, Garzzone C N. 2007. Climatic variation in the Linxia basin, NE Tibetan Plateau, from 13.1 to 4.3 Ma: The stable isotope record. *Palaeogeogr Palaeoclimatol Palaeoecol*, 247: 313–328
- Fang X M, Garzzone C, Van V R, Li J J, Fan M J. 2003. Flexural subsidence by 29 Ma on the NE edge of Tibet from the magnetostratigraphy of Linxia Basin, China. *Earth Planet Sci Lett*, 210: 545–560
- Fang X M, Wang J Y, Zhang W L, Zan J B, Song C H, Yan M D, Appel E, Zhang T, Wu F L, Yang Y S, Lu Y. 2016. Tectonosedimentary evolution model of an intracontinental flexural (foreland) basin for paleoclimatic research. *Glob Planet Change*, 145: 78–97
- Fang X M, Zhang W L, Meng Q Q, Gao J P, Wang X M, King J, Song C H, Dai S, Miao Y F. 2007. High-resolution magnetostratigraphy of the Neogene Huaitoutala section in the eastern Qaidam Basin on the NE Tibetan Plateau, Qinghai Province, China and its implication on tectonic uplift of the NE Tibetan Plateau. *Earth Planet Sci Lett*, 258: 293–306
- Flynn L J, Downs W, Opdyke N, Huang K N, Lindsay E, Ye J, Xie G P, Wang X M. 1999. Recent advances in the small mammal biostratigraphy and magnetostratigraphy of Lanzhou Basin. *Chin Sci Bull*, 44 (Suppl): 105–118
- Flynn L J, Lindsay E H, Pilbeam D, Raza S M, Morgan M E, Barry J C, Badgley C E, Behrensmeyer A K, Cheema I U, Rajpar A R, Opdyke N D. 2013. The Siwaliks and Neogene evolutionary biology in South Asia. In: Wang X M, Flynn L J, Fortelius M, eds. *Fossil Mammals of Asia: Neogene Biostratigraphy and Chronology*. New York: Columbia University Press. 353–309
- Garzzone C N, Dettman D L, Quade J, DeCelles P G, Butler R F. 2000a. High times on the Tibetan Plateau: Paleoelevation of the Thakkhola graben, Nepal. *Geology*, 28: 339–342
- Garzzone C N, Quade J, DeCelles P G, English N B. 2000b. Predicting paleoelevation of Tibet and the Himalaya from  $\delta^{18}\text{O}$  vs. altitude gradients in meteoric water across the Nepal Himalaya. *Earth Planet Sci Lett*, 183: 215–229
- Geng G C, Tao J R. 1982. Tertiary plants from Xizang (in Chinese). In: *The Comprehensive Scientific Expedition to the Qinghai-Xizang Plateau, the Chinese Academy of Sciences, ed. Palaeontology of Xizang*, Book 5. Beijing: Science Press. 110–124
- Gilder S, Chen Y, Sen S. 2001. Oligo-Miocene magnetostratigraphy and rock magnetism of the Xishuigou section, Subei (Gansu Province, western China) and implications for shallow inclinations in central Asia. *J Geophys Res*, 106: 30505–30521
- Gu Z G, Zhang X D, Xie G P. 1988. The Pliocene beds in Mount Hongyazi, in the main range of Qilian Mountains and the northern rimland of Chaidam Basin (in Chinese). *J Lanzhou Univ Nat Sci*, 24: 78–83
- Guo Z T, Ruddiman W F, Hao Q Z, Wu H B, Qiao Y S, Zhu R X, Peng S Z, Wei J J, Yuan B Y, Liu T S. 2002. Onset of Asian desertification by 22 Myr ago inferred from loess deposits in China. *Nature*, 416: 159–163
- He H Y, Deng C L, Pan Y X, Deng T, Luo Z H, Sun J M, Zhu R X. 2011. New  $^{40}\text{Ar}/^{39}\text{Ar}$  dating results from the Shanwang Basin, eastern China: Constraints on the age of the Shanwang Formation and associated biota. *Phys Earth Planet Inter*, 187: 66–75
- He H Y, Sun J M, Li Q L, Zhu R X. 2012. New age determination of the Cenozoic Lunpola basin, central Tibet. *Geol Mag*, 149: 141–145
- Hilgen F, Aziz H A, Bice D, Iaccarino S, Krijgsman W, Kuiper K, Montanari A, Raffi I, Turco E, Zachariasse W J. 2005. The Global boundary Stratotype Section and Point (GSSP) of the Tortonian Stage (Upper Miocene) at Monte Dei Corvi. *Episodes*, 28: 6–17
- Hilgen F J, Iaccarino S, Krijgsman W, Villa G, Langereis C G, Zachariasse W J. 2000. The Global Boundary Stratotype Section and Point (GSSP) of the Messinian Stage (uppermost Miocene). *Episodes*, 23: 172–178
- Hilgen F J, Lourens L J, Van Dam J A. 2012. The Neogene Period. In: *The Geological Time Scale 2012*. Amsterdam: Elsevier Scientific Publishing Company. 923–978
- Hou S K, Deng T. 2014. A new species of *Chleuastochoerus* (Artiodactyla: Suidae) from the Linxia Basin, Gansu Province, China. *Zootaxa*, 3872: 401–439
- Hou S K, Cydylo M, Danowitz M, Solounias N. 2019. Comparisons of *Schansitherium tafeli* with *Samotherium boissieri* (Giraffidae, Mammalia) from the Late Miocene of Gansu Province, China. *PLoS ONE*, 14: e0211797
- Hough B G, Garzzone C N, Wang Z, Lease R O, Burbank D W, Yuan D. 2011. Stable isotope evidence for topographic growth and basin segmentation: Implications for the evolution of the NE Tibetan Plateau. *Geol Soc Am Bull*, 123: 168–185
- Hsu J, Tao J R, Sun X J. 1973. On the discovery of a *Quercus semicarpifolia* bed in Mount Shisha Pangma and its significance in botany and geology (in Chinese). *Acta Bot Sin*, 1973, 15: 103–119
- Hu F, Song B W, Sun Y Y, Huang W, Luo M S, Ji J L, Lin Q X, Algeo T J, Zhang K X. 2021. Paleodietary and paleoclimatic reconstruction of *Hipparion* Fauna at ~9 Ma from the Xunhua Basin on the Northeastern Tibetan Plateau. *Front Earth Sci*, 9: 717720

- Huang C X, Li B Y, Zhang Q S, Liang Y L, Wang F B. 1980. An analysis of the pollen-spores assemblages and the age of the stratum from Dati palaeo-lake basin at Nainnainxunla, South Xizang (in Chinese). In: *The Scientific Expedition to Tibet*, Chinese Academy of Sciences, ed. Palaeontology of Xizang, Book 1. Beijing: Science Press. 97–106
- Huang W B, Ji H X, Chen W Y, Hsu C Q, Zheng S H. 1980. Pliocene stratum of Guizhong and Bulong Basin, Xizang. In: *The Scientific Expedition to Tibet*, Chinese Academy of Sciences, ed. Palaeontology of Xizang, Book 1. Beijing: Science Press. 4–17
- Ji H X, Hsu C Q, Huang W P. 1980. The *Hipparion* fauna from Guizhong Basin, Xizang (in Chinese). In: *The Scientific Expedition to Tibet*, Chinese Academy of Sciences, ed. Palaeontology of Xizang, Book 1. Beijing: Science Press. 18–32
- Jiangzuo Q G, Li S J, Fu J, Wang S Q, Ji X P, Duan M, Che D C. 2022a. Fossil Felidae (Carnivora: Mammalia) from the Yuanmou hominid site, southern China (Late Miocene) and its significance in the living environment of the fossil ape. *Zool J Linnean Soc*, 196: 1156–1174
- Jiangzuo Q G, Niu K C, Li S J, Fu J, Wang S Q. 2022b. A diverse metalurine guild from the Latest Miocene Xingjiawan Fauna, Yongdeng, Northwestern China, and generic differentiation of metalurine felids. *J Mammal Evol*, 29: 845–862
- Jiangzuo Q G, Wang S Q, Li C X, Sun D H, Zhang X X. 2019. New material of *Gobicyon* (Carnivora, Amphicyonidae, Haplocyoninae) from northern China and a review of Aktaucyonini evolution. *Pap Palaeont*, 7: 307–327
- Jiangzuo Q G, Wang S Q, Deng T. 2023. Chronological framework and palaeoecology of Carnivora from the Linxia Basin, China. *Palaeogeogr Palaeoclimatol Palaeoecol*, 615: 111463
- Johnson G D, Zeitler P, Naeser C W, Johnson N M, Summers D M, Frost C D, Opdyke N D, Tahirkheli R A K. 1982. The occurrence and fission-track ages of late Neogene and Quaternary volcanic sediments, Siwalik group, Northern Pakistan. *Palaeogeogr Palaeoclimatol Palaeoecol*, 37: 63–93
- Johnson N M, Stix J, Tauxe L, Cervený P F, Tahirkheli R A K. 1985. Paleomagnetic chronology, fluvial processes, and tectonic implications of the Siwalik Deposits near Chinji Village, Pakistan. *J Geol*, 93: 27–40
- Kempf O, Blisniuk P M, Wang S F, Fang X M, Wrozyńska C, Schwab A. 2009. Sedimentology, sedimentary petrology, and paleoecology of the monsoon-driven, fluvio-lacustrine Zhada Basin, SW-Tibet. *Sediment Geol*, 222: 27–41
- Kent-Connors M L, Ritts B D, Zhuang G, Bovet P M, Graham S A, Chamberlain C P. 2009. Stable isotopic constraints on the tectonic, topographic, and climatic evolution of the northern margin of the Tibetan Plateau. *Earth Planet Sci Lett*, 282: 158–166
- Khan A M, Iqbal A, Waseem M T, Ahmad R M, Ali Z. 2020. Palaeodietary and palaeoclimatic interpretations for herbivore fauna from Late Pliocene to Early Pleistocene Siwaliks of Pakistan. *J Anim Plant Sci*, 30: 355–363
- Kimura Y, Jacobs L L, Cerling T E, Uno K T, Ferguson K M, Flynn L J, Patnaik R. 2013. Fossil mice and rats show isotopic evidence of niche partitioning and change in dental ecomorphology related to dietary shift in Late Miocene of Pakistan. *PLoS ONE*, 8: e69308
- Kordikova E G, Heizmann E P J, de Bruijn H. 2004. Early-Middle Miocene vertebrate faunas from Western Kazakhstan. Part 1. Rodentia, Insectivora, Chiroptera, and Lagomorpha. *N Jb Geol Paläont Abh*, 231: 219–276
- Kutzbach J E, Prell W L, Ruddiman W F. 1993. Sensitivity of Eurasian climate to surface uplift of the Tibetan Plateau. *J Geol*, 101: 177–190
- Leary R J, Quade J, DeCelles P G, Reynolds A. 2017. Evidence from paleosols for low to moderate elevation of the India-Asia suture zone during mid-Cenozoic time. *Geology*, 45: 399–402
- Lei Q L, Fu X Y, Lu Y P. 1996. Petroleum geological features of Tertiary terrestrial Lunpola Basin, Xizang (Tibet) (in Chinese). *Ear Sci J China Univ Geosci*, 21: 168–173
- Li B F, Sun D H, Wang X, Zhang Y B, Hu W E, Wang F, Li Z J, Ma Z W, Liang B Q. 2016.  $\delta^{18}\text{O}$  and  $\delta^{13}\text{C}$  records from a Cenozoic sedimentary sequence in the Lanzhou Basin, Northwestern China: Implications for palaeoenvironmental and palaeoecological changes. *J Asian Earth Sci*, 125: 22–36
- Li C K, Qiu Z D. 1980. Early Miocene mammalian fossils of Xining Basin, Qinghai (in Chinese). *Vert Palasiat*, 18: 198–214
- Li C K, Wu W Y, Qiu Z D. 1984. Chinese Neogene: Subdivision and correlation (in Chinese). *Vert Palasiat*, 22: 163–178
- Li C X, Ji X P, Zhang S T, Luo J, Su Y P, Li Y B, Zhen M, Hou S K, Jiangzuo Q G, Zhang X X, Zhu Y S, Xu H L, Bai X C, Yang Y, Wang S Q. 2021. The new fossil record of *Stegolophodon latidens* from the Xiaolongtan locality, Yunnan, China, and the discussion on the age of the *Lufengpithecus keiyuanensis* (in Chinese). *Chin Sci Bull*, 66: 1469–1481
- Li F L, Li D L. 1990. Latest Miocene *Hipparion* (*Plesiohipparion*) of Zanda Basin (in Chinese). In: Yang Z Y, Nie Z T, eds. *Paleontology of the Ngari Area, Tibet* (Xizang). Wuhan: China Univ Geoscience Press. 186–193
- Li H B, Yang J S, Shi R D, Wu C L, Tapponnier P, Wan Y S, Zhang J X, Meng F C. 2002. Determination of the Altyn Tagh strike-slip fault basin and its relationship with mountains. *Chin Sci Bull*, 47: 572–577
- Li J J, Zhang J, Song C H, Zhao Z J, Zhang Y, Wang X X, Zhang J M, Cui Q Y. 2006. Miocene Bahean stratigraphy in the Longzhong Basin, northern central China and its implications in environmental change. *Sci China Ser D*, 49: 1270–1279
- Li L, Garzione C N, Pullen A, Chang H. 2016. Early-middle Miocene topographic growth of the northern Tibetan Plateau: Stable isotope and sedimentation evidence from the southwestern Qaidam basin. *Palaeogeogr Palaeoclimatol Palaeoecol*, 461: 201–213
- Li J X, Yue L P, Pan F, Zhang R, Guo L, Xi R G, Guo L. 2014. Intensified aridity of the Asian interior recorded by the magnetism of red clay in Altun Shan, NE Tibetan Plateau. *Palaeogeogr Palaeoclimatol Palaeoecol*, 411: 30–41
- Li P. 1955. A preliminary understanding of the geology of eastern Tibet (in Chinese). *Chin Sci Bull*, 6: 62–71
- Li Q. 2010. Note on the cricetids from the Pliocene Gaotege locality, Nei Mongol. *Vert Palasiat*, 48: 247–261
- Li Q, Stidham T A, Ni X J, Li L Z. 2017. Two new Pliocene hamsters (Cricetidae, Rodentia) from southwestern Tibet (China), and their implications for rodent dispersal ‘into Tibet’. *J Vertebrate Paleontol*, 37: e1403443
- Li Q, Wang S Q, Xie G P. 2011. Discovery of fossil *Equus* near Menshi (Mioncer, or Menci), Ngari, Xizang (Tibet) (in Chinese). *Quat Sci*, 31: 689–698
- Li Q, Wang X M. 2014. *Qaidamomys fortellii*, a new Late Miocene murid from Qaidam Basin, North Qinghai-Xizang Plateau, China. *Ann Zool Fennici*, 51: 17–26
- Li Q, Wang X M. 2015. Discovery of Neogene beavers (Castoridae, Mammalia) in central Qaidam Basin, and their palaeoenvironmental significance. *Quat Sci*, 35: 584–595
- Li Q, Wang X M, Xie G P, Yin A. 2013. Oligocene-Miocene mammalian fossils from Hongyazi Basin and its bearing on tectonics of Danghe Nanshan in Northern Tibetan Plateau. *PLoS ONE*, 8: e82816
- Li Q, Xie G P, Takeuchi G T, Deng T, Tseng Z J, Grohé C, Wang X M. 2014. Vertebrate fossils on the roof of the world: Biostratigraphy and geochronology of high-elevation Kunlun Pass Basin, northern Tibetan Plateau, and basin history as related to the Kunlun strike-slip fault. *Palaeogeogr Palaeoclimatol Palaeoecol*, 411: 46–55
- Li Q, Zhou X Y, Ni X J, Fu B H, Deng T. 2020. Latest Middle Miocene fauna and flora from Kumkol Basin of northern Qinghai-Xizang Plateau and paleoenvironment. *Sci China Earth Sci*, 63: 188–201
- Li S, Deng C L, Dong W, Sun L, Liu S Z, Qin H F, Yin J Y, Ji X P, Zhu R X. 2015. Magnetostratigraphy of the Xiaolongtan Formation bearing *Lufengpithecus keiyuanensis* in Yunnan, southwestern China: Constraint on the initiation time of the southern segment of the Xianshuihe-Xiaojiang fault. *Tectonophysics*, 655: 213–226
- Li T D, Qi S J. 1982. Tertiary System in the middle section of the Altyn Mountains, Xinjiang (in Chinese). *Northwestern Geol*, 15: 1–11
- Li Y, Xiong W Y, Wang L, He W, Sun B Y. 2022. First record of *Ma-*

- chairoodus aphanistus* KAUP, 1833 (Carnivora, Felidae, Machairodontinae) in East Asia from a late Miocene deposit of the Linxia Basin, Gansu Province, China. *Historical Biol*, 34: 930–939
- Li Y K. 2015. *Gazella* fossils of the Late Miocene Yangjiashan fauna from the Linxia Basin, Gansu Province (in Chinese). *Quat Sci*, 35: 550–560
- Li Y K, He W, Chen S Q, Wang S Q, Sun B Y, Li Y. 2017. *Hipparion* material from Gaojiashan locality in the Late Miocene of Linxia Basin, Gansu, China and associated mammalian fossil assemblage. *Historical Biol*, 30: 677–693
- Li Y K, Mennecart B, Aiglstorfer M, Ni X J, Li Q, Deng T. 2022. The early evolution of cranial appendages in Bovoidea revealed by new species of *Amphimoschus* (Mammalia: Ruminantia) from China. *Zool J Linnean Soc*, 196: 1039–1053
- Liu G W, Li J G. 2016. Miocene fossil floral horizons in the Oiyug Basin, southern central Tibet, and related stratigraphic problems (in Chinese). *J Stratigr*, 40: 92–99
- Liu J, Wang T X, Zhang X W, Song A, Li S F, Huang J, Spicer T, Spicer R A, Wu F X, Su T, Zhou Z K. 2021. Snapshot of the Pliocene environment of West Kunlun region, Northwest China. *Palaeobio Palaeoenv*, 101: 163–176
- Lu H J, Fu B H, Shi P L, Ma Y X, Li H B. 2016. Constraints on the uplift mechanism of northern Tibet. *Earth Planet Sci Lett*, 453: 108–118
- Lu J Y, Algeo T J, Zhuang G S, Yang J L, Xiao G Q, Liu J S, Huang J H, Xie S C. 2020. The Early Pliocene global expansion of C<sub>4</sub> grasslands: A new organic carbon-isotopic dataset from the north China plain. *Palaeogeogr Palaeoclimatol Palaeoecol*, 538: 109454
- Luo B J, Dai G Y, Pan Z X. 1996. Oil and gas potential in Paleogene terrestrial Bangonghu-Dingqing suture zone (in Chinese). *Earth Sci J China Univ Geosci*, 21: 163–167
- Lydekker R. 1881. Observations on the ossiferous beds of Hündes in Tibet. *Rec Geol Surv India*, 14: 178–184
- Mao Z Q, Meng Q Q, Fang X M, Zhang T, Wu F L, Yang Y B, Zhang W L, Zan J B, Tan M Q. 2019. Recognition of tuffs in the middle-upper Dingqinghu Fm., Lunpola Basin, central Tibetan Plateau: Constraints on stratigraphic age and implications for paleoclimate. *Palaeogeogr Palaeoclimatol Palaeoecol*, 525: 44–56
- Martin C, Bentaleb I, Antoine P O. 2011. Pakistan mammal tooth stable isotopes show paleoclimatic and paleoenvironmental changes since the early Oligocene. *Palaeogeogr Palaeoclimatol Palaeoecol*, 311: 19–29
- Molnar P. 2005. Mio-Pliocene growth of the Tibetan Plateau and evolution of East Asian climate. *Palaeont Electr*, 8: 2A
- Morgan M E, Behrensmeyer A K, Badgley C, Barry J C, Nelson S, Pilbeam D. 2009. Lateral trends in carbon isotope ratios reveal a Miocene vegetation gradient in the Siwaliks of Pakistan. *Geology*, 37: 103–106
- Morgan M E, Kingston J D, Marino B D. 1994. Carbon isotopic evidence for the emergence of C<sub>4</sub> plants in the Neogene from Pakistan and Kenya. *Nature*, 367: 162–165
- Murphy M A, Yin A, Kapp P, Harrison T M, Manning C E, Ryerson F J, Ding L, Guo J H. 2002. Structural evolution of the Gurla Mandhata detachment system, southwest Tibet: Implications for the eastward extent of the Karakoram fault system. *Geol Soc Am Bull*, 114: 428–447
- Nelson S V. 2007. Isotopic reconstructions of habitat change surrounding the extinction of *Sivapithecus*, a Miocene hominoid, in the Siwalik Group of Pakistan. *Palaeogeogr Palaeoclimatol Palaeoecol*, 243: 204–222
- Ni X J, Qiu Z D. 2002. The micromammalian fauna from the Leilao, Yuanmou hominoid locality: Implications for biochronology and paleoecology. *J Hum Evol*, 42: 535–546
- Ogg J G, Ogg G, Cradstein F M. 2016. *A Concise Geologic Time Scale 2016*. Amsterdam: Elsevier. 1–213
- Pan G T, Liu Y P, Zheng L L, Gen Q R, Wang L Q, Yin F G, Li G M, Liao Z L, Zhu D C. 2013. The Collision Tectonic and Effect on Qinghai-Tibet Plateau (in Chinese). Guangzhou: Guangdong Science and Technology Press. 466
- Passey B H, Ayliffe L K, Kaakinen A, Zhang Z Q, Eronen J T, Zhu Y M, Zhou L Q, Cerling T E, Fortelius M. 2009. Strengthened East Asian summer monsoons during a period of high-latitude warmth? Isotopic evidence from Mio-Pliocene fossil mammals and soil carbonates from northern China. *Earth Planet Sci Lett*, 277: 443–452
- Patnaik R, Cerling T E, Uno K T, Fleagle J G. 2014. Diet and habitat of Siwalik primates *Indopithecus*, *Sivaladapis* and *Theropithecus*. *Ann Zool Fennici*, 51: 123–142
- Patnaik R, Singh N P, Paul D, Sukumar R. 2019. Dietary and habitat shifts in relation to climate of Neogene-Quaternary proboscideans and associated mammals of the Indian subcontinent. *Quat Sci Rev*, 224: 105968
- Pilgrim G E. 1912. The vertebrate fauna of the Gaj Series in the Bugti Hills and the Punjab. *Palaeont Ind N S*, 4: 1–83
- Prell W L, Kutzbach J E. 1992. Sensitivity of the Indian monsoon to forcing parameters and implications for its evolution. *Nature*, 360: 647–652
- Qian F. 1990. Preliminary study of horizontal movement since Late Pliocene by palaeomagnetic method in Ali area, Xizang (Tibet) (in Chinese). In: Chinese Academy of Geological Sciences, ed. *Tectonic Evolution of the Lithosphere of the Himalayas: Contribution to the Geophysics of Xizang (Tibet)*. Beijing: Geological Publishing House. 198–206
- Qian F, Zhou G X, et al. 1991. Quaternary Geology and Palaeoanthropology of Yuanmou, Yunnan, China (in Chinese). Beijing: Science Press. 1–184
- Qiu Z D. 1996. Middle Miocene Micromammalian Fauna from Tunggur, Nei Mongol (in Chinese). Beijing: Science Press. 1–216
- Qiu Z D. 2000. Insectivore, Dipodoidean and Lagomorph from the Middle Miocene Quantougou fauna of Lanzhou, Gansu (in Chinese). *Vert Palasiat*, 38: 287–302
- Qiu Z D. 2001a. Cricetid rodents from the Middle Miocene Quantougou fauna of Lanzhou, Gansu (in Chinese). *Vert Palasiat*, 39: 204–214
- Qiu Z D. 2001b. Glirid and gerbillid rodents from the Middle Miocene Quantougou fauna of Lanzhou, Gansu (in Chinese). *Vert Palasiat*, 39: 297–305
- Qiu Z D, Li C K, Wang S J. 1981. Miocene mammalian fossils from Xining Basin, Qinghai (in Chinese). *Vert Palasiat*, 19: 156–173
- Qiu Z D, Li Q. 2008. Late Miocene micromammals from the Qaidam Basin in the Qinghai-Xizang Plateau. *Vert Palasiat*, 46: 284–306
- Qiu Z D, Li Q. 2016. Neogene rodents from central Nei Mongol, China (in Chinese). *Palaeont Sin New Ser C* 30: 1–684
- Qiu Z D, Wang B Y, Li L. 2023. Middle Cenozoic micromammals from Linxia Basin, Gansu Province, China, and their implications for biostatigraphy and palaeoecology. *Palaeogeogr Palaeoclimatol Palaeoecol*, 616: 111467
- Qiu Z X. 1990. The Chinese Neogene mammalian biochronology: Its correlation with the European Neogene mammalian zonation. In: Lindsay E H, Fahlbusch V, Mein P, eds. *European Neogene Mammal Chronology*. New York: Plenum Press. 527–556
- Qiu Z X, Deng T, Wang B Y. 2014. A Late Miocene *Ursavus* skull from Guanghe, Gansu, China. *Vert Palasiat*, 52: 265–302
- Qiu Z X, Huang W L, Guo Z H. 1987. The Chinese hipparionine fossils (in Chinese). *Palaeont Sin New Ser C* 25: 1–243
- Qiu Z X, Qiu Z D. 1990. The sequence and division of mammalian local faunas in the Neogene of China (in Chinese). *J Stratigr*, 14: 241–260
- Qiu Z X, Qiu Z D. 1995. Chronological sequence and subdivision of Chinese Neogene mammalian faunas. *Palaeogeogr Palaeoclimatol Palaeoecol*, 116: 41–70
- Qiu Z X, Qiu Z D, Deng T, Li C K, Zhang Z Q, Wang B Y, Wang X M. 2013. Neogene land mammal stages/ages of China: Toward the goal to establish an Asian land mammal stage/age scheme. In: Wang X M, Flynn L J, Fortelius M, eds. *Fossil Mammals of Asia: Neogene Biostatigraphy and Chronology*. New York: Columbia University Press. 29–90
- Qiu Z X, Wang B Y, Li H, Deng T, Sun Y. 2007. First discovery of deinotherium in China (in Chinese). *Vert Palasiat*, 45: 261–277
- Qiu Z X, Wu W Y, Qiu Z D. 1999. Miocene mammal faunal sequences of China: Palaeozoogeography and Eurasian relationships. In: Rössner G E, Heissig K, eds. *The Miocene Land Mammals of Europe*. Munich: Dr. Friedrich Pfeil. 443–472

- Qiu Z X, Xie J Y, Yan D F. 1988. Discovery of the skull of *Dinocrocota gigantea* (in Chinese). *Vert Palasiat*, 26: 128–138
- Qiu Z X, Xie J Y, Yan D F. 1991. Discovery of Late Miocene *Agriotherium* from Jiegou, Gansu, and its taxonomic implications (in Chinese). *Vert Palasiat*, 29: 286–295
- Quade J, Cater J M L, Ojha T P, Adam J, Harrison T M. 1995. Late Miocene environmental change in Nepal and the northern Indian subcontinent: Stable isotopic evidence from paleosols. *Geol Soc Am Bull*, 107: 1381–1397
- Quade J, Cerling T E. 1995. Expansion of C<sub>4</sub> grasses in the Late Miocene of Northern Pakistan: Evidence from stable isotopes in paleosols. *Palaeogeogr Palaeoclimatol Palaeoecol*, 115: 91–116
- Quade J, Cerling T E, Barry J C, Morgan M E, Pilbeam D R, Chivas A R, Lee-Thorp J A, van der Merwe N J. 1992. A 16-Ma record of paleodiet using carbon and oxygen isotopes in fossil teeth from Pakistan. *Chem Geol*, 94: 183–192
- Quade J, Cerling T E, Bowman J R. 1989. Development of Asian monsoon revealed by marked ecological shift during the latest Miocene in northern Pakistan. *Nature*, 342: 163–166
- Quade J, Roe L J. 1999. The stable-isotope composition of early groundwater cements from sandstone in paleoecological reconstruction. *J Sediment Res*, 69: 667–674
- Raffi I, Wade B S, Pälke H, Beu A G, Cooper R, Crundwell M P, Krijgsman W, Moore T, Raine I, Sardella R, Vernyhorova Y V. 2020. The Neogene Period. In: Gradstein F M, Ogg J G, Schmitz M D, Ogg G M, eds. *Geologic Time Scale 2020, Volume 2*. Amsterdam: Elsevier. 1141–1215
- Raza S M, Meyer G E. 1984. Early Miocene geology and paleontology of the Bugti Hills. *Geol Surv Pakistan*, 11: 43–63
- Royle J F. 1839. *Illustrations of the Botany and Other Branches of the Natural History of the Himalayan Mountains, and of the Flora of Cashmere, Volume I*. London: Wm. H. Allen and Co
- Ruddiman W F, Kutzbach J E. 1989. Forcing of late Cenozoic northern hemisphere climate by plateau uplift in southern Asia and the American west. *J Geophys Res*, 94: 18409–18427
- Salvador A. 1994. *International Stratigraphic Guide: A Guide to Stratigraphic Classification, Terminology, and Procedure*. 2nd ed. Boulder: Geological Society of America. 1–214
- Sanyal P, Bhattacharya S K, Kumar R, Ghosh S K, Sangode S J. 2004. Mio-Pliocene monsoonal record from Himalayan foreland basin (Indian Siwalik) and its relation to vegetational change. *Palaeogeogr Palaeoclimatol Palaeoecol*, 205: 23–41
- Sanyal P, Bhattacharya S K, Kumar R, Ghosh S K, Sangode S J. 2005. Palaeovegetational reconstruction in Late Miocene: A case study based on early diagenetic carbonate cement from the Indian Siwalik. *Palaeogeogr Palaeoclimatol Palaeoecol*, 228: 245–259
- Saylor J E, Quade J, Dettman D L, DeCelles P G, Kapp P A, Ding L. 2009. The late Miocene through present paleoelevation history of southwestern Tibet. *Am J Sci*, 309: 1–42
- Shen X Y, Wan S M, Colin C, Tada R, Shi X F, Pei W Q, Tan Y, Jiang X J, Li A C. 2018. Increased seasonality and aridity drove the C<sub>4</sub> plant expansion in Central Asia since the Miocene-Pliocene boundary. *Earth Planet Sci Lett*, 502: 74–83
- Shi Q Q, He W, Chen S Q. 2014. A new species of *Shaanxispira* (Bovidae, Artiodactyla) from the upper Miocene of China. *Zootaxa*, 3794: 501–513
- Singh A P, Sehgal R K, Singh N P, Kharya A. 2023. Diet and habitat of late Miocene herbivore mammals from Narpur, District Kangra, Himachal Pradesh, India. *Geol J*, 58: 740–754
- Song C H, Gao D L, Fang X M, Cui Z J, Li J J, Yang S L, Jin H B, Burbank D W, Kirschvink J L. 2005. Late Cenozoic high-resolution magnetostratigraphy in the Kunlun Pass Basin and its implications for the uplift of the northern Tibetan Plateau. *Chin Sci Bull*, 50: 1912–1922
- Spicer R A, Harris N B W, Widdowson M, Herman A B, Guo S S, Valdes P J, Wolfe J A, Kelley S P. 2003. Constant elevation of southern Tibet over the past 15 million years. *Nature*, 421: 622–624
- Steininger F F, Aubry M P, Berggren W A, Biolzi M, Borsetti A M, Cartlidge J E, Cati F, Corfield R, Gelati R, Iaccarino S, Napoleone C, Ottner F, Rögl F, Roetzel R, Spezzaferrri S, Tateo F, Villa G, Zeevenboom D. 1997. The Global Stratotype Section and Point (GSSP) for the base of the Neogene. *Episodes*, 20: 23–28
- Steininger F F. 1999. Chronostratigraphy, geochronology and biochronology of the Miocene “European Land Mammal Mega-Zones” (ELMMZ) and the Miocene “Mammal-Zones (MN-Zones)”. In: Rössner G E, Heissig K, eds. *The Miocene Land Mammals of Europe*. München: Verlag Dr. Friedrich Pfeil. 9–24
- Stern L A, Johnson G D, Chamberlain C P. 1994. Carbon isotope signature of environmental change found in fossil ratite eggshells from a South Asian Neogene sequence. *Geology*, 22: 419–422
- Sun B, Wang Y F, Li C S, Yang J, Li J F, Li Y L, Deng T, Wang S Q, Zhao M, Spicer R A, Ferguson D K, Mehrotra R C. 2015. Early Miocene elevation in northern Tibet estimated by palaeobotanical evidence. *Sci Rep*, 5: 10379
- Sun B Y. 2013. The Miocene *Hipparion* (Equidae, Perissodactyla) from Shihuiba locality, Lufeng, Yunnan (in Chinese). *Vert Palasiat*, 51: 141–161
- Sun B Y, Deng T. 2021. New specimens of anchitheriine from the Linxia Basin, Gansu and evolution of East Asian anchitheriines (in Chinese). *Chin Sci Bull*, 66: 1492–1502
- Sun J M, Li J G, Liu W G, Windley B F, Farnsworth A, Jin C S, Zhang Z L, Xiao W J. 2023. Middle Miocene paleoenvironmental change and paleoelevation of the Lunpola Basin, Central Tibet. *Glob Planet Change*, 220: 104009
- Sun J M, Li Y, Zhang Z Q, Fu B H. 2009. Magnetostratigraphic data on Neogene growth folding in the foreland basin of the southern Tianshan Mountains. *Geology*, 37: 1051–1054
- Sun J M, Liu W G, Liu Z H, Deng T, Windley B F, Fu B H. 2017. Extreme aridification since the beginning of the Pliocene in the Tarim Basin, western China. *Palaeogeogr Palaeoclimatol Palaeoecol*, 485: 189–200
- Sun J M, Xu Q H, Liu W M, Zhang Z Q, Xue L, Zhao P. 2014. Palynological evidence for the latest Oligocene-early Miocene paleoelevation estimate in the Lunpola Basin, central Tibet. *Palaeogeogr Palaeoclimatol Palaeoecol*, 399: 21–30
- Sun J M, Zhu R X, An Z S. 2005. Tectonic uplift in the northern Tibetan Plateau since 13.7 Ma ago inferred from molasse deposits along the Altyn Tagh Fault. *Earth Planet Sci Lett*, 235: 641–653
- Sun L, Deng C L, Deng T, Kong Y F, Wu B L, Liu S Z, Li Q, Liu G. 2023. Magnetostratigraphy of the Oligocene and Miocene of the Linxia Basin, northwestern China. *Palaeogeogr Palaeoclimatol Palaeoecol*, 613: 111404
- Sun Z, Han A, Li Y, Jiangzuo Q G, Wang S Q, Li S J. 2022. New material of *Amphicyon zhanxiangi* from Laogou, Linxia Basin suggests a possible southern dispersal with increasing omnivory. *Historical Biol*, 34: 857–864
- Tapponnier P, Peltzer G, Le Dain A Y, Armijo R, Cobbold P. 1982. Propagating extrusion tectonics in Asia: New insights from simple experiments with plasticine. *Geology*, 10: 611–616
- Tapponnier P, Xu Z Q, Roger F, Meyer B, Arnaud N, Wittlinger G, Yang J S. 2001. Oblique stepwise rise and growth of the Tibet Plateau. *Science*, 294: 1671–1677
- Tedford R H. 1995. Neogene mammalian biostratigraphy in China: Past, present and future. *Vert Palasiat*, 33: 272–289
- Tong Y S, Zheng S H, Qiu Z D. 1995. Cenozoic mammal ages of China (in Chinese). *Vert Palasiat*, 33: 290–314
- Tseng Z J, Li Q, Wang X M. 2013. A new cursorial hyena from Tibet, and analysis of biostratigraphy, paleozoogeography, and dental morphology of *Chasmaporthetes* (Mammalia, Carnivora). *J Vertebr Paleontol*, 33: 1457–1471
- Tseng Z J, Wang X M, Li Q, Xie G P. 2022. *Qurlignoria* (Mammalia: Bovidae) fossils from Qaidam Basin, Tibetan Plateau and deep-time endemism of the Tibetan antelope lineage. *Zool J Linnean Soc*, 196: 990–1012
- van Couvering J A, Castradori D, Cita M B, Hilgen F J, Rio D. 2000. The base of the Zanclean Stage and of the Pliocene Series. *Episodes*, 23:



- 179–187
- Vögeli N, Najman Y, van der Beek P, Huyghe P, Wynn P M, Govin G, van der Veen I, Sachse D. 2017. Lateral variations in vegetation in the Himalaya since the Miocene and implications for climate evolution. *Earth Planet Sci Lett*, 471: 1–9
- Wang B Y. 2003. Dipodidae (Rodentia, Mammalia) from the middle Tertiary deposits in Danghe area, Gansu, China (in Chinese). *Vert Palasiat*, 41: 89–103
- Wang B Y. 2017. Discovery of *Yuomys* from Altun Shan, Xinjiang, China. *Vert Palasiat*, 55: 227–232
- Wang B Y, Qiu Z X. 2000. Micromammal fossils from red mudstone of lower member of Xianshuihe Formation in Lanzhou Basin, China (in Chinese). *Vert Palasiat*, 38: 255–273
- Wang B Y, Qiu Z X. 2002. A new species of *Platybelodon* (Gomphotheriidae, Proboscidea, Mammalia) from Early Miocene of the Danghe area, Gansu, China (in Chinese). *Vert Palasiat*, 40: 291–299
- Wang B Y, Qiu Z X, Wang X M, Xie G P, Xie J Y, Downs W, Qiu Z D, Deng T. 2003. Cenozoic stratigraphy in Danghe area, Gansu Province, and uplift of Tibetan Plateau (in Chinese). *Vert Palasiat*, 41: 66–75
- Wang K F, Yang J W, Li Z, Li Z R. 1975. On the Tertiary sporopollen assemblages from Lunpola Basin of Xizang, China and their palaeogeographic significance (in Chinese). *Sci Geol Sin*, : 366–374
- Wang L, Lü H Y, Wu N Q, Chu D, Han J M, Wu Y H, Wu H B, Gu Z Y. 2004. Discovery of  $C_4$  species at high altitude in Qinghai-Tibetan Plateau. *Chin Sci Bull*, 49: 1392–1396
- Wang N, Chang M. 2010. Pliocene cyprinids (Cypriniformes, Teleostei) from Kunlun Pass Basin, northeastern Tibetan Plateau and their bearings on development of water system and uplift of the area. *Sci China Earth Sci*, 53: 485–500
- Wang N, Chang M. 2012. Discovery of fossil Nemacheilids (Cypriniformes, Teleostei, Pisces) from the Tibetan Plateau, China. *Sci China Earth Sci*, 55: 714–727
- Wang P X. 2005. Cenozoic deformation and history of sea-land interactions in Asia. *Earth Sci J China Univ Geosci* (in Chinese), 30: 1–18
- Wang P X. 2021. Low-latitude forcing: A new insight into paleo-climate changes. *Innovation*, 2: 100145
- Wang S F, Zhang W L, Fang X M, Dai S, Kempf O. 2008. Magnetostatigraphy of the Zanda Basin in southwest Tibet Plateau and its tectonic implications. *Chin Sci Bull*, 53: 1393–1400
- Wang S Q, Ji X P, Deng T, Fu L Y, Zhang J H, Li C X, He Z L. 2019. Yunnan, a refuge for trilophodont proboscideans during the late Miocene aridification of East Asia. *Palaeogeogr Palaeoclimatol Palaeoecol*, 515: 162–171
- Wang S Q, Ji X P, Jablonski N G, Su D F, Ge J Y, Ding C F, Yu T S, Li W Q, Duangkrayom J. 2016. The oldest cranium of *Sinomastodon* (Proboscidea, Gomphotheriidae), discovered in the uppermost Miocene of Southwestern China: Implications for the origin and migration of this taxon. *J Mammal Evol*, 23: 155–173
- Wang S Q, Li Y, Duangkrayom J, Chen S K, He W, Chen S Q. 2017a. Early *Mammot* from the Upper Miocene of northern China, and its implications for the evolution and differentiation of Mammotidae. *Vert Palasiat*, 55: 233–256
- Wang S Q, Li Y, Duangkrayom J, Yang X W, He W, Chen S Q. 2017b. A new species of *Gomphotherium* (Proboscidea, Mammalia) from China and the evolution of *Gomphotherium* in Eurasia. *J Vertebrate Paleontology*, 37: e1318284
- Wang W M, Deng T. 2009. Palynoflora from the stratotype section of the Neogene Xiejian Stage and its significance (in Chinese). *Acta Palaeont Sin*, 48: 1–8
- Wang W T, Zheng W J, Zhang P Z, Li Q, Kirby E, Yuan D Y, Zheng D W, Liu C C, Wang Z C, Zhang H P, Pang J Z. 2017. Expansion of the Tibetan Plateau during the Neogene. *Nat Commun*, 8: 15887
- Wang X M, Li Q, Qiu Z D, Xie G P, Wang B Y, Qiu Z X, Tseng Z J, Takeuchi G T, Deng T. 2013a. Neogene mammalian biostratigraphy and geochronology of the Tibetan Plateau. In: Wang X M, Flynn L J, Fortelius M, eds. *Fossil Mammals of Asia: Neogene Biostratigraphy and Chronology*. New York: Columbia University Press. 274–292
- Wang X M, Li Q, Tseng Z J. 2023. Primitive Tibetan antelope, *Qurlignoria hundesiensis* (Lydekker, 1881) (Bovidae, Artiodactyla), from Pliocene Zanda and Kunlun Pass basins and paleoenvironmental implications. *J Mammal Evol*, 30: 245–268
- Wang X M, Li Q, Xie G P, Saylor J E, Tseng Z J, Takeuchi G T, Deng T, Wang Y, Hou S K, Zhang C F, Wang N, Wu F X. 2013b. Mio-Pleistocene Zanda Basin biostratigraphy and geochronology, pre-Ice Age fauna, and mammalian evolution in western Himalaya. *Palaeogeogr Palaeoclimatol Palaeoecol*, 374: 81–95
- Wang X M, Qiu Z D, Li Q, Wang B Y, Qiu Z X, Downs W, Xie G P, Xie J Y, Deng T, Takeuchi G, Tseng Z J, Chang M M, Liu J, Wang Y, Biasatti D, Sun Z C, Fang X M, Meng Q Q. 2007. Vertebrate paleontology, biostratigraphy, geochronology, and paleoenvironment of Qaidam Basin in northern Tibetan Plateau. *Palaeogeogr Palaeoclimatol Palaeoecol*, 254: 363–385
- Wang X M, Qiu Z X. 2004. Late Miocene *Promephitis* (Carnivora, Mephitidae) from China. *J Vertebr Paleontol*, 24: 721–731
- Wang X M, Qiu Z X, Wang B Y. 2004. A new leptarcine (Carnivora: Mustelidae) from the early Miocene of the northern Tibetan Plateau: Implications for the phylogeny and zoogeography of basal mustelids. *Zool J Linnean Soc*, 142: 405–421
- Wang X M, Tseng Z J, Li Q, Takeuchi G T, Xie G P. 2014. From ‘third pole’ to north pole: A Himalayan origin for the arctic fox. *Proc R Soc B*, 281: 20140893
- Wang X M, Wang B Y, Qiu Z X. 2008. Early explorations of Tabenbuluk region (western Gansu Province) by Birger Bohlin: Reconciling classic vertebrate fossil localities with modern stratigraphy. *Vert Palasiat*, 46: 1–19
- Wang X M, Wang B Y, Qiu Z X, Xie G P, Xie J Y, Downs W, Qiu Z D, Deng T. 2003. Danghe area (western Gansu, China) biostratigraphy and implications for depositional history and tectonics of northern Tibetan Plateau. *Earth Planet Sci Lett*, 208: 253–269
- Wang X M, Wang Y, Li Q, Tseng Z J, Takeuchi G T, Deng T, Xie G P, Chang M M, Wang N. 2015. Cenozoic vertebrate evolution and paleoenvironment in Tibetan Plateau: Progress and prospects. *Gondwana Res*, 27: 1335–1354
- Wang X M, Xie G P, Li Q, Qiu Z D, Tseng Z J, Takeuchi G T, Wang B Y, Fortelius M, Rosenstrom-Fortelius A, Wahlouist H, Downs W R, Zhang C F, Wang Y. 2011. Early explorations of Qaidam Basin (Tibetan Plateau) by Birger Bohlin: Reconciling classic vertebrate fossil localities with modern biostratigraphy. *Vert Palasiat*, 49: 285–310
- Wang Y, Deng T. 2005. A 25 m.y. isotopic record of paleodiet and environmental change from fossil mammals and paleosols from the NE margin of the Tibetan Plateau. *Earth Planet Sci Lett*, 236: 322–338
- Wang Y, Deng T, Biasatti D. 2006. Ancient diets indicate significant uplift of southern Tibet after ca. 7 Ma. *Geology*, 34: 309–312
- Wang Y, Kromhout E, Zhang C F, Xu Y F, Parker W, Deng T, Qiu Z D. 2008a. Stable isotopic variations in modern herbivore tooth enamel, plants and water on the Tibetan Plateau: Implications for paleoclimate and paleoelevation reconstructions. *Palaeogeogr Palaeoclimatol Palaeoecol*, 260: 359–374
- Wang Y, Wang X M, Xu Y F, Zhang C F, Li Q, Tseng J, Takeuchi G, Deng T. 2008b. Stable isotopes in fossil mammals, fish and shells from Kunlun Pass Basin, Tibetan Plateau: Paleo-climatic and paleo-elevation implications. *Earth Planet Sci Lett*, 270: 73–85
- Wang Y, Xu Y F, Khawaja S, Passey B H, Zhang C F, Wang X M, Li Q, Tseng Z J, Takeuchi G T, Deng T, Xie G P. 2013. Diet and environment of a mid-Pliocene fauna from southwestern Himalaya: Paleo-elevation implications. *Earth Planet Sci Lett*, 376: 43–53
- Wang Z J, Huang Z G, Yao J X, Ma X L. 2014. Characteristics and main progress of the stratigraphic chart of China and directions (in Chinese). *Acta Geosci Sin*, 35: 271–276
- Waseem M T, Khan A M, Ghaffar A, Iqbal A, Ahmad R M. 2021a. Palaeodietary and palaeoclimatic reconstruction for Late Miocene hipparionines from the Siwaliks of Pakistan. *Pak J Zool*, 53: 801–1200
- Waseem M T, Khan A M, Quade J, Krupa A, Dettman D, Rafah A, Ahmad R M. 2021b. Stable isotope analysis of middle Miocene mammals from

- the Siwalik sub-Group of Pakistan. *Acta Palaeontol Polon*, 66: s123
- Woodburne M O, Bernor R L, Swisher C C III. 1996. An appraisal of the stratigraphic and phylogenetic bases for the “*Hipparion*” datum in the Old World. In: Bernor R L, Fahlbusch V, Mittmann H W, eds. *The Evolution of Western Eurasian Neogene Mammal Faunas*. New York: Columbia University Press. 124–136
- Woodburne M O, Tedford R H, Lindsay E H. 2013. North China Neogene biochronology. In: Wang X M, Flynn L J, Fortelius M, eds. *Fossil Mammals of Asia: Neogene Biostratigraphy and Chronology*. New York: Columbia University Press. 91–123
- Wu F L, Fang X M, Yang Y B, Dupont-Nivet G, Nie J S, Fluteau F, Zhang T, Han W X. 2022. Reorganization of Asian climate in relation to Tibetan Plateau uplift. *Nat Rev Earth Environ*, 3: 684–700
- Wu R K, Wu X Z, Zhang S S. 1989. Early Humankind in China (in Chinese). Beijing: Science Press. 1–437
- Wu S, Zhang F, Edwards S V, Wu W, Ye J, Bi S, Ni X, Quan C, Meng J, Organ C L. 2014. The evolution of bipedalism in jerboas (Rodentia: Dipodoidea): Origin in humid and forested environments. *Evolution*, 68: 2108–2118
- Wu Y F, Chen Y Y. 1980. Fossil cyprinid fishes from the late Tertiary of North Xizang, China (in Chinese). *Vert Palasiat*, 18: 15–20
- Xie G P. 2004. The Tertiary and local mammalian faunas in Lanzhou Basin, Gansu (in Chinese). *J Stratigr*, 28: 67–80
- Xu Q, Ding L, Zhang L Y, Yang D, Cai F L, Lai Q Z, Liu J, Shi R D. 2010. Stable isotopes of modern herbivore tooth enamel in the Tibetan Plateau: Implications for paleoelevation reconstructions. *Chin Sci Bull*, 55: 45–54
- Yang H B. 1998. First discovery of fresh water fossils of the Early Cretaceous in the West Kunlun Mountains of Xinjiang (in Chinese). *Xinjiang Geol*, 16: 288–289
- Yang L R, Li J X, Yue L P, Wang H L, Guo H J, Zhu X H, Zhu T, Du K, Zhang R, Zhang Y X, Gong H J. 2017. Paleogene-Neogene stratigraphic realm and tectonic-sedimentary evolution of the Qilian Mountains and their surrounding areas. *Sci China Earth Sci*, 60: 992–1009
- Yang Z H, Wang H J, Su C Q, Deng Y T, Liu Z T. 2005. A brief introduction to the geology and tectonics in Waka area, west Kunlun Mt (in Chinese). *Geol Shannxi*, 23: 32–48
- Yin A, Harrison T M. 2000. Geologic evolution of the Himalayan-Tibetan Orogen. *Annu Rev Earth Planet Sci*, 28: 211–280
- Yin A, Rumelhart P E, Butler R E, Cowgill E, Harrison T M, Foster D A, Ingersoll R V, Zhang Q, Zhou X Q, Wang X F, Hanson A, Raza A. 2002. Tectonic history of the Altyn Tagh fault system in northern Tibet inferred from Cenozoic sedimentation. *Geol Soc Am Bull*, 114: 1257–1295
- Yue L P, Deng T, Zhang R, Zhang Z Q, Heller F, Wang J Q, Yang L R. 2004a. Paleomagnetic chronology and record of Himalayan movements in the Longgugou Section of Gyirong-Oma Basin in Xizang (Tibet). *Chin J Geophys*, 47: 1135–1142
- Yue L P, Deng T, Zhang Y X, Wang J Q, Zhang R, Yang L R, Heller F. 2004b. Magnetostratigraphy of stratotype section of the Baode Stage (in Chinese). *J Stratigr*, 28: 48–51
- Zachos J, Pagani M, Sloan L, Thomas E, Billups K. 2001. Trends, rhythms, and aberrations in global climate 65 Ma to present. *Science*, 292: 686–693
- Zdansky O. 1923. Fundorte der *Hipparion*-Fanna um Pao-Te-Hsien in NW-Shansi. *Bull Geol Surv China*, 5: 69–81
- Zhang C F, Wang Y, Deng T, Wang X M, Biasatti D, Xu Y F, Li Q. 2009. C<sub>4</sub> expansion in the central Inner Mongolia during the latest Miocene and early Pliocene. *Earth Planet Sci Lett*, 287: 311–319
- Zhang C F, Wang Y, Li Q, Wang X M, Deng T, Tseng Z J, Takeuchi G T, Xie G P, Xu Y F. 2012. Diets and environments of late Cenozoic mammals in the Qaidam Basin, Tibetan Plateau: Evidence from stable isotopes. *Earth Planet Sci Lett*, 333-334: 70–82
- Zhang J D, Zhang Z L, Wei W T, Guo J C, et al. 2015a. Regional Geological Report of Yare and Burang County Maps of the People’s Republic of China (in Chinese). Beijing: Geological Publishing House. 1–283
- Zhang K X, Wang G C, Ji J L, Luo M S, Kou X H, Wang Y M, Xu Y D, Chen F N, Chen R M, Song B W, Zhang J Y, Liang Y P. 2010. Paleogene-Neogene stratigraphic realm and sedimentary sequence of the Qinghai-Tibet Plateau and their response to uplift of the plateau. *Sci China Earth Sci*, 53: 1271–1294
- Zhang Q S, Wang F B, Ji H X, Huang W B. 1981. Pliocene stratigraphy of Zhada Basin, Tibet. *J Stratigr*, 5: 216–220
- Zhang S Z, Li J H, Zhang H B, Wang L J, et al. 2015b. Regional Geological Report of Rixin, Zanda County and Qiangyema Maps of the People’s Republic of China (in Chinese). Beijing: Geological Publishing House. 1–224
- Zhang W L, Yan M D, Fang X M, Zhang D W, Zhang T, Zan J B, Song C H. 2019. High-resolution paleomagnetic constraint on the oldest hominoid-fossil-bearing sequence in the Xiaolongtan Basin, southeast margin of the Tibetan Plateau and its geologic implications. *Glob Planet Change*, 182: 103001
- Zhang W L, Zhang T, Song C H, Appel E, Mao Z Q, Fang Y H, Lu Y, Meng Q Q, Yang R S, Zhang D W, Li B S, Li J. 2017. Termination of fluvial-alluvial sedimentation in the Xining Basin, NE Tibetan Plateau, and its subsequent geomorphic evolution. *Geomorphology*, 297: 86–99
- Zhang X. 1993. New discovery of the mammalian fossils in Baode period of later Miocene Epoch in Lanzhou Basin (in Chinese). *Acta Geol Gansu*, 2: 1–5
- Zhang X D, Xie G P. 1988. The first discovery of the Hongyazi *Hipparion* fauna and its significance for upheaval of the Qinghai-Xizang Plateau (in Chinese). *Gansu Geol*, (1): 87–91
- Zhang Y X, Che Z C, Liu L, Luo J L. 1996. Tertiary in the Kumkol Basin, Xinjiang (in Chinese). *Region Geol Chin*, (4): 311–316
- Zhang Z Q. 2005. New materials of *Dinocrocota* (Percrocutidae, Carnivora) from Lantian, Shaanxi Province, China, and remarks on Chinese Late Miocene biochronology. *Geobios*, 38: 685–689
- Zheng S H. 1980. The *Hipparion* fauna of Bulong Basin, Biru, Xizang. In: *The Scientific Expedition to Tibet*, Chinese Academy of Sciences, ed. *Palaeontology of Xizang*, Book 1. Beijing: Science Press. 33–47
- Zheng S H, Li Y. 1982. Some Pliocene lagomorphs and rodents from Loc. 1 of Songshan, Tianzu Xian, Gansu Province. *Vert Palasiat*, 20: 35–44
- Zheng Y, Qiu Z, Qiu Z, Li L, Wei X, Zhang R, Yue L, Deng T. 2023. Revised magnetostratigraphy of the Linxia Basin in the northeast Tibetan Plateau, constrained by micromammalian fossils. *Palaeogeogr Palaeoclimatol Palaeoecol*, 623: 111620
- Zhu D G, Meng X G, Shao Z G, Yang C B, Wang J, Han J E, Yu J, Meng Q W, Lü R P. 2008. Division and correlation of Pliocene and Early Pleistocene fluvio-lacustrine strata in the Zhada Basin, Tibet, China (in Chinese). *Acta Geosci Sin*, 29: 137–144
- Zhuang G S, Hourigan J K, Koch P L, Ritts B D, Kent-Corson M L. 2011. Isotopic constraints on intensified aridity in Central Asia around 12 Ma. *Earth Planet Sci Lett*, 312: 152–163
- Zin-Maung-Maung-Thein, Takai M, Nishioka Y, Wynn J, Uno H, Thaug-Htike H, Egi N, Tsubamoto T, Maung-Maung T. 2021. Stable isotope geochemistry of Gwebin mammalian fauna with implications for late Neogene paleoenvironmental changes in central Myanmar. *J Asian Earth Sci*, 218: 104884
- Zin-Maung-Maung-Thein, Takai M, Uno H, Wynn J G, Egi N, Tsubamoto T, Thaug-Htike T, Aung-Naing-Soe T, Maung-Maung T, Nishimura T, Yoneda M. 2011. Stable isotope analysis of the tooth enamel of Chaingzauk mammalian fauna (late Neogene, Myanmar) and its implication to paleoenvironment and paleogeography. *Palaeogeogr Palaeoclimatol Palaeoecol*, 300: 11–22
- Zong G F, Chen W Y, Huang X S, Xu Q Q. 1996. *Cenozoic Mammals and Environment of Hengduan Mountains Region*. Beijing: Ocean Press. 1–279